Volume 72 • Issue 1 • January-March 2023

ISSN : 0003-2778

Scopus
Indexed

JASI

JOURNAL OF THE ANATOMICAL SOCIETY OF INDIA

An International Journal

An Official Publication of Anatomical Society of India

Full text online at **www.jasi.org.in**
Submit articles online at **https://review.jow.medknow.com/jasi**

Editor-in-Chief
Dr. Vishram Singh

Wolters Kluwer

Medknow

Journal of the Anatomical Society of India

Print ISSN: 0003-2778

GENERAL INFORMATION

About the Journal

Journal of the Anatomical Society of India (ISSN: Print 0003-2778) is peer-reviewed journal. The journal is owned and run by Anatomical Society of India. The journal publishes research articles related to all aspects of Anatomy and allied medical/surgical sciences. Pre-Publication Peer Review and Post-Publication Peer Review Online Manuscript Submission System Selection of articles on the basis of MRS system Eminent academicians across the globe as the Editorial board members Electronic Table of Contents alerts Available in both online and print form. The journal is published quarterly in the months of January, April, July and October.

Scope of the Journal

The aim of the *Journal of the Anatomical Society of India* is to enhance and upgrade the research work in the field of anatomy and allied clinical subjects. It provides an integrative forum for anatomists across the globe to exchange their knowledge and views. It also helps to promote communication among fellow academicians and researchers worldwide. The Journal is devoted to publish recent original research work and recent advances in the field of Anatomical Sciences and allied clinical subjects. It provides an opportunity to academicians to disseminate their knowledge that is directly relevant to all domains of health sciences.

The Editorial Board comprises of academicians across the globe.

JASI is indexed in Scopus, available in Science Direct.

Abstracting and Indexing Information

The journal is registered with the following abstracting partners:

Baidu Scholar, CNKI (China National Knowledge Infrastructure), EBSCO Publishing's Electronic Databases, Ex Libris – Primo Central, Google Scholar, Hinari, Infotrieve, Netherlands ISSN center, ProQuest, TdNet, Wanfang Data

The journal is indexed with, or included in, the following:

SCOPUS, Science Citation Index Expanded, IndMed, MedInd, Scimago Journal Ranking, Emerging Sources Citation Index.

Impact Factor® as reported in the Journal Citation Reports® (Clarivate Analytics, 2021): 0.26

Information for Authors

Article processing and publication charges will be communicated by the editorial office. All manuscripts must be submitted online at https://review.jow.medknow.com/jasi.

Subscription Information

A subscription to JASI comprises 4 issues. Prices include postage. Annual Subscription Rate for non-members-		
Rates of Membership (with effect from 1.1.2022)		
	India	**International**
Ordinary membership	INR 1500	US $ 100
Couple membership	INR 2250	
Life membership	INR 8000	US $ 900
Subscription Rates (till 31st August)		
Individual	INR 6000	US $ 650
Library/Institutional Trade discount of 10% for agencies only	INR 12000	US $ 1000
Subscription Rates (after 31st August)		
Individual	INR 6500	US $ 700
Library/Institutional	INR 12500	US $ 1050
The Journal of Anatomical Society of India (ISSN: 0003-2778) is published quarterly **Subscriptions** are accepted on a prepaid basis only and are entered on a calendar year basis. Issues are sent by standard mail Priority rates are available upon request.		

Information to Members/Subscribers

All members and existing subscribers of the Anatomical Society of India are requested to send their membership/existing subscription fee for the current year to the Treasurer of the Society on the following address: Prof (Dr.) Punit Manik, Treasurer, ASI, Department of Anatomy, KGMU, Lucknow - 226003. Email: punitamanik@yahoo.co.in. All payments should be made through an account payee bank draft drawn in favor of the **Treasurer, Anatomical Society of India,** payable at **Lucknow** only, preferably for **Allahabad Bank, Medical College Branch, Lucknow.** Outstation cheques/drafts must include INR 70 extra as bank collection charges.

All complaints regarding non-receipt of journal issues should be addressed to the Editor-in-Chief, JASI at editorjasi@gmail.com. The new subscribers may, please contact wkhlrpmedknow_subscriptions@wolterskluwer.com.

Requests of any general information like travel concession forms, venue of next annual conference, etc. should be addressed to the General Secretary of the Anatomical Society of India.

For mode of payment and other details, please visit www.medknow.com/subscribe.asp

Claims for missing issues will be serviced at no charge if received within 60 days of the cover date for domestic subscribers, and 3 months for subscribers outside India. Duplicate copies cannot be sent to replace issues not delivered because of failure to notify publisher of change of address. The journal is published and distributed by Wolters Kluwer India Pvt. Ltd. Copies are sent to subscribers directly from the publisher's address. It is illegal to acquire copies from any other source. If a copy is received for personal use as a member of the association/society, one cannot resale or give-away the copy for commercial or library use.

The copies of the journal to the subscribers are sent by ordinary post. The editorial board, association or publisher will not be responsible for non receipt of copies. If any subscriber wishes to receive the copies by registered post or courier, kindly contact the publisher's office. If a copy returns due to incomplete, incorrect or changed address of a subscriber on two consecutive occasions, the names of such subscribers will be deleted from the mailing list of the journal. Providing complete, correct and up-to-date address is the responsibility of the subscriber.

Nonmembers: Please send change of address information to subscriptions@medknow.com.

Advertising Policies

The journal accepts display and classified advertising. Frequency discounts and special positions are available. Inquiries about advertising should be sent to Wolters Kluwer India Pvt. Ltd, advertise@medknow. com.

The journal reserves the right to reject any advertisement considered unsuitable according to the set policies of the journal.

The appearance of advertising or product information in the various sections in the journal does not constitute an endorsement or approval by the journal and/or its publisher of the quality or value of the said product or of claims made for it by its manufacturer.

Addresses

Editorial Office

Dr. Vishram Singh, Editor-in-Chief, JASI
B5/3 Hahnemann Enclave, Plot No. 40, Sector 6, Dwarka Phase – 2,
New Delhi - 110 075, India.
Email: editorjasi@gmail.com

Published by

Wolters Kluwer India Pvt. Ltd
A-202, 2nd Floor, The Qube,
C.T.S. No.1498A/2 Village Marol, Andheri (East),
Mumbai - 400 059, India.
Phone: 91-22-66491818
Website: www.medknow.com

Printed at

Nikeda Art Printers Pvt. Ltd.,
Building No. C/3 - 14,15,16, Shree Balaji Complex, Vehele Road,
Village Bhatale, Taluka Bhiwandi, District Thane - 421302, India.

Journal of the Anatomical Society of India

Print ISSN: 0003-2778

EDITORIAL BOARD

Journal of the Anatomical Society of India

Volume 72 | Issue 1 | January-March 2023

CONTENTS

continued...

Teaching Should be Preferred over Research in Peripheral Medical Institutions - A view point

The main purpose of medical education is to ensure that medical students acquire sufficient knowledge, skills, and professional efficiency that prepares them to provide good health education, and good health care or enhance existing medical knowledge, depending on the aptitude and conditions available to them in the future.

This entails proficiency both in teaching and research. The teaching enhances the development of students while research advances new knowledge.

Therefore, linking teaching and research is essential to both teachers and students. There are many ways of linking research to teaching; the most important of these is to set specific teaching and research goals.

However, the problem comes when some teachers have no inclination or may not have time to do research due to a poor teacher–student ratio. Most of the peripheral medical colleges have a very poor teacher–student ratio as compared to one that was recommended by the Mudalier Committee in 1962.[1,2]

Therefore, research should not be forced to teachers, particularly if they do not have any aptitude for it or they do not have time to pursue such activities. Contrary to this, if they have a good interest and aptitude for teaching, students taught by them excel in all fields of their later life such as teaching, patient care, research, and interpersonal relationship.

Recently, the National Medical Council of India has recommended an introductory course in medical education technology[3-5] and basic research in biomedical research as mandatory for promotion. Not only that, this body has also made it mandatory that one should also publish a requisite number of research articles in indexed journals for their promotion.[6]

For this reason, teachers who were already under pressure to complete the course were forced to do research, on the cost of teaching. As a result, the quality of producing good Indian Medical Graduates is defeated. Not only that, forced research has adulterated the already existing good scientific data with false-positive results. Not only that, the number of predatory scientific journals has started worldwide purely for business purposes. They started charging exorbitantly, and poor teachers have no option but to pay it.

To conclude, teaching and patient care should be given more weightage over research, particularly in peripheral medical colleges, for the following reasons: Teacher–student ratio is very poor, institutions are not well equipped with research facilities, all teachers are forced to do research whether they have an aptitude for it or not. As a result, medical teaching and patient care are on a decline.

Vishram Singh, Rashi Singh[1]

Department of Anatomy, Kasturba Medical College, Manipal Academy of Higher Education, Mangalore, Karnataka, [1]Department of Pediatric and Preventive Dentistry, Santosh Dental College and Hospital, Ghaziabad, Uttar Pradesh, India

Address for correspondence: *Prof. Vishram Singh, B5/3 Hahnemann Enclave, Plot No. 40, Sector 6, Dwarka Phase – 2, New Delhi - 110 075, India.*
E-mail: drvishramsingh@gmail.com

References

1. Carballido Coria L. The mudaliar committee (1962): Assessing the beginnings. Estud Asia Áfr 2020;55:571-98.
2. Sahai A. Medical education in India: Introspection, challenges and reforms – A vision. J Anat Soc India 2016;65:167-74.
3. Available from: https://www.nmc.org.in/ActivitiWebClient/open/getDocument?path=/Documents/Public/Portal/Gazette/TEQ-17.02.2019.pdf. [Last accessed on 2023 Mar 15].
4. Ministry of Family Welfare, Government of India. Sneh Bhargav Committee Report. Available from: https://www.google.com/search?q=sneha+bhargava+committeeandrlz=1C1CHZN_enIN971IN971 andoq=sneha+bhargava+committeeandaqs=chrome. 69i57j0i390.9261j0j15andsourceid=chrome and ie=UTF8. [Last accessed on 2023 Jan 18].
5. Medical Council of India. Competency Based Undergraduate Curriculum for the Indian Medical Graduate; 2018. p. 1-3. Available from: https://www.mciindia.org/CMS/informationdesk/forcolleges/ugcurriculum. [Last accessed on 2019 Mar 05].
6. Aggarwal R. Why must faculty members in medical institutions engage in research? Int J Adv Med Health Res 2021;8:1.

Article Info

Received: 15 March 2023
Accepted: 17 March 2023
Available online: 24 March 2023

Access this article online	
Quick Response Code:	**Website:** www.jasi.org.in
	DOI: 10.4103/jasi.jasi_25_23

How to cite this article: Singh V, Singh R. Teaching should be preferred over research in peripheral medical institutions - A view point. J Anat Soc India 2023;72:1.

Original Article

The Morphological Features of Anencephaly in North Indian Population

Rashmi, Nitish Kumar Singh, Ashish, Abhay Kumar Yadav, Manpreet Kaur, Royana Singh

Department of Anatomy, Institute of Medical Sciences, Banaras Hindu University, Varanasi, Uttar Pradesh, India

Abstract

Background: Anencephaly occurs due to the complete absence of cranial vault and subsequent disruption of the cerebral cortex with a severely damaged brain. In anencephaly, the forebrain and brain stem are exposed. Forebrain either does not develop or is destroyed, leading to the absence of cerebrum and cerebellum. **Methodology:** Neural tube defects were taken in the study group. During the autopsy, clinical findings, external examination, internal examination, and photography were done along with the histopathology of the specimens to confirm the anomalies at microscopic level using hematoxylin and eosin staining. **Results:** In our study, we observed a simian crease in 4 out of 5 (80%) cases. Furthermore, there was presence of tooth which was not seen in previous studies. Central nervous system anomalies like spina bifida, gastro intestinal tract (GIT) anomalies like cleft palate, intestinal obstruction of megacolon, and malrotation of gut were some of the common anomalies which were observed in our study. **Conclusion:** It may be suggested that Anencephaly shows a female predisposition and the cases seems to be associated more in the primigravida females.The classical phenotypic presentation of anencephaly having absent cranial vault ,low set ears, protruding eyes were present in all subjects studied. In our study, we observed a simian crease in 4 out of 5 (80%) cases. Furthermore, there was presence of tooth which was not seen in previous studies. Central nervous system anomalies like spina bifida, GIT anomalies like cleft palate, intestinal obstruction of megacolon, and malrotation of gut were some of the common anomalies which were observed in our study.

Keywords: *Anencephaly, Meckel–Gruber syndrome, neural tube defects*

Introduction

Neural tube defects (NTDs) are a group of congenital malformation with an incidence of 1/1000 live birth worldwide.[1] NTD can be classified into open or closed type. Open NTDs are the most common type of defect which include anencephaly which occurs most predominantly after spina bifida.[2] Anencephaly which results in the absence of cranial vault and subsequent disruption of the cerebral cortex development with severely damaged brain.[3] In anencephaly, forebrain and brain stem are exposed. Forebrain either does not develop or is destroyed leading to the absence of cerebrum and cerebellum. Several factors both genetic and environmental were known to be associated with NTD. Newborns with anencephaly are stillbirth or survive for few hours (30 h). Anencephaly is a lethal malformation, and several associated deformities are known to be associated with NTD. The different malformation which occurred along with anencephaly includes cleft lip, cleft palate, polycystic kidney, spina bifida, simian crease, malrotation of gut, intestinal obstruction, esophageal atresia, diaphragmatic hernia, bladder exstrophy, or renal agenesis. Meckel–Gruber syndrome (MKS) is a lethal ciliopathy characterized by the triad of cystic renal dysplasia, occipital encephalocele, and postaxial polydactyly. The diagnosis of anencephaly can be done either by ultrasound examination or by alpha-fetoprotein test. However, since anencephaly is associated with several anomalies both systemic and nonsystemic, hence pathological examination of abortus is to be done.[4] Only a few studies of this type have been done in southern India; however, in northern India, no study has been done.[5] Hence, the proposed study was undertaken to assess the deformities and systematic anomalies associated with anencephaly and also with histological findings in anencephaly and associated different anomalies.

Methodology

During the study, stillbirth samples of NTDs were collected from the Department of Gynecology and Obstetrics, SS Hospital,

How to cite this article: Rashmi, Singh NK, Ashish, Yadav AK, Kaur M, Singh R. The morphological features of anencephaly in North Indian population. J Anat Soc India 2023;72:2-7.

Article Info

Received: 08 November 2020
Revised: 07 August 2022
Accepted: 11 October 2022
Available online: 24 March 2023

Address for correspondence:
Dr. Royana Singh,
Department of Anatomy,
Institute of Medical Sciences,
Banaras Hindu University,
Varanasi - 221 005,
Uttar Pradesh, India.
E-mail: royanasingh@bhu.ac.in

Access this article online

Website: www.jasi.org.in
DOI: 10.4103/jasi.jasi_245_20
Quick Response Code:

Banaras Hindu University. This is a prospective study where all the patients diagnosed with features of NTD by ultrasound or delivered babies with NTD were taken in the study group. During the autopsy, clinical findings, external examination, internal examination, and photography were done along with the histopathology of the specimens to confirm the anomalies at microscopic level using hematoxylin and eosin staining.

Methods of preparation of egg albumin

Egg albumin solution was prepared by mixing equal amount of egg white and glycerin. It was filtered and few crystals of thymol were added to it to prevent the growth of molds in it.

Results

The study shown here determines six cases of anencephaly with different systemic anomalies. During the study, the minimum maternal age having anencephaly baby was 21 and maximum 35 years with a mean age of 26 years. Out of six mothers, four were primigravida (66.66%), one was gravida 2 (16.66%), and the last one was gravida 3 (16.66%). A study shown here determines that out of six cases, four cases were female (80%), one was male (20%), and in one case, sex was undetermined. The gestational age ranged from 14 to 36 weeks with a mean of 23.2 weeks. The head circumference ranged from 10 cm to 26 cm with a mean of 16 cm. On dissection, the entire six fetuses showed different associated systemic anomalies (100%) along with anencephaly. During the study, anencephaly fetuses were suffering from different types of anomalies.

A 24-year-old female presented with 25 weeks 5 days of gestation for routine antenatal examination. There was no history of consanguineous marriage and no history of teratogenic drugs was there. Routine antenatal screening showed a female fetus having features of anencephaly. Case 1 presented with cleft palate in the oral cavity. Ultrasound report showed that supraorbital skull bones and brain tissue is not visualized showing a case of anencephaly and bradycardia of the fetus. Club foot was also seen in both legs. The fetal autopsy was done of the anencephalic subjects after obtaining consent from their parents. All the anencephalic subjects displayed absence of the cerebrum, cerebellum and a poorly developed brain stem. The fetus showed excess hairs on the whole body, i.e., lanugo. There was dilation in the bowel loop leading to intestinal obstruction and the sigmoid colon shifted toward the right side leading to malrotation of the gut. Other visceral organs were normal. A 24-year-old female presented with primigravida for 19 weeks of gestation for routine antenatal examination. She was not on any teratogenic drugs. Routine antenatal screening showed features of anencephaly. On autopsy, the male fetus Case 2 showed a cleft palate with syndactyly in the right hand. X-ray showed the presence of four metatarsals and two phalanges in the right hand. There was dilation in the bowel loop leading to intestinal obstruction and the sigmoid colon shifted towards the right side leading to malrotation of the gut. The fetus has a right lobe of the liver smaller than left lobe. A 35-year-old female presented at 19 weeks 6 days of gestation to the OPD for routine antenatal examination. There was no significant medical and surgical history with no history of consanguineous marriage. Her second daughter died due to jaundice at the age of 23 days. On clinical examination, she was of average nutrition. Ultrasound report showed features of fetal occipital calvarial defect with herniation of occipital lobes leading to anencephaly with postaxial polydactyly and nephromegaly with echogenic medulla which can be correlated with cystic dysplasia of the kidney. Hence, the termination of pregnancy was done after proper counseling and consent and the baby was sent for autopsy. On external examination, the baby was male and showed features of microcephaly with anencephaly. The brain stem was present; however, cerebellum and cerebrum were absent. Oral cavity showed the presence of cleft palate and lobulated tongue. All the four limbs showed postaxial polydactyly with seven fingers in the right and six fingers in the left hand and six fingers in both legs. On autopsy, malrotation of the gut was observed along with bilateral polycystic kidney. The kidney specimen was sent for histopathology for confirmation. On histological observation, multiple cysts were observed in the kidney of fetus. Other visceral organs were normal. The characteristic features of anencephaly, postaxial polydactyly, cleft palate, and polycystic kidney correlated with MKS [Figures 1-3].

A 21-year-old female presented with 14 weeks of gestation and came to a gynecologist for routine antenatal examination. There was no history of consanguineous marriage. She was not on any teratogenic drug. A gravida 2 female fetus Case 4 showed central nervous system anomalies, i.e., spina bifida. USG report showed that the cranium is not opacified. Only facial bones are visualized and brain material is lying in closed sac. On dissection, brain showed the absence of cerebrum and cerebellum with

Figure 1: Ventral and dorsal surface of fetus showing encephalocele and polydactyly

the absence of brain stem. Oral cavity showed the presence of cleft palate. Webbed neck is also observed. The vertebral column shows spina bifida. The only skeletal deformity showed shifting of the spinal cord from the center toward the right side evidence kyphoscoliosis. A bilateral simian crease is observed. Other visceral organs were normal [Table 1]. A 28-year second gravida at 36 weeks of gestation in labor presented in the emergency. Her previous pregnancy was uneventful with a 3-year-old male baby. She delivered a stillborn female fetus. On external examination, there was anencephaly with protruding eyes. Oral cavity showed cleft palate, two teeth. There was presence of simian crease in the right palm along with low-set ears. On autopsy, the forebrain of fetus has thalamus, but cerebrum was absent. The corpus callosum showed the development of only splenium. It was observed that the cerebellum was absent. The medulla oblongata and pons were present. Abnormal rotation of the gut was also observed. Other visceral organs were normal. Again, this fetus showed characteristic features of anencephaly, cleft palate, and polycystic kidney closely correlating with the diagnosis of MKS. Histological examination was done to check multiple cysts in the kidney of fetus. We observed multiple cysts in the kidney of fetus [Figures 4, 5 and Table 1].

The different systematic anomalies associated with anencephaly with the number of cases are represented in Table 2.

Discussion

The incidence of anencephaly varies in different countries. In India, a study of Cherian showed that the incidence rate is 6·57–8·21 per 1000 live births.[6] Other studies showed the incidence rate to be 0.5–6.5 per 1000 live birth.[7-10] A hospital-based study has been done to check the incidence of NTD.[11] A study shows that the incidence of anencephaly varies in different countries with an incidence of 0.54 per 1000 births in Singapore,[12] 12 per 10,000 in Iran, and 10.4 per 10,000 in China. A previous study showed the prevalence of anencephaly to be more in mother of age below 20 and above 35. In our study, the mean age was 26 years with a minimum age of 21 and maximum 35 years; our findings were similar to previous studies reported.[13-16]

In our study, four out of six showed primigravida which is similar to the previous study observed.[17,18] The anencephaly cases were diagnosed at the time when the mother came to SS Hospital for regular check-up. The ultrasound examination showed a defect in fetus and termination of pregnancy was advised. During the study, some cases were spontaneous abortion and some were stillborn with gestational age of 14–36 weeks. Furthermore, there is preponderance of anencephaly more in female fetus (4/6) than males in our study. Some studies showed male preponderance than females.[17] Phenotypic features of anencephaly such as acrania (absence of skull),

Table 1: Different anomalies associated with anencephaly in different cases

Case ID	Sex (years)	Disease + HC	Oral	Low-set ears + neck	Upper limb + simian crease	Lower limb	Age	Polycystic kidney	Spina bifida	Intestine malrotation of gut
Case 1	Female 24	Anencephaly 18 cm	Cleft palate	Present	Absent, present	Club foot	25 weeks 5 days	Absent	Absent	Intestinal obstruction mega colon present malrotation of gut
Case 2	Male 24	Anencephaly 24 cm microcephaly	Cleft palate	Present	Syndactyly only 4 metatarsals in right hand, 2 phalanges, absent	Absent	18 weeks	Absent	Absent	Intestinal obstruction mega colon present malrotation of gut
Case 3	Female 35	Occipital myelomeningocele 14 cm microcephaly	Cleft palate lobulated tongue	Present	Postaxial polydactyly 7 fingers in right hand 6 fingers in left hand, present	6 fingers in both legs	20 weeks 6 days	Nephromegaly with echogenic medulla is noted correlated with cystic dysplasia of kidney, polycystic kidney (bilateral)	Absent	Absent present malrotation of gut
Case 4	Female 21	Anencephaly 10 cm	Cleft palate	Present webbed neck	Absent, present (bilateral)	Absent	14 weeks	Absent	Present kyphoscoliosis	Absent
Case 5	Female	Anencephaly 26 cm	Cleft palate witch tooth	Present	Absent, present	Absent	36 weeks	Present	MMC present	Absent present malrotation of gut
Case 6	Female 28	Anencephaly	Absent	Present	Absent, absent	Absent		Absent	Present	Absent

HC: Head circumference, MMC: myelomeningocele

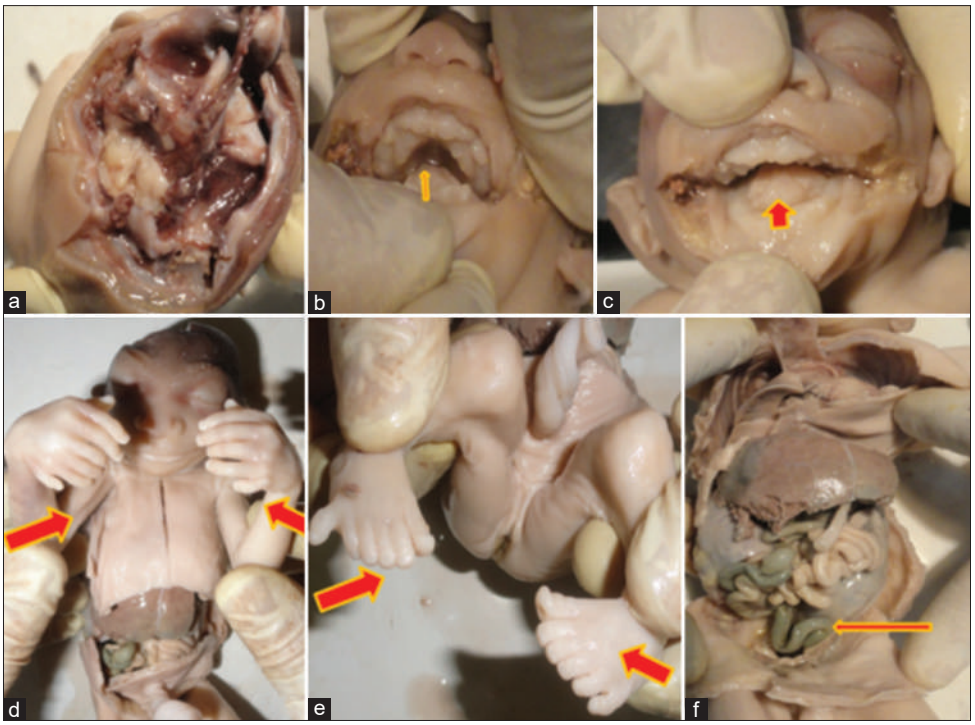

Figure 2: (a) Absence of cerebellum and cerebrum, (b) cleft palate, (c) lobulated tongue, (d and e) polydactyly in all four limbs, (f) malrotation of gut

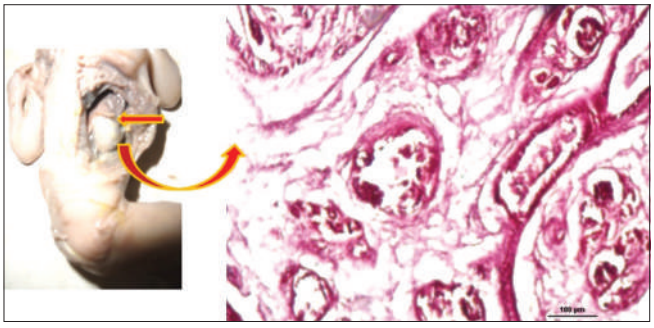

Figure 3: Microphotograph of the kidney showing multiple cysts

acephaly (absence of head), and meroanencephaly were present in all cases. Some other features such as low-set ears and protruding eyes were also present in all the cases. A very interesting feature simian crease which is known to be associated with Down's syndrome was observed in 4 out of 5 (80%) cases. Studies show that anencephaly is associated with anomalies of different systems. In our study out of six cases obtained, two showed spina bifida. Spina bifida is the most common anomaly associated with anencephaly. GIT anomalies were the second most common anomalies associated with anencephaly. In our study, GIT anomalies included cleft palate, lobulated tongue, witched teeth, and intestinal obstruction of megacolon and malrotation of the gut. In our study, we have noticed polycystic kidney in two cases out of five. During the study, we observed two cases having MKS. Studies show the presence of anencephaly which is a defect of the central nervous system (90%), polydactyly (83.3%), and renal dysplasia because the internal structure does not develop properly leading to polycystic kidney (100%).[19-21] MGS shows an autosomal recessive inheritance pattern. In MKS, both male and female are affected equally with a recurrence rate in subsequent pregnancy of 1 in 4 (25%). The survivor rate of infants affected with MKS is very less. Only ten infants have been known to survive after birth with the highest age of 28 months.[2,6,8-10,17] Mortality rate is 100% [Table 3].

Table 2: Systemic anomalies associated with anencephaly

System	Associated anomalies (number of cases)
Central nervous system	Spina bifida (2)
Brain	Brain stem (2, 2 poorly developed), Cerebrum (5 absent), cerebellum (4 absent, 1 poorly developed)
Head and neck	Cleft palate, webbed neck (1)
Respiratory	No defect
Cardiovascular	No defect
GIT	Malrotation of gut (4), intestinal obstruction of megacolon (2)
Skeletal	Polydactyly (1), syndactyly (1), kyphoscoliosis (1)

GIT: Gastro intestinal tract

Conclusion

Anencephaly is associated with multiple congenital anomalies with observed percentage of 100%. In our study, we conclude that anencephaly is observed in women conceiving at the third decade (20–29 years) of life. It may be concluded from the observations made that Anencephaly showed a female preponderance .The ratio of female to male being 4:1 .Further it was seen that the

Table 3: Comparison of pathological parameters done in a previous study with the present study

System	David	Vare	Golalipour	Tan	Nielsen	David	Panduranga	Eslavath	Present study
Total anomaly	33.3	Not mentioned	42.9	9.4	43	23.6	73	77.7	100
Head and neck	3.5	7.5	3.5	NO	14	4.6	2.5	NO	83.33
Respiratory	1	NO	NO	3	NO	0.6	2.5	11.1	NO
Cardiovascular	5.8	7.5	1.7	3	4.75	11	14.5	11.1	NO
GIT	8	32	5.3	29	NO	5.7	14.5	33.3	66.66
Skeletal	1.5	14.5	8.9	20	16.5	1.7	14.5	22.2	50
Renal	16.3	27	3.5	3	12	5.2	NAD	14.5	33.33
Genital	0.6	5	NO	NO	NO	0.6	12	11.1	NO

GIT: Gastro intestinal tract, NAD: Not observed, NO: Not observed

Figure 4: (a and b) Ventral and dorsal surface of fetus showing encephalocele. (c) Left lateral showing low set ears, (d) presence of tooth, (e) cleft palate, (f) simian crease, (g) malrotation of gut, (h) polycystic kidney

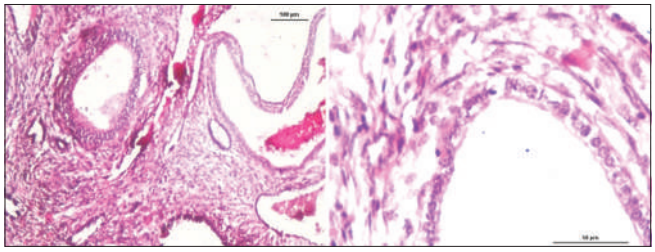

Figure 5: Gross photograph of cut surface of kidney showing multiple cysts

primigravida showed an increased association with that of anencephaly than multigravida. In our study, we observed a simian crease in 4 out of 5 (80%) cases. Furthermore, there was presence of tooth which was not seen in previous studies. Central nervous system anomalies like spina bifida, GIT anomalies like cleft palate, intestinal obstruction of megacolon, and malrotation of gut were some of the common anomalies which were observed in our study. Club foot, polydactyly, syndactyly, and kyphoscoliosis are the commonly associated anomalies of the skeletal system. Diagnosis of anencephaly can be done by Ultrasonography (USG) examination during early weeks of pregnancy and further pathological examination of abortus should be done. Further to determine the reason associated with anencephaly and other systemic anomalies, genetic studies can be done.

Acknowledgment

This research was sponsored by Multi-Disciplinary Research Units (MRUs), a grant by ICMR-Department of Health Research.

Author contributions

R.S., R., N.K.S. contributed to the conception, design, and writing of the study protocol and the design of search strategies; A., A.K.Y., M.K. located and obtained reports, helped to select and assess cases, conducted the data analysis, and drafted and approved the final paper. All authors contributed to the conception, design, and writing of the study protocol, conducted data analysis, and revised and approved the final paper.

Financial support and sponsorship

Nil.

Conflicts of interest

There are no conflicts of interest.

References

1. Cook RJ, Erdman JN, Hevia M, Dickens BM. Prenatal management of anencephaly. Int J Gynaecol Obstet 2008;102:304-8.
2. Godbole K, Deshmukh U, Yajnik C. Nutri-genetic determinants of neural tube defects in India. Indian Pediatr 2009;46:467-75.
3. Copp AJ, Bernfield M. Etiology and pathogenesis of human neural tube defects: Insights from mouse models. Curr Opin Pediatr 1994;6:624-31.
4. Malina RM. The developing human: Clinically oriented embryology (5th edition). xi+493 pp. By Keith L. Moore and T.V.N. Persaud. Philadelphia: W. B. Saunders, 1993. $31.95 (paper). Am J Hum Biol 1993;5:507.
5. Panduranga C, Patil P, Pilli G, Suranagi V, Kangle R. Anencephaly: A pathological study of 41 cases. J Sci Soc 2012;39:81.
6. Cherian A, Seena S, Bullock RK, Antony AC. Incidence of neural tube defects in the least-developed area of India: A population-based study. Lancet 2005;366:930-1.
7. Bhat BV, Babu L. Congenital malformations at birth – A prospective study from south India. Indian J Pediatr 1998;65:873-81.
8. Mahadevan B, Bhat BV. Neural tube defects in Pondicherry. Indian J Pediatr 2005;72:557-9.
9. Sood M, Agarwal N, Verma S, Bhargava SK. Neural tubal defects in an East Delhi hospital. Indian J Pediatr 1991;58:363-5.
10. Kulkarni ML, Mathew MA, Ramachandran B. High incidence of neural-tube defects in south India. Lancet 1987;329:1260.
11. Rai SK, Singh R, Pandey S, Singh K, Shinde N, Rai S, *et al*. High incidence of neural tube defects in Northern part of India. Asian J Neurosurg 2016;11:352-5.
12. Mobasheri E, Keshtkar A, Golalipour MJ. Maternal folate and vitamin b (12) status and neural tube defects in northern Iran: A case control study. Iran J Pediatr 2010;20:167-73.
13. Leck I, Rogers SC. Changes in the Incidence of Anencephalus. Br J Prev Soc Med 1967;21:177–80. PMCID: PMC1059097.
14. Horowitz I, McDonald AD. Anencephaly and spina bifida in the Province of Quebec. Can Med Assoc J 1969;100:748-55.
15. Edwards JH. Congenital malformations of the central nervous system in Scotland. Br J Prev Soc Med 1958;12:115-30.
16. Golalipour MJ, Najafi L, Keshtkar AA. Prevalence of anencephaly in Gorgan, Northern Iran. Arch Iran Med 2010;13:34-7.
17. Singh J, Kapoor K, Kaur A, Kochhar S and Huria A. Incidence of Anencephaly in a tertiary care hospital in North West India; Int J Sci Res Publ 2018;5:1-17.
18. Eslavath A. Anencephaly: A 3 years study. IOSR J Dent Med Sci 2013;12:12-5.
19. Alexiev BA, Lin X, Sun CC, Brenner DS. Meckel-Gruber syndrome: Pathologic manifestations, minimal diagnostic criteria, and differential diagnosis. Arch Pathol Lab Med 2006;130:1236-8.
20. Paavola P, Salonen R, Baumer A, Schinzel A, Boyd PA, Gould S, *et al*. Clinical and genetic heterogeneity in Meckel syndrome. Hum Genet 1997;101:88-92.
21. Verma M, Sharma S, Suthar K, Thada B. Meckel Gruber syndrome: A rare case report. Int J Contemp Pediatr 2017;5:262.

Original Article

Analysis of the Effects of Total Pneumatized Turbinate Volume on Septum Deviation, Maxillary Sinus Volume, and Maxillopalatal Parameters: A Multidetector Computerized Tomography Study

Abstract

Introduction: The aim of this study was to examine the effects of pneumatized turbinate volume (PTV) on nasal septum deviation (NSD), maxillary sinus volume (MSV), and maxillopalatal parameters with multidetector computed tomography (MDCT). **Material and Methods:** MDCT images of a total of 73 patients (35 females and 38 males) between the ages of 25 and 58 years were used in the study. PTV, MSV, and NSD angle and direction and interalveolar distance (IAD), maxillary spin distance (MSD), and maxillopalatal angle (MPA) measurements were made on images brought to the orthogonal plane in 3 plans. **Results:** Turbinate pneumatization (superior, middle, or inferior) was found in a total of 55 (75.3%) patients (28 females and 27 males). The number of patients with turbinate pneumatization on the right side was 14 (19.2%), while the number of patients with turbinate pneumatization on the left side was 15 (20.5%) and the number of bilateral pneumatization was 26 (35.6%). While no significant association was found between the presence of turbinate pneumatization and septal deviation angle, MSV, MPA, IAD, and MSD measurements, a significant difference was found between the groups in terms of PTV ($P < 0.05$). No significant association was found between NSD direction and all parameters. **Discussion and Conclusion:** In this study, we conducted with MDCT images, in addition to the highest incidence in turbinate pneumatization with 75.3%; it was found that PTV did not have an effect on NSD amount, MSV, and maxillopalatal parameters. Men were found to have higher NSD angle, higher maxillary sinus aeration, and larger IAD when compared with women.

Keywords: *Concha bullosa, interalveolar distance, maxillary spin distance, maxillopalatal angle, multidetector computed tomography, nasal septal deviation*

Deniz Senol, Serkan Oner[1], Yusuf Secgin[2], Zulal Oner[3], Seyma Toy[2]

Department of Anatomy, Düzce University Faculty of Medicine, Düzce, [1]Department of Radiology, İzmir Bakırçay University Faculty of Medicine, [3]Department of Anatomy, İzmir Bakırçay University Faculty of Medicine, İzmir, [2]Department of Anatomy, Karabük University Faculty of Medicine, Karabük, Turkey

Introduction

A large number of congenital anomalies and anatomic variations of the anatomical structures that make up the paranasal region have been identified. Concha bullosa, septum pneumatization, paradox middle concha, Haller cell, Onodi cell, anterior clinoid process pneumatization, and uncinate process pneumatization can be listed as common variations.[1] The most common of these is concha bullosa (also known as middle turbinate pneumatization) and it is an anatomical variation of the lateral nasal wall within the nasal cavity.[2,3]

Certain pathologies such as the excessive pneumatization of concha, ethmoid bulla pneumatization, uncinate process pneumatization, and secondary middle concha can show significant growth in nasal cavity and obstruct the nasal cavity.[4] Although the mechanism of concha bullosa is not fully known, it is thought that it may be due to the enlargement of sinus pneumatization in the concha in intrauterine period, fusion anomaly during intrauterine development or mucosal invagination of conchal bone microfractures into the bullosa cavity in late adolescence.[1] Another theory suggests that anterior and posterior ethmoidal cells cause turbinate pneumatization.[5]

Although turbinate pneumatization is frequently seen in the middle concha, it is also rarely seen in the superior concha.[6] Inferior concha bullosa is a very rare condition in which the inferior concha body is pneumatized. Although generally asymptomatic, severely pneumatized and hypertrophic concha may cause nasal congestion and rhinogenic

How to cite this article: Senol D, Oner S, Secgin Y, Oner Z, Toy S. Analysis of the effects of total pneumatized turbinate volume on septum deviation, maxillary sinus volume, and maxillopalatal parameters: A multidetector computerized tomography study. J Anat Soc India 2023;72:8-14.

Article Info

Received: 05 March 2021
Revised: 13 June 2022
Accepted: 16 August 2022
Available online: 24 March 2023

Address for correspondence:
Dr. Deniz Senol, Department of Anatomy, Düzce University Faculty of Medicine, Düzce, Turkey. E-mail: denizanatomi@gmail.com

Access this article online

Website: www.jasi.org.in
DOI: 10.4103/jasi.jasi_46_21
Quick Response Code:

headache.[1] Concha enlargement due to pneumatization may cause compression related contact headache. It also causes mucosal edema by obstructing the nasal passage and disrupting mucus drainage.[7] Another cause of headaches is the narrowed posterior nasal passage due to nasal septum deviation (NSD), another pathological condition of this region, which is known to accompany pneumatized and hypertrophic concha frequently. NSD is also associated with hypertrophic concha or concha bullosa and it is a developmental or acquired condition that may affect the maxillopalatal parameters.[8,9] Maxillary sinus anatomy is especially important in dentistry since it closely concerns the area they work.[10] Anatomical variations such as NSD and concha bullosa may cause narrowing or obstruction of the sinus drainage canals, resulting in decreased ventilation of the maxillary sinus, impaired mucociliary activity, and narrowing of the sinus volume in chronic cases.[11]

Multidetector computed tomography (MDCT) is a frequently used extremely effective method to examine the pathologies in the paranasal region and their anatomical relationship. In addition, MDCT is helpful in evaluating the ostiomeatal complex, soft tissue details and their relationship to bone and air containing sinuses.[1,2,5]

The relationship between total pneumatized turbinate volume (PTV) and anatomical variations in the nasal cavity and paranasal sinusitis has been frequently studied in the literature.[8,12] The objective of the present study is to examine the effects of total PTV in nasal cavity on NSD, MSV and maxillopalatal parameters with MDCT.

Material and Methods

This study was carried out with the approval of Karabük University Noninvasive Clinical Research Ethics Committee (protocol number: 2021/481, date: 24/2/2021). In the study, patients who underwent paranasal sinus CT with various complaints between January 2019 and January 2020 were retrospectively examined and a total of 150 patient images were randomly selected. The measurements were made by a radiologist and anatomist with at least 10 years of experience in the field. In the findings, the average of the values obtained by the two experts is given. Among these, patients who did not have significant sinusitis, tumor, polyposis, surgery and trauma history that could affect the paranasal anatomy were included in the study. CT images with artifacts that adversely affected the evaluation were excluded from the study. Finally, a total of 73 patients (35F, 38M) between the ages of 25 and 58 were included in the study.

All scans were performed on a 16-detector spiral CT device (Aquilion 16; Toshiba Medical Systems, Otawara, Japan) with 120 kV and 120 mA parameters. In the routine imaging protocol, sagittal and coronal reformat images were obtained by performing axial scans with a slice thickness of 3 mm when the patients were in head front and supine position on the scanning table. All images were analyzed with an expert radiologist and anatomist of at least 10 years of experience by using OsiriX MD software (v8.0, Pixmeo, Geneva, Switzerland). All measurements were made on images brought to orthogonal plane in three plans [Figure 1].

Estimated volume measurements were calculated with ½ × transverse diameter × craniocaudal diameter × anteroposterior diameter formula. The angles were shown as degree (°), distances were shown in millimeter (mm). The evaluated measurement parameters were as follows:

Pneumatized turbinate volume

Right, left and bilateral total PTV of the patients with nasal turbinate pneumatization were measured [Figure 2].

Septal deviation angle

The Septal deviation angle (SDA) of the patients with NSD was measured and the septal deviation direction was determined [Figure 3].

Maxillary sinus volume

Right maxillary sinus volume (R-MSV) and left side (L-MSV) MSV were measured [Figure 4].

Maxillopalatal angle

The angle between the line perpendicular to the palatal bone at the junction of maxilla and palatine bones in the right maxillopalatal angle (R-MPA) and left side (L-MPA) alveolar process was measured [Figure 5].

Interalveolar distance

Distance at the medial margins of alveolar process was measured at the dentation level [Figure 5].

Maxillary spin distance

Distance from palatal bone to interalveolar distance (IAD). After measurement of IAD, nasal spin distance was measured at perpendicular plane to this line [Figure 5].

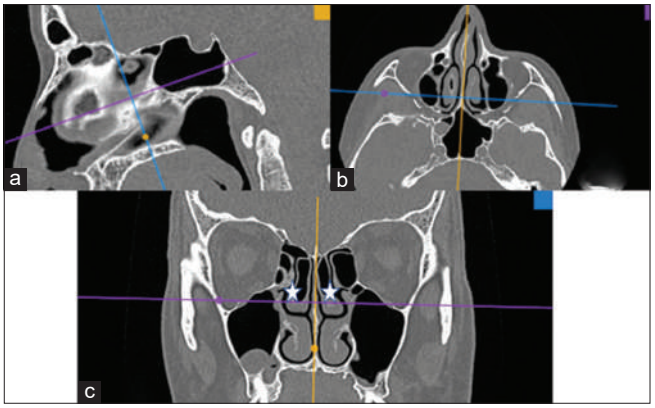

Figure 1: CT images brought to orthogonal plane in sagittal (a), axial (b) and coronal (c) plans. Asterisk show bilateral pneumatized middle turbinate, CT: Computed tomography

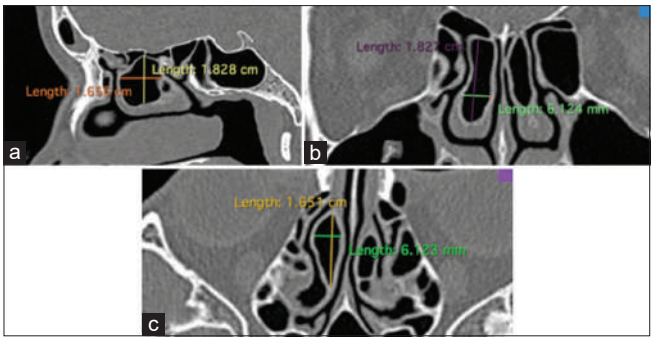

Figure 2: Right side volume measurement on sagittal (a), coronal (b) and axial (c) CT images of patients with bilateral pneumatized middle turbinate, CT: Computed tomography

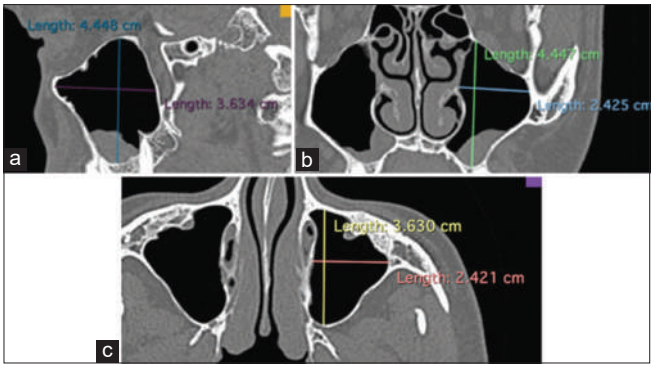

Figure 4: Left side MSV measurement on sagittal (a), coronal (b) and axial (c) CT images, CT: Computed tomography, MSV: Maxillary sinus volume

Statistical analysis

Normality distribution of the data was examined with Kolmogorov Smirnov test and it was found that the data were not normally distributed. Median, minimum (min) and maximum (max) values of the data were given. Mann–Whitney U-test was applied to data to compare the parameters of male and female patients. Kruskall–Wallis *H*-test was applied on data to compare the parameters of the patients between groups. The intraclass correlation coefficient (ICC) test was used for inter-measurer reliability analysis. $P < 0.05$ values were considered significant. Spss version 22 (IBM CO., Armonk, NY, USA) for Windows was used in statistical analyses.

Results

The mean age of 27 male patients with turbinate pneumatization was 32 (25–58), while the mean age of 28 female patients was 35 (25–58) ($P > 0.05$). While total PTVs were compared in terms of gender, they were not statistically significant although they were found to be higher in men ($P > 0.05$). SDA and MSV values were found to be significantly higher in men [Table 1].

Turbinate pneumatization was found in a total of 55 patients (75.3%). The patients were grouped in 4 in terms of pneumatization of the turbinate. Bilateral pneumatization was found to be the highest with

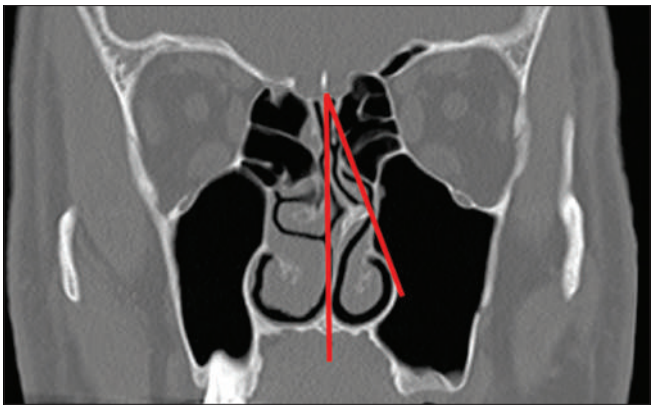

Figure 3: Coronal CT image showing SDA measurement with significant deviation to the left, CT: Computed tomography, SDA: Septal deviation angle

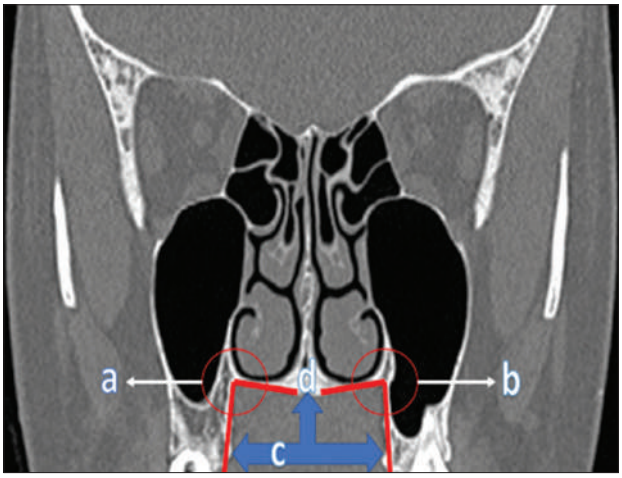

Figure 5: Coronal CT image showing right MPA (a), left MPA (b), IAD (c) and MSD (d) measurements, CT: Computed tomography, MPA: Maxillopalatal angle, IAD: Interalveolar distance, MSD: Maxillary spin distance

26 patients and no significant difference was found between the genders [Table 2]. When viewed according to their level without gender discrimination; 20 right superior turbinate pneumatization (20.4%), 16 left superior turbinate pneumatization (16.3%), 30 right middle turbinate pneumatization (30.6%), and 31 left middle turbinate pneumatization (31.6%) were found. Inferior turbinate pneumatization was seen on the left side in only one female patient (1%). Five male and four female patients had both superior and middle turbinate pneumatization.

While no significant association was found between the state of pneumatization of the turbinate and SDA and MSV, the difference was found between groups in terms of PTV ($P < 0.05$). PTV was found to be the highest (911.26 mm^3) in patients with bilateral turbinate pneumatization; it was found to be the lowest in patients with left side pneumatization (156.28 mm^3) [Table 3].

No statistically significant difference was found between pneumatized turbinate groups in terms of MPA, IAD, and maxillary spin distance (MSD)

measurements ($P > 0.05$) [Table 4]. In the comparison of these parameters in terms of genders, IAD was found to be higher in men when compared with women ($P < 0.05$) [Table 5].

In all the images evaluated, NSD direction was mostly on the right side with 29 patients. Deviation to left was found in 15 patients, while "S" shaped deviation was found in 11 patients and no deviation was found in 18 patients [Table 6]. No significant association was found between NSD direction and all parameters [Table 7].

According to ICC test, 0.87 in PTV, 0.81 in SDA, 0.88 R-MSV 0.86 on L-MSV, 0.83 on R-MPA, 0.87 on L-MPA, Confidence ratio of 0.85 to 0.81 was obtained in IAD, MSD. This result demonstrates the reliability of our measurements.

Table 1: Age, pnomatized turbinate volume, septal deviation angle, right maxillar sinüs volume and left maxillar sinüs volume parameters in terms of gender

Gender	Frequency	Age	PTV	SDA	R-MSV	L-MSV
Male	Median	32	447.41	20.83	19.41	18.55
	Minimum-maximum	25-58	25.37-4470.25	6.30-60.23	1.79-36.89	5.10-38.45
Female	Median	35	356.18	15.09	15.12	14.85
	Minimum-maximum	25-58	27.07-3564.98	5.91-38.24	6.09-29.16	5.36-27.53
P		0.230	0.683	0.017	0.005	0.012

P<0.05: Significant. PTV: Pnomatized turbinate volume, SDA: Septal deviation angle, R-MSV: Right maxillar sinüs volume, L-MSV: Left maxillar sinüs volume

Table 2: Patient distribution according to the presence of turbinate pneumatization

Groups	Patients	Male	Female	Total	Distribution (%)
I	Patients with normal nasal cavity	8	10	18	24.7
II	Patients with pneumatization on the right side	7	7	14	19.2
III	Patients with pneumatization on the left side	7	8	15	20.5
IV	Patients with bilateral pneumatization	13	13	26	35.6

Table 3: Age, pnomatized turbinate volume, septal deviation angle, right maxillar sinüs volume and left maxillar sinüs volume values in terms of pneumatized turbinate groups

Groups	Frequency	Age	PTV	SDA	R-MSV	L-MSV
I	Median	32.5	-	17.96	14.3	14.85
	Minimum-maximum	26-49	-	5.91-43.21	8.53-35.92	7.51-38.4
II	Median	41	430.99	18	18.61	17.76
	Minimum-maximum	25-58	25.37-3564.9	7.69-60.23	13.04-22.55	12.70-26.2
III	Median	33.5	156.28	17.07	15.23	17.34
	Minimum-maximum	28-49	39.47-1385.1	6.30-54.72	1.79-29.16	10.68-27.5
IV	Median	32.5	911.26	15.15	17.19	14.79
	Minimum-maximum	25-58	72.32-4470.2	6.94-57.57	6.09-36.89	5.10-33.24
P		0.875	0.007	0.873	0.497	0.328

P<0.05: Significant. PTV: Pnomatizedturbinatevolume, SDA: Septaldeviationangle, R-MSV: Right maxillar sinüs volume, L-MSV: Leftmaxillar sinüs volume

Table 4: Maxillopalatal parameters according to pneumatized turbinate groups

Groups	Frequency	R-MPA	L-MPA	IAD	MSD
I	Median	110.67	111.58	36.67	13.04
	Minimum-maximum	73.19-141.02	71.30-143.92	28.29-40.83	7.82-19.39
II	Median	111.11	109.92	33.91	14.74
	Minimum-maximum	99.45-129.94	96.54-131.83	27.21-41.68	10-20.28
III	Median	119.55	112.18	32.89	13.22
	Minimum-maximum	83.59-129.33	94.92-137.84	27.48-42.41	10.22-18.30
IV	Median	113.45	117.62	33.85	13.31
	Minimum-maximum	86.76-140.37	76.65-135.37	27.16-40.53	10.11-21.15
P		0.949	0.844	0.372	0.397

P<0.05: Significant. IAD: Inter alveollar distance, MSD: Maxillary spin distance, R-MPA: Right maxillo palatal angle, L-MPA: Left maxillo palatal angle

Table 5: Comparison of maxillopalatal parameters in terms of gender

Groups	Frequency	R-MPA	L-MPA	IAD	MSD
Male	Median	113.94	112.94	36.61	13.22
	Minimum-maximum	73.19-141.02	71.30-143.92	27.16-42.41	7.82-21.15
Female	Median	111.05	112.71	33.41	13.31
	Minimum-maximum	83.59-140.37	94.92-137.84	27.42-40.53	10.37-18.70
P		0.731	0.555	0.014	0.782

P<0.05: Significant. R-MPA: Right maxillo palatal angle, L-MPA: Left maxillo palatal angle, IAD: Inter alveollar distance, MSD: Maxillary spin distance

Table 6: Nasal septum deviation direction and frequency

Deviation direction	Frequency (%)
Absent	18 (25)
Right	29 (38)
Left	15 (22)
"S" shaped	11 (15)

Discussion

In this study in which the relationship of NSD, MSV, and maxillopalatal parameters with total PTV was examined, it was concluded that pneumatized turbinate frequency was 75.3%, while unilateral pneumatized concha frequency was 39.7% and bilateral pneumatized concha frequency was 35.6%. No significant association was found between pneumatized turbinate and MPA, IAD, and MSD. In the comparison of these parameters in terms of gender, IAD was found to be higher in men when compared with women. This situation may be related to the fact that men generally have larger structural sizes in terms of paranasal components than women as in many parts of the body and the fact that they are more prone to NSD.

Kim *et al*. reported a significant link between NSD and asymmetric facial development.[13] In a study conducted by Cengiz *et al*., narrowing of the maxillary curve and a decrease in IAD was found in patients with NSD.[14] Holton *et al*. reported that NSD caused asymmetry in the hard palate and lateral wall of the nasal passage.[15] Sapmaz *et al*. reported that right-left MSV differences will cause facial asymmetry.[16]

Kucybała *et al*., in their study on 214 patients, have found a relationship between the presence of unilateral or dominant concha bullosa and the direction of contralateral septal deviation.[17] Al-Rawi *et al*., in their study on 106 patients, have found a relationship between concha bullosa and high MSV.[18] Shetty *et al*., in their study on 200 patients, have found significant differences between the presence of NSD and concha bullosa and the size of the palate of the patients.[19] These studies support us, and significant relationships were obtained between pneumatization and MSV and maxillopalatal parameters.

Although the fact that there are no studies in literature examining the relationship between pneumatized concha and MSV and maxillopalatal parameters limits the discussion of this study, it is important that the results of the study will pave the way for studies to be conducted in the field. Although congenital anomalies and anatomical variations of the paranasal region are rare, they are of clinical importance once they are identified. While turbinate pneumatization, which is one of the most common variations, is generally seen in the middle concha, it can also be seen in superior concha with a less frequency and in inferior concha although very rarely.[20]

The prevalence of pneumatized turbinate is in a wide range (13.2%-72.2%) in previous studies.[1,3,6] The prevalence of pneumatized turbinate was found as 75.3% in the present study, which is a high rate compared to the literature. The formation mechanism is concha bullosa has not been fully clarified and different theories have been put forward on the issue. According to "e vacua" theory, which is one of the most known of these theories, after the formation of NSD, the cavity on the opposite side of the deviation and the turbulent airflow pattern of the nasal cavity predispose to the formation of concha bullosa.[21] In their study supporting this theory, Uzun and Savranlar. Examined the CT images of a series consisting of 10 cases and reported that the prevalence of concha bullosa increased in cases with advanced NSD.[22] However, there is also strong evidence that incidence of concha bullosa does not change with the degree of NSD.[3,8]

In the present study, findings contrary to this theory were found. Similar NSD angle was found in patients with bilateral high PTV and in patients who were not found to have any pneumatized concha. In addition, higher pneumatization volume was found in right concha than the left when NSD was higher in the right side. These findings suggest no relationship between NSD and pneumatized turbinate. This is thought to be due to the small size of some pneumatization found in images brought to the orthogonal plane by using MDCT, which cannot be associated with NSD.

In literature, the frequency of unilateral and bilateral concha bullosa is very close. Bilateral concha bullosa rate has been reported as 45%–61.5%.[23] In a study conducted by Erkuş and Turan, on 150 patients, concha bullosa was found in 22 (15.1%) patients, 10 of these were unilateral, while 12 were bilateral.[24] In this study, the rates were similar with 39.7% unilateral and 35.6% bilateral pneumatized concha.

Table 7: Kruskall-Wallis *H*-test between nasal septum deviation direction and variables

Test	PTV	SDA	R-MSV	L-MSV	R-MPA	L-MPA	IAD	MSD
χ^2	4.336	0.007	3.807	2.549	0.200	0.490	0.139	2.144
df	2	1	2	2	2	2	2	2
Asymptotic significance	0.114	0.933	0.149	0.280	0.905	0.783	0.933	0.342

PTV: Pnomatized turbinate volume, SDA: Septal deviation angle, R-MSV: Right maxillar sinüs volume, L-MSV: Leftmaxillar sinüs volume, R-MPA: Right maxillo palatal angle, L-MPA: Left maxillo palatal angle, IAD: Inter alveollar distance, MSD: Maxillary spin distance

The fact that it is seen bilaterally seems to support the thesis that concha bullosa formation is independent from NSD.

In their study conducted on 146 patients, Subramanian *et al*. found 49.5% concha bullosa and they reported that it was statistically higher in women (66%) when compared with men.[25] In the present study, concha bullosa was found to be almost equal in women and men.

The fact that there are such big differences in concha bullosa rates in many studies in literature can be explained with racial differences in populations of the studies, criteria differences for pneumatization, and sensitivity of analysis methods. The criteria prescribed for pneumatization can vary between researchers. While low pneumatization rates indicate only large concha bullosa, high rates may include pneumatization observed in any degree. Pneumatization may also be affected by the sensitivity of analysis methods.[26]

In this study, images brought to orthogonal position on 3 planes were studied using MDCT. A higher rate of concha bullosa may have been obtained when compared with previous studies, since it is possible to evaluate even the smallest pneumatization in this way.

Relatively low number of cases can be shown as the limitation of the study. In addition, since the anatomical effect of pneumatized concha on other maxillofacial parameters constituted the main subject of the study, an evaluation covering the clinical findings was not made.

Conclusion

While the highest incidence found so far in studies conducted with MDCT images were found in the present study with a pneumatized turbinate rate of 75.3%, it was also found that total PTV did not have an effect on NSD amount, MSV, and maxillopalatal parameters. It was found that men had higher curvature rates in the nasal septum, higher maxillary sinus aeration, and a larger IAD. Larger studies are needed to understand the relationship of paranasal sinus structures with each other and their clinical effect.

Financial support and sponsorship

Nil.

Conflicts of interest

There are no conflicts of interest.

References

1. Bolger WE, Butzin CA, Parsons DS. Paranasal sinus bony anatomic variations and mucosal abnormalities: CT analysis for endoscopic sinus surgery. Laryngoscope 1991;101:56-64.
2. İla K, Yilmaz N, Öner S, Başaran E, Öner Z. Evaluation of superior concha bullosa by computed tomography. Surg Radiol Anat 2018;40:841-6.
3. Uygur K, Tüz M, Doğru H. The correlation between septal deviation and concha bullosa. Otolaryngol Head Neck Surg 2003;129:33-6.
4. Kantarci M, Karasen RM, Alper F, Onbas O, Okur A, Karaman A. Remarkable anatomic variations in paranasal sinus region and their clinical importance. Eur J Radiol 2004;50:296-302.
5. Stallman JS, Lobo JN, Som PM. The incidence of concha bullosa and its relationship to nasal septal deviation and paranasal sinus disease. AJNR Am J Neuroradiol 2004;25:1613-8.
6. Hatipoğlu HG, Cetin MA, Yüksel E. Concha bullosa types: Their relationship with sinusitis, ostiomeatal and frontal recess disease. Diagn Interv Radiol 2005;11:145-9.
7. Zinreich SJ, Mattox DE, Kennedy DW, Chisholm HL, Diffley DM, Rosenbaum AE. Concha bullosa: CT evaluation. J Comput Assist Tomogr 1988;12:778-84.
8. Aktas D, Kalcioglu MT, Kutlu R, Ozturan O, Oncel S. The relationship between the concha bullosa, nasal septal deviation and sinusitis. Rhinology 2003;41:103-6.
9. Al-Qudah M. The relationship between anatomical variations of the sino-nasal region and chronic sinusitis extension in children. Int J Pediatr Otorhinolaryngol 2008;72:817-21.
10. Aktuna Belgin C, Colak M, Adiguzel O, Akkus Z, Orhan K. Three-dimensional evaluation of maxillary sinus volume in different age and sex groups using CBCT. Eur Arch Otorhinolaryngol 2019;276:1493-9.
11. Orhan İ, Soylu E, Altın G, Yılmaz F, Çalım ÖF, Örmeci T. Analysis of anatomic variations of paranasal sinus by computed tomography. Abant Medical Journal 2014;3:145-9.
12. Javadrashid R, Naderpour M, Asghari S, Fouladi DF, Ghojazadeh M. Concha bullosa, nasal septal deviation and paranasal sinusitis; a computed tomographic evaluation. B-ENT 2014;10:291-8.
13. Kim YM, Rha KS, Weissman JD, Hwang PH, Most SP. Correlation of asymmetric facial growth with deviated nasal septum. Laryngoscope 2011;121:1144-8.
14. Cengiz C, Hanifi B, Ercan A, Yasar C. Assessment of the relationship between palatum durum and maxillary bone in patients with nasal polyp, chronic sinusitis or septum deviation. Indian J Otolaryngol Head Neck Surg 2013;65:421-5.
15. Holton NE, Yokley TR, Figueroa A. Nasal septal and craniofacial form in European- and African-derived populations. J Anat 2012;221:263-74.
16. Sapmaz E, Kavaklı A, Sapmaz HI, Ögetürk M. Impact of hard palate angulation caused by septal deviation on maxillary sinus volume. Turk Arch Otorhinolaryngol 2018;56:75-80.

17. Kucybała I, Janik KA, Ciuk S, Storman D, Urbanik A. Nasal septal deviation and concha Bullosa – Do they have an impact on maxillary sinus volumes and prevalence of maxillary sinusitis? Pol J Radiol 2017;82:126-33.
18. Al-Rawi NH, Uthman AT, Abdulhameed E, Al Nuaimi AS, Seraj Z. Concha Bullosa, nasal septal deviation, and their impacts on maxillary sinus volume among Emirati people: A cone-beam computed tomography study. Imaging Sci Dent 2019;49:45-51.
19. Shetty SR, Al Bayatti SW, Al-Rawi NH, Kamath V, Reddy S, Narasimhan S, *et al.* The effect of concha bullosa and nasal septal deviation on palatal dimensions: A cone beam computed tomography study. BMC Oral Health 2021;21:607.
20. Kucur C, Erdoğan O, Sermin T, Şanal B, Özkan M, Yıldırım N. Giant concha bullosa pyocele. Cumhuriyet Medical Journal 2014;36:256-60.
21. Stammberger H, Posawetz W. Functional endoscopic sinus surgery. Concept, indications and results of the Messerklinger technique. Eur Arch Otorhinolaryngol 1990;247:63-76.
22. Uzun L, Savranlar A. Pneumatization of the Middle Turbinate: A Computed Tomography Study in 140 Patients. Journal of ear nose throat and head neck surgery 2004;12:2:54-8.
23. Unlü HH, Akyar S, Caylan R, Nalça Y. Concha bullosa. J Otolaryngol 1994;23:23-7.
24. Erkuş S, Kaya T, Turan T. Choncha Bullosa (Pneumatized Middle Turbinate). Turk Arch Otorhinolaryngol 1992;30:220-4.
25. Subramanian S, Lekhraj Rampal GR, Wong EF, Mastura S, Razi A. Concha bullosa in chronic sinusitis. Med J Malaysia 2005;60:535-9.
26. Havas TE, Motbey JA, Gullane PJ. Prevalence of incidental abnormalities on computed tomographic scans of the paranasal sinuses. Arch Otolaryngol Head Neck Surg 1988;114:856-9.

Original Article

Anatomical Evaluation of Sphenoid Sinus, Foramen Rotundum, and Vidian Canal for Ventrolateral Skull Base Surgery: A Radiological Study

Eda Duygu Ipek, Nazli Gulriz Ceri, Zehra Seznur Kasar

Department of Anatomy, Faculty of Medicine, Aydin Adnan Menderes University, Aydin, Turkey

Abstract

Introduction: We aimed to evaluate the pneumatization of the sphenoid sinus (SS) and configuration of the vidian canal (VC) and foramen rotundum (FR). **Materials and Methods:** This study was performed on a total of 259 coronal and sagittal computed tomography (CTs) scans that we divided into rhinosinusitis (RS), nasal septum deviation (NSD), nasal polyposis (NP), and control (C) groups. We performed various morphometric measurements on CTs and evaluated the SS pneumatization and the position and protrusion of the FR and VC. **Results:** The mean age was found to be 42.42 ± 1.28 and 44.06 ± 1.45 in 149 males and 110 females, respectively. Significant differences were found among all morphometric measurements in the right and left side measurements and between genders except for the distance between VC and FR on both sides. The rotundum angle and bilateral VC distance values were found to be high in the NP and NSD groups. There was a difference in the distribution of categorical data between patient groups. We found prevalence of the FR and VC Type I as 3.3% and 13.3%, Type II as 35.5% and 43.65%; Type III as 61.2% and 43.05%, respectively. The position of FR was medial in 45.15%, online in 35.95%, and lateral in 18.9% of cases and SS pneumatization with lateral recess in 41.6%, tangent in 16.7%, and less pneumatized in 41.7% of cases in total. **Discussion and Conclusion:** Our findings show that the configuration of the structures, which are important anatomical landmarks for ventrolateral skull base surgery, changes in patients with anatomical variations and inflammatory sinonasal diseases.

Keywords: *Foramen rotundum, Sphenoidal sinus, transpterygoid surgery, vidian canal*

Introduction

Endoscopic endonasal transsphenoidal approach (EETA) is widely used in the surgery of ventral skull base lesions,[1] because it eliminates the need for manipulation and retraction of critical neurovascular structures concerning the sphenoid sinus (SS),[1] accelerates the postoperative recovery process, and significantly reduces the risk of complications.[2-4] The configuration and the degree of pneumatization of the SS play a key role in planning how to access the targeted area.[5-8] A wide pneumatized SS provides an advantage for surgical manipulation and access to a wider area, but the protrusion of neurovascular structures passing through the vidian canal (VC) and foramen rotundum (FR) into the SS increase with the extent of pneumatization.[2,3,5,8-13]

SS pneumatization is classified according to the sagittal plane traditionally,[3,14,15] and anatomical variations of the carotid artery and optic canal, which are used as landmarks in anterior skull base surgeries, have been investigated in many studies. However, there are very few studies examining the SS pneumatization according to coronal plane and evaluating the anatomical structures located on the sinus floor. In the coronal plane, EETA allows access to the Meckel's cave, the middle third of the clivus, petrous apex, the middle cranial fossa, parapharyngeal space, sinus cavernosus, and infratemporal fossa. The transpterygoid approach which allows wide observation of this area is frequently used to access the ventrolateral skull base with endoscopic surgery.[1] The VC is a consistent and reliable anatomical landmark for detecting the anterior genu of petrous internal carotid artery at the transition point from the horizontal segment to the vertical paraclival segment in ventrolateral skull base surgeries.[1,13,16] Furthermore, if the SS does not show a lateral recess pneumatization, the bone between the VC and the FR must be drilled.[3] After bone drilling, the

How to cite this article: Ipek ED, Ceri NG, Kasar ZS. Anatomical evaluation of sphenoid sinus, foramen rotundum, and vidian canal for ventrolateral skull base surgery: A radiological study. J Anat Soc India 2023;72:15-21.

Article Info

Received: 07 January 2022
Revised: 11 August 2022
Accepted: 13 September 2022
Available online: 24 March 2023

Address for correspondence:
Dr. Eda Duygu Ipek, Department of Anatomy, Faculty of Medicine, Aydin Adnan Menderes University, Efeler 09010, Aydin, Turkey.
E-mail: eda.cakir@adu.edu.tr

Access this article online

Website: www.jasi.org.in
DOI: 10.4103/jasi.jasi_6_22
Quick Response Code:

dural opening is started from the FR, and the maxillary nerve is followed toward to the Meckel's cave to protect the abducens nerve.[1] FR individualization is difficult and requires an understanding of its anatomical relationships.[16] Therefore, the lateral extension of the SS pneumatization and the position of the FR and the VC are very important in ventrolateral surgical approaches to the skull base.[1,12,17] On the other hand, anatomical variations and diseases of the paranasal sinuses and nasal cavity are frequently encountered in clinical practice.[18] Although anatomical variations have been reported to vary depending on gender, age, and ethnicity, most of these have also been associated with the etiopathogenesis of inflammatory sinonasal diseases. Nasal septum deviation (NSD) is the most common anatomical variant of the paranasal sinuses and nasal cavity.[5] Poorey and Gupta[15] reported that there is a relationship among inflammatory paranasal sinus diseases, middle turbinate abnormalities, and enlarged ethmoid bulla on the contralateral side with an increased angle of septal deviation. According to Kaya *et al.*,[18] anatomic variations accompanying NSD result in chronic rhinosinusitis (RS). Akgül *et al.*[11] reported that the SS cavity was divided asymmetrically in patients with septal deviation, and Orhan *et al*.[5] found that the volume of the SS was smaller on the side of the nasal septal deviation. Anatomical variations often disrupt the aeration of the paranasal sinuses, causing chronic RS and nasal polyps defined as inflammatory growths of the sinonasal tissue. Increasing awareness of these variations plays an important role not only in diagnosis but also in reducing intraoperative difficulties and postoperative complications and elucidating the pathogenesis of processes that may occur in the sinus cavity.[4,8,18] In this study, we aimed to evaluate SS pneumatization on the coronal plane and position of FR and VC between genders and patient groups with septal deviation, chronic RS, and nasal polyposis (NP).

Materials and Methods

This is a prospective, cross-sectional study of patients who underwent the head computed tomography (CT) scan at Radiology Department of Aydin Adnan Menderes University Practice and Research Hospital in Aydin, Turkey. This study was approved by the Institutional Ethics Committee with the approval protocol number of 2018/1486. CT scans of paranasal sinuses and nasal cavity were performed with Toshiba Aquilion 150 slice CT scanner (Toshiba Medical Systems, Otawara, Japan) of contiguous coronal and sagittal cuts of 2-mm slice thickness (scan setting; tube voltage 120 kV, effective 270 mAs and 0,75 pitch). We searched our radiology database for 2 years (November 2018–November 2020). One hundred and twenty-eight patients diagnosed with a sinonasal disease that cannot be detected on CT scans (for example, nasal dripping, anosmia, and allergic rhinitis), history of maxillofacial trauma including fractures, skull base pathology, head and neck tumors, previous surgery history, and younger than 20 years, and sagittal CT scans with haziness of SS ostium were excluded from this study among a total of 387 CT scans.

A total of 259 patients using CT scans in this study were classified as follows: RS group (RS group, n = 66) with chronic RS radiological findings reported by Kaya *et al.*,[18] NP group (NP group, n = 63) with polyps in the nasal cavity on CT scans, and NSD group (NSD group, n = 64) determined according to Orhan *et al.*[5] criteria. Patients without sinonasal disease classified as control group (C group, n = 66). We performed the morphometric measurements are shown in Figures 1 and 2 and the assessment of the FR, VC position, and the SS pneumatization as indicated in Figure 3 with Sectra 18.2 (Linköping, Sweden) radiological imaging and image analysis program. In coronal CT scans, the distance between the right and left FR (FRL) [CE line in Figure 1], the distance between the right FR (FRr) and the FRl to the midline [CB, CE lines in Figure 1], the distance between the right and left VC (VCL) [DF line in Figure 1], and the distance between the FR and the VC on the right (VCFRr) and left sides (VCFRl) [DC, FE lines in Figure 1] were measured. The angulation of the FR (VCFRAr and VCFRAl on the right and left sides, respectively) assessed by measuring the angle between two lines; first line is extending from FR to VC [H line in Figure 1] and the other is vertical line [G line in Figure 1] passing through VC. On the sagittal CT scans, the distance from nasal floor, in other words, the posterior end of the palatum durum, to the floor [National Science Foundation; AD line in Figure 2], orificium [NSO; AB line in Figure 2], and roof [National Skills Registry (NSR); AC line in Figure 2] of the SS anterior wall were measured. We evaluated the pneumatization degree of SS, position of the FR and VC protrusion into the SS cavity and classified the FR with respect to the lateral pterygoid plate (Lpp).

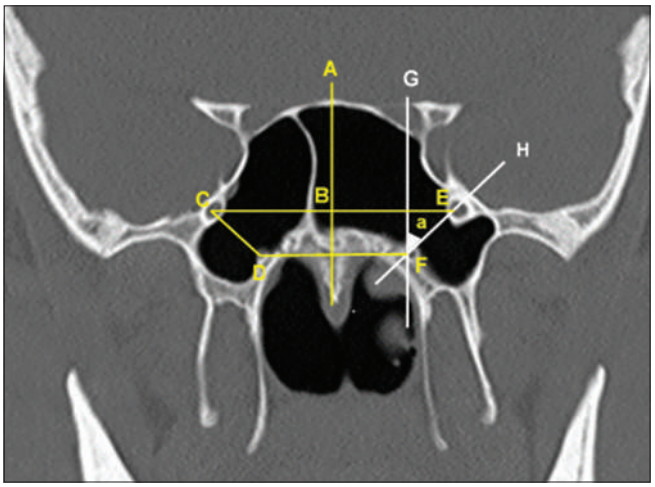

Figure 1: A; imaginary midline, CB, BE; FRr, FRl distance, CE; FRL distance, DF; VCL distance, a; FR angulation between G and H lines. FR: Foramen rotundum, VCL: Vidian canal left, FRL: Foramen rotundum left, FRr: Foramen rotundum right

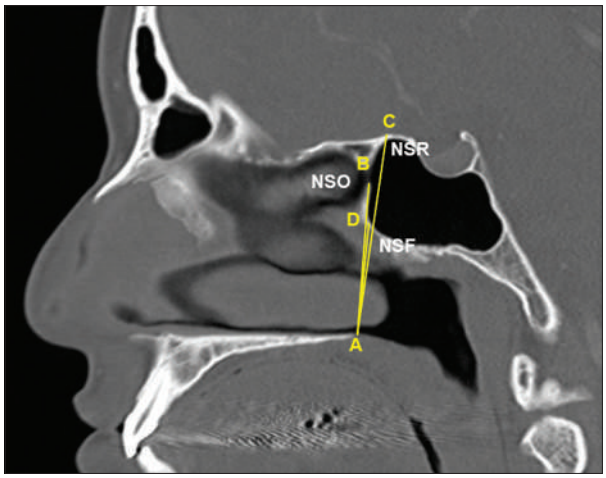

Figure 2: Sagittal CT image showing AB, AC, AD; distance from the posterior end of the palatum durum to the sphenoid orifice, roof and floor of anterior wall of sphenoid sinus, respectively. CT: Computed tomography

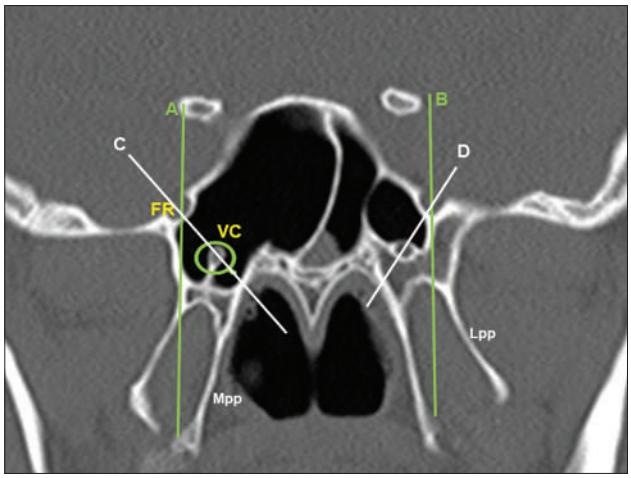

Figure 3: A coronal CT image showing the evaluation of FR, VC position, and SS pneumatization. Mpp: medial pterygoid plate, Lpp: Lateral pterygoid plate. CT: Computed tomography, FR: Foramen rotundum, VC: Vidian canal, SS: Sphenoid sinus

Lateralization of FR according to imaginary line descending perpendicularly from FR [A and B lines in Figure 3]:

- Medial– When the imaginary line is medial to the base of the Lpp
- Online– When the imaginary line intersects with the base of the Lpp
- Lateral– When the imaginary line is lateral to the base of the Lpp.

We defined FR and VC according to their protrusion into the SS cavity:

- Type I FR or VC– When FR or VC is located completely in the SS cavity
- Type II FR or VC– When FR or VC is partially protruding into the SS cavity or tangent
- Type III FR or VC– When FR or VC is embedded in the sphenoid bone.

SS pneumatization according to the imaginary line connecting the centers of FR and VC [C and D lines in Figure 3]:

- Lateral recess– If the SS is pneumatized lateral to the imaginary line
- Tangent– If the SS tangent to the imaginary line
- Less pneumatized– If the imaginary line passes through the sphenoid bone.

Statistical Package for Social Sciences (Version 22.0, SPSS Inc., Chicago, IL, USA) software was used in the statistical analysis. The normality of variables was evaluated by the Kolmogorov–Smirnov test. According to results, parametric variables are expressed as mean ± standard deviation and nonparametric variables expressed as median value. Differences between genders, right and left sides were evaluated using Student's *t*-test, Mann–Whitney *U*-test, paired *t*-test, and Wilcoxon, respectively. One-way ANOVA, Tukey, Games-Howell *post hoc* tests, Kruskal–Wallis test, and *post hoc* Dunnett's T3 test were used in patient groups. The Pearson's Chi-square test was used to determine the differences of categorical variables expressed by frequency (n) and ratio (%) between patient groups and genders. Fisher's exact test was used in the evaluation of only FR position, since the minimum expected count values were >5 in patient groups and between genders.

Results

Coronal and sagittal CT scans of 259 patients, 149 males (57.5%) and 110 females (42.5%), were used in this study, and the mean age was found to be 42.42 ± 1.28 for males and 44.06 ± 1.45 for females. A significant difference was found in all quantitative values except for VCFRr and VCFRl between genders. The differences, mean, and median values of the morphometric parameters between the genders, right and left sides are shown in Tables 1 and 2.

The statistical differences in patient groups that we formed as chronic RS group (RS, 32 males and 34 females), NSD group (NSD, 41 males and 23 females), NP group (47 males and 16 females), and control group (29 males and 37 females) are given in Table 3.

The frequency and ratio values of the categorical variables in the patient groups and between the genders are given in Tables 4 and 5. According to Chi-square and Fisher's exact test results, FR, VC, and SS pneumatization types differed significantly in patient groups.

Discussion

In the present study, the FRL distance was found significantly higher in males than in females, consistent with the findings of Inal *et al*.[16] However, our mean FRL value is slightly lower compared to Mohebbi *et al*.[17] mean value of 38.48 ± 3.87 and Inal *et al*.[16] mean values of 35.22 ± 3.68 mm in females and 37.20 ± 3.86 mm in males. In the studies of Inal *et al*.[16] and Mohebbi

et al.,[17] CTs of patients with RS, nasal septal deviation, and NP were excluded; therefore, their FRL values may be higher than ours. Because, it is seen that the lowest FRL value in our study was detected in RS group ($P < 0.05$), and the mean FRL values were lower in the NP and NSD groups compared to the C group in Table 3. Furthermore, Mohebbi *et al.*[17] reported the total average value of males and females regardless of gender. In the present study, FRr and FRl were found to be statistically higher in males consistent with the findings of Serindere *et al.*,[8] Mohebbi *et al.*,[17] and Awadalla *et al.*[9] values of FRr as 19.00 ± 2.07, 20.06 ± 2.38 and values of FRl as 19.34 ± 2.17, 19.8 ± 1.4 on the right and left sides, respectively, significantly different from each other similarly our results. Prabu *et al.*[12] reported the FRr value as 17.06 ± 0.2, FRl as 18.9 ± 0.2 mm, and they found the FRl was significantly higher than the right side. However, we found the FRr value to be significantly higher compared to FRl value. Table 5 shows that lateral FR was found more on the right side in both genders in our study. While our FRL and FRr values differed significantly between the patient groups, the FRl value did not differ. In Table 4, it is seen that the medial, online, and lateral positions of the FR differed in the patient groups on the right side, but not on the left side. We found a significant difference in the distance between the VCL between genders consistent with Inal *et al.*[16] finding. Inal *et al.*[16] reported the VCL value as 25.04 ± 3.22 mm in males and 22.82 ± 3.10 mm in females; these results are higher than our VCL values. Although our FRL, FRr, and FRl measurements were found to be significantly higher in males, we did not find a significant difference between VCFRl and VCFRr between genders and patient groups too. However, we found a significant difference in our VCFRr and VCFRl values between the right and left sides contrary to Papavasileiou *et al.*[2] and Mohebbi *et al.*[17] findings. Papavasileiou *et al.*[2] VCFRr value of 6.2 mm (range 0.5–11 mm) and VCFRl value of 6.7 mm (range 0.4–12 mm), Serindere *et al.*[6] VCFRr value of 6.36 ± 2.42 and 5.89 ± 2 and VCFRl value of 6.54 ± 2.17 and 6.54 ± 1.75 in females and males, respectively, are closer to our control grou*P* value than Mato *et al.*[20] reported VCFRr value as 6.5 (1–13) and VCFRl as 7.2 (1–15.7). Mohebbi *et al.*[17] VCFRr

Table 1: Student *t*-test and Mann-Whitney *U*-test results between genders

	Male (*n*=149)	Female (*n*=110)	*P*
FRL	35.81±3.3	34.39±3.92	0.002
FRr	17.87±1.81	17.23±2.05	0.008
FRl	17.59±2.07	16.83±2.17	0.004
VCL	20.5 (15-27.3)	18.5 (13.09-26.74)	0.001
VCFRr	4.53±0.16	4.64±0.18	0.639
VCFRl	4.2 (0.95-8.3)	4.5 (1.21-7.89)	0.678
VCFRAr	74.56±3.54	60.81±3.04	0.004
VCFRAl	83.95±3.37	64.79±3.18	0.001
NSF	27.33±3.3	25.44±2.95	0.001
NSO	36.67±3.32	35.52±3.31	0.007
NSR	47.62±3.45	44.71±3.32	0.001

FR: Foramen rotundum, FRl: FR left, FRr: FR right, VC: Vidian canal, VCL: VC left, VCFRr: VCFR right, VCFRl: VCFR left, VCFRAr: VCFR angulation right, VDFRAl: VCFR angulation left, NS: Nasal septum, NSF: NS floor, NSO: NS orificium, NSR: NS roof

Table 2: Comparison of right and left measurements with paired *t*-test and Wilcoxon test (*n*=259)

Measurements	Descriptive values	*P*
FRr	17.6±0.12	0.006
FRl	17.27±0.13	
VCFRr	4.5 (1.6-8.3)	0.001
VCFRl	4.08±0.12	
VCFRAr	53.4 (24.2-140.5)	0.001
VCFRAl	58 (33.5-142)	

FR: Foramen rotundum, FRl: FR left, FRr: FR right, VC: Vidian canal, VCFRr: VCFR right, VCFRl: VCFR left, VCFRAr: VCFR angulation right, VDFRAl: VCFR angulation left

Table 3: Mean±standard deviation and median values of patient groups

	RS group (*n*=66)	NP group (*n*=63)	NSD group (*n*=64)	C group (*n*=66)	*P*
FRL	34.08±0.4$^{‡,|,||}$	35.8±0.47†	35.83±0.46†	36.16±0.44	0.019
FRr	16.91±0.22$^{‡,|}$	18.1±0.26†	18.05±0.22†	17.39±0.22	0.001
FRl	16.81±0.23	17.54±0.28	18.49±0.28	17.24±0.26	0.192
VCL	19.65$^{||}$	20.9	21.05$^{||}$	18.3$^{‡,|}$	0.000
VCFRr	4.7	4.1	4.9	5.65	0.425
VCFRl	4.13±0.22	3.82±0.21	4.27±0.29	5.1±0.24	0.636
VCFRAr	48.15 $^{‡,|,||}$	110.6$^{†,||}$	110.15$^{†,||}$	51.45$^{†,‡,|}$	0.000
VCFRAl	49.45$^{‡,|,||}$	128.7$^{†,||}$	114.6$^{†,||}$	54.9$^{†,‡,|}$	0.000
NSF	26.66±0.42	26.89±0.41	26.42±0.41	26.15±0.39	0.614
NSO	36.52±0.45	35.51±0.39	36.07±0.41	36.59±0.39	0.237
NSR	45.45±0.44$^{‡,|}$	47.39±0.55†	46.99±0.46	45.77±0.31	0.006

†As compared to RS group, ‡As compared to NP group, $^{|}$As compared to NSD group, $^{||}$As compared to C group statistically different (P<0.05). RS: Rhinosinusitis, NP: Nasal polyposis, NS: Nasal septum, NSD: NS deviation, C: Control, FR: Foramen rotundum, FRl: FR left, FRr: FR right, VC: Vidian canal, VCL: VC left, VCFRr: VCFR right, VCFRl: VCFR left, VCFRAr: VCFR angulation right, VDFRAl: VCFR angulation left, NSF: NS floor, NSO: NS orificium, NSR: NS roof

Table 4: Pearson's Chi-square and Fisher's exact test (*) results according to patient groups, ratio, and *n* values of categorical variables

Type of anatomical structure	RS (*n*=66)		NP (*n*=63)		NSD (*n*=64)		C (*n*=66)		*P*
	Right, *n* (%)	Left, *n* (%)	Right, *n* (%)	Left, *n* (%)	Right, *n* (%)	Left, *n* (%)	Right, *n* (%)	Left, *n* (%)	Right-left
Medial FR	32 (48.5)	33 (50)	22 (34.9)	27 (42.9)	18 (28.1)	29 (45.3)	33 (50)	40 (60.6)	0.003-0.297
Online FR	21 (31.8)	21 (31.8)	33 (52.4)	28 (44.4)	29 (45.3)	24 (37.5)	14 (21.2)	16 (24.2)	0.003-0.297
Lateral FR	13 (19.7)	12 (18.2)	8 (12.7)	8 (12.7)	17 (26.6)	11 (17.2)	19 (28.8)	10 (15.2)	0.003-0.297
Type I FR	2 (3)	2 (3)	4 (6.3)	3 (4.8)	1 (1.6)	1 (1.6)	2 (3)	2 (3)	0.001-0.002*
Type II FR	13 (19.7)	13 (19.7)	31 (49.2)	26 (41.3)	32 (50)	34 (53.1)	18 (27.3)	17 (25.8)	0.001-0.002*
Type III FR	51 (77.3)	51 (77.3)	28 (44.4)	34 (54)	31 (48.4)	29 (45.3)	46 (69.7)	47 (71.2)	0.001-0.002*
Type I VC	6 (9.1)	7 (10.6)	8 (12.7)	7 (11.1)	13 (20.3)	11 (17.2)	8 (12.1)	9 (13.6)	0.001-0.001
Type II VC	19 (28.8)	18 (27.3)	32 (50.8)	35 (55.6)	35 (54.7)	37 (57.8)	23 (34.8)	27 (40.9)	0.001-0.001
Type III VC	41 (62.1)	41 (62.1)	23 (36.5)	21 (33.3)	16 (25)	16 (25)	35 (53.1)	30 (45.5)	0.001-0.001
Lateral recess	22 (33.3)	21 (31.8)	28 (44.4)	26 (41.3)	35 (54.7)	32 (50)	26 (39.4)	25 (37.9)	0.058-0.024
Tangent	10 (15.2)	8 (12.1)	15 (23.8)	18 (28.6)	6 (9.4)	10 (15.6)	9 (13.6)	11 (16.7)	0.058-0.024
Less pneumatized	34 (51.5)	37 (56.1)	20 (31.7)	19 (30.2)	23 (35.9)	22 (34.4)	31 (47)	30 (45.5)	0.058-0.024

RS: Rhinosinusitis, NP: Nasal polyposis, NS: Nasal septum, NSD: NS deviation, C: Control, VC: Vidian canal, FR: Foramen rotundum

Table 5: Pearson's Chi-square and Fisher's exact test (*) results according to genders, ratio, and *n* values of categorical variables

Type of anatomical structure	Male (*n*=149)		Female (*n*=110)		*P*
	Right, *n* (%)	Left, *n* (%)	Right, *n* (%)	Left, *n* (%)	Right-left
Medial FR	59 (39.6)	75 (50.3)	46 (41.8)	54 (49.1)	0.325-0.658
Online FR	61 (40.9)	53 (35.6)	36 (32.7)	36 (32.7)	0.325-0.658
Lateral FR	29 (19.5)	21 (14.1)	28 (25.5)	20 (18.2)	0.325-0.658
Type I FR	7 (4.7)	6 (4)	2 (1.8)	2 (1.8)	0.219-0.072*
Type II FR	58 (38.9)	59 (39.6)	36 (32.7)	31 (28.2)	0.219-0.072*
Type III FR	84 (56.4)	84 (56.4)	72 (65.5)	77 (70)	0.219-0.072*
Type I VC	19 (12.3)	19 (12.8)	16 (14.5)	15 (13.6)	0.696-0.911
Type II VC	66 (44)	69 (46.3)	43 (39.1)	48 (43.6)	0.696-0.911
Type III VC	64 (43.7)	61 (40.9)	51 (46.4)	47 (42.8)	0.696-0.911
Lateral recess	64 (43)	62 (41.6)	47 (42.7)	42 (38.2)	0.526-0.849
Tangent	26 (17.4)	26 (17.4)	14 (12.8)	21 (19.1)	0.526-0.849
Less pneumatized	59 (39.6)	61 (41)	49 (44.5)	47 (42.7)	0.526-0.849

VC: Vidian canal, FR: Foramen rotundum

value of 8.16 ± 2.27 and VCFRl value of 9.20 ± 2.15 are considerably higher than our average values. The most striking difference in morphometric parameters is in our VCFRAr and VCFRAl values were considerably higher in the NP and NSD groups compared to C and RS groups; therefore, our mean rotundum angle values between genders and sides are higher than the findings of Mohebbi *et al.*,[17] Papavasileiou *et al.*,[2] and Serindere *et al.*[6] Vaezi *et al.*[3] reported that the increase in the distance between the VC and the FR was associated with the pneumatization of the lateral recess of the SS which was evaluated by the depth of the lateral recess; however, pneumatization was not related to the rotundum angle and gender. Acar *et al.*[21] reported the distance between VC and FR in cases with lateral recess pneumatization as 9.6 ± 2.1, which was significantly higher than the mean value of 7.2 ± 2.0 in patients without lateral recess pneumatization, and Prabu *et al.*[12] reported that there was no significant difference between the distance of the VC to the midline on both sides, but FRr and FRr values were significantly higher in patients with lateral recess pneumatization. The high rotundum angle may be affected mainly by the lateralization of the FR. This may be due to the high rotundum angle value in the NSD group with the most lateral recess pneumatization and higher FRr and FRl values. The higher rotundum angle in the NSD group may be due to the higher FRr and FRl values and the percentage of lateral pneumatization. However, lateral FR was found to be different only on the right side and was the lowest in the NP group with a high rotundum angle, whereas SS pneumatization was different only on the left side and VCFR was not different in patient groups anyway. Furthermore, the average value of all the morphometric measurements, which were performed on the anterior wall of the SS on sagittal CTs in this study, was significantly higher in males; in the patient groups, only the NSR was found to be lower in the RS group than NP

and NSD groups. This finding may indicate that the SS was also enlarged anterosuperiorly in the NP and NSD groups. Supporting this, Akgül *et al*.[11] reported that most of the cases with NSD showed presellar-type pneumatization; however, Famurewa *et al*.[19] reported the rate of lateral recess pneumatization as 45.1% and detected it only in cases with sellar- and postsellar-type pneumatization. It is reported that a positive correlation between right and left hemisinus pneumatization and affects bone aeration in all directions, thus coronal and sagittal pneumatization are also interrelated.[3] We agree with Vaezi *et al*.[3] finding that pneumatization is not related to the rotundum angle; however, it is clear from our findings that there are different factors affecting the configuration of FR and VC in the NP and NSD groups.

While the prevalence of categorical data differed significantly between patient groups, there was no significant difference found in any of them between genders. In this study, medial, online, and lateral FR were detected in 45.15%, 35.95%, and 18.9%, respectively, in total, and FR position frequency was significantly different on the right side between patient groups. Compared to the findings of Mohebbi *et al*.,[17] our online FR values are less and our lateral FR values are quite high. Serindere *et al*.[6] found a significant difference between the online FR and the medial and lateral FR according to genders unlike our findings. SS pneumatization was found as a lateral recess in 41.6%, tangent in 16.7%, and less pneumatized in 41.7% in our study. Mohebbi *et al*.[17] and Vaezi *et al*.[3] were categorized to be lateral recess in 54%, 36.5%, tangent 26%, 39%, and less pneumatized 20%, 24.5%, respectively. Parvathy[22] detected the lateral recess ratio as 50.7%, and similar to our findings, did not find any difference between males and females. We found the prevalence of the VC and FR Type I as %13.3, %3.3, Type II as 43.65%, 35.5%, and Type III as 43.05%, 61.2%, respectively. Rahmati *et al*.[10] found lateral recess as 38.9% and reported that VC and FR protruding partially or completely into the sinus cavity were mostly detected in these cases. Prabu *et al*.[12] also reported that protrusion of FR and VC into the SS cavity increased in patients with lateral pneumatization. Acar *et al*.[21] detected a lateral recess in 72.4% of Type II VC cases. Similarly, Lakshman *et al*.,[14] who stated that there was a relationship between lateral recess pneumatization and VCl types, also reported that the lateral recess frequency as 54.8%, and Type II VC was found as a common configurations in their study. Consistent with these findings, it can be said that Type II FR and Type II VC are more common configurations in NP and NSD groups with a higher lateral recess frequency. In addition, the Type 1 FR and VC were detected higher in the NP and NSD groups, respectively.

Conclusion

Although preoperative radiological evaluations play very important role in the planning of the surgical approach, they do not provide visualization of all elements, and also the knowledge of anatomical relations and variations provides a minimum level of operative risk. Our results show that inflammatory sinonasal diseases and anatomical variations change the configuration of important anatomical landmarks for ventrolateral skull base surgery. By classifying certain variations and diseases, more specific studies can increase awareness about postoperative complications, help understand the pathogenesis of nasal cavity and paranasal sinus diseases, and even provide the opportunity for early intervention.

Financial support and sponsorship

Nil.

Conflicts of interest

There are no conflicts of interest.

References

1. Oyama K, Tahara S, Hirohata T, Ishii Y, Prevedello DM, Carrau RL, *et al*. Surgical anatomy for the endoscopic endonasal approach to the ventrolateral skull base. Neurol Med Chir (Tokyo) 2017;57:534-41.
2. Papavasileiou G, Hajiioannou J, Kapsalaki E, Bizakis I, Fezoulidis I, Vassiou K. Vidian canal and sphenoid sinus: An MDCT and cadaveric study of useful landmarks in skull base surgery. Surg Radiol Anat 2020;42:589-601.
3. Vaezi A, Cardenas E, Pinheiro-Neto C, Paluzzi A, Branstetter BF 4th, Gardner PA, *et al*. Classification of sphenoid sinus pneumatization: Relevance for endoscopic skull base surgery. Laryngoscope 2015;125:577-81.
4. Yeğin Y, Çelik M, Altıntaş A, Şimşek BM, Olgun B, Kayhan FT. Vidian canal types and dehiscence of the bony roof of the canal: An anatomical study. Turk Arch Otorhinolaryngol 2017;55:22-6.
5. Orhan I, Ormeci T, Bilal N, Sagiroglu S, Doganer A. Morphometric analysis of sphenoid sinus in patients with nasal septum deviation. J Craniofac Surg 2019;30:1605-8.
6. Serindere G, Gunduz K, Avsever H. The measurement indexes and the relationships with adjacent structures of vidian canal and foramen rotundum using computed tomography. J Anat Soc India 2020;69:144-9.
7. Locatelli M, Di Cristofori A, Draghi R, Bertani G, Guastella C, Pignataro L, *et al*. Is Complex sphenoidal sinus anatomy a contraindication to a transsphenoidal approach for resection of sellar lesions? Case series and review of the literature. World Neurosurg 2017;100:173-9.
8. Štoković N, Trkulja V, Dumić-Čule I, Čuković-Bagić I, Lauc T, Vukičević S, *et al.* Sphenoid sinus types, dimensions and relationship with surrounding structures. Ann Anat 2016;203:69-76.
9. Awadalla AM, Hussein Y, ELKammash TH. Anatomical and radiological parameters of the sphenoid sinus among Egyptians and its impact on sellar region surgery. Egypt J Neurosurg 2015;30:1-12.
10. Rahmati A, Ghafari R, AnjomShoa M. Normal variations of sphenoid sinus and the adjacent structures detected in cone beam computed tomography. J Dent (Shiraz) 2016;17:32-7.
11. Akgül MH, Muluk NB, Burulday V, Kaya A. Is there a relationship between sphenoid sinus types, septation and symmetry; and septal deviation? Eur Arch Otorhinolaryngol

2016;273:4321-8.
12. Prabu SS, Veerapandian R, Prgadhees R, Pradeep S, Rajendran M. Neurovascular variations of sphenoid sinus: Impact on transsphenoidal surgery. Int J Sci Stud 2018;6:5-9.
13. Lakshman N, Viveka S, Thondupadath A, Fahad B. Anatomical relationship of pterygoid process pneumatization and vidian canal. Braz J Otorhinolaryngol 2020;88:303-8.
14. Tarabishia ME, Rabiea H, Youssef T, Elsharnouby M, Fawaz S, Nada I, *et al*. The transnasal endoscopic management of spontaneous cerebrospinal fluid rhinorrhea from the lateral recess of the sphenoid sinus. Egypt J Otolaryngol 2016;32:13-20.
15. Poorey VK, Gupta N. Endoscopic and computed tomographic evaluation of influence of nasal septal deviation on lateral wall of nose and its relation to sinus diseases. Indian J Otolaryngol Head Neck Surg 2014;66:330-5.
16. Inal M, Muluk NB, Arikan OK, Şahin S. Is there a relationship between optic canal, foramen rotundum, and vidian canal? J Craniofac Surg 2015;26:1382-8.
17. Mohebbi A, Rajaeih S, Safdarian M, Omidian P. The sphenoid sinus, foramen rotundum and vidian canal: A radiological study of anatomical relationships. Braz J Otorhinolaryngol 2017;83:381-7.
18. Kaya M, Çankal F, Gumusok M, Apaydin N, Tekdemir I. Role of anatomic variations of paranasal sinuses on the prevalence of sinusitis: Computed tomography findings of 350 patients. Niger J Clin Pract 2017;20:1481-8.
19. Famurewa OC, Ibitoye BO, Ameye SA, Asaleye CM, Ayoola OO, Onigbinde OS. Sphenoid sinus pneumatization, septation, and the internal carotid artery: A computed tomography study. Niger Med J 2018;59:7-13.
20. Mato D, Yokota H, Hirono S, Martino J, Saeki N. The vidian canal: Radiological features in Japanese population and clinical implications. Neurol Med Chir (Tokyo) 2015;55:71-6.
21. Açar G, Çiçekcibaşı AE, Çukurova İ, Özen KE, Şeker M, Güler İ. The anatomic analysis of the vidian canal and the surrounding structures concerning vidian neurectomy using computed tomography scans. Braz J Otorhinolaryngol 2019;85:136-43.
22. Parvathy P. Role of high-resolution computed tomography in the evaluation of anatomical variations of sphenoid sinus and its clinical importance in FESS. J Evol Med Dent Sci 2020;9:1874-80.

Original Article

Correlation of Some Anatomical Angles of the Shoulder with Rotator Cuff Syndrome

Busra Candan, Ebru Torun[1], Rumeysa Dikici, Seda Avnioglu, Mehmet Yalcin Gunal[2]

Departments of Anatomy, [1]Radiology and [2]Physiology, School of Medicine, Alanya Alaaddin Keykubat University, Alanya, Turkey

Abstract

Background: Shoulder movement occurs through the coordinated work of muscles, tendons, ligaments, and bones, primarily that affect the glenohumeral joint. Some distances and the angles between the bones forming this joint are important in shoulder pathologies. In this study, we aimed to determine the evaluation of nine different radiological parameters related to acromion and humerus in rotator cuff syndrome and control group patients. **Materials and Methods:** A total of 400 patients' routine clinic radiographs were retrospectively assessed, which have rotator cuff syndrome (n = 210), and control group (n = 190). We measured the critical shoulder angle (CSA), distance of glenoid-acromion (GA), distance of glenoid-humeral head (GH), acromial index, lateral acromial angle (LAA), total shoulder arthroplasty angle (TSA), reverse shoulder arthroplasty angle (RSA), Point T represents the superior border of the glenoid cavity, Point S represents the inferior border of the glenoid cavity, point R represents the intersection of the supraspinatus fossa line with the glenoid surface. RST angle, and greater tuberosity angle (GTA) angle. We determined the type of acromion. **Results:** We determined that the GH, TSA, RST, and GTA were significantly different between rotator cuff syndrome and control group patients. When we evaluated the acromion type, Type 2 was the most common type. Different from the literature, when we evaluated the relationship between acromion types and angles, we determined that LAA, GA, and TSA parameters were significantly different between acromion types. **Conclusions:** In this study, we determined the importance of measurements and angles in rotator cuff syndrome. We think that the relationship between acromion types and parameters can contribute to the literature. Moreover, we believe that our study will contribute to the literature in terms of gathering many angles that are important in shoulder pathologies in a single study.

Keywords: *Acromial index, acromion type, rotator cuff syndrome, shoulder joint*

Introduction

The humerus, scapula, and clavicula form the shoulder girdle. Also, the shoulder girdle consists of three main joints, the sternoclavicular joint, the acromioclavicular joint, and the glenohumeral joint. The glenohumeral joint is one of the most mobile joints in the body, and it is formed between the glenoid cavity of the scapula and humeral head.[1] It is frequently stated in the literature that the angles between the bones forming this joint are important in shoulder pathologies such as rotator cuff syndrome.[2] And, acromion morphology has been related to shoulder pathologies, and the shape of the acromion is among the primary causes of shoulder impingement; thus, various attempts have been made to classify acromion's morphologic appearance on standard radiographs.[3] Radiographs allow imaging of acromion anomalies, tendinitis, fractures, and neoplasms and diagnose impingement and shoulder pain.[1]

This study's primary purpose was to investigate the efficacy of angles between the scapula and humerus on the presence of rotator cuff syndrome on standard radiographs, as well as to identify the supporting literature for this conclusion.

Materials and Methods

This study was a retrospective, observational study, and it was carried out on 400 (200 male and 200 female) patients who attended to the hospital for various reasons and had shoulder radiographs between January 2018 and December 2020. This study was performed in line with the principles of the Declaration of Helsinki. This study was approved by the Non-Interventional Clinical Research Ethics Committee (Decision No. 2020:20–27).

How to cite this article: Candan B, Torun E, Dikici R, Avnioglu S, Gunal MY. Correlation of some anatomical angles of the shoulder with rotator cuff syndrome. J Anat Soc India 2023;72:22-8.

Article Info

Received: 15 November 2021
Revised: 29 August 2022
Accepted: 13 September 2022
Available online: 24 March 2023

Address for correspondence:
Dr. Busra Candan, Departments of Anatomy, School of Medicine, Alanya Alaaddin Keykubat University, Alanya, Turkey.
E-mail: busra.candan@alanya.edu.tr

Access this article online

Website: www.jasi.org.in
DOI: 10.4103/jasi.jasi_186_21
Quick Response Code:

Study design

After obtaining ethical approval, all measurements were taken electronically on radiographs displayed on a PACS. Four hundred radiographs of the shoulders were reviewed. Patients were included in the study if they had routine clinical radiographs of the shoulder taken within the last 2 years of acceptable quality. All patients with previous shoulder surgery, fractures, infections, and tumors were excluded. The patients were divided into two groups according to syndromes, as follows:

- Group 1: Patients with rotator cuff syndrome (210 patients)
- Group 2: Control group (190 patients): Radiographs of the patients in this group were radiographs taken for routine diagnosis and examination.

We determined the acromion type according to the Bigliani classification observationally: Type 1 represents acromion being flat in shape, Type 2 represents a curved acromion that lies parallel to the humeral head, and Type 3 represents a hooked undersurface of the acromion.[4] In addition, the relationship between acromion type and angles was evaluated. We measured the following nine different parameters: the critical shoulder angle (CSA) was measured as the angle between a line connecting the glenoid's superior and inferior margins and a line between the inferolateral border of the acromion and the glenoid's inferior margin [Figure 1a]. The acromial index (AI) was obtained by dividing the distance from the glenoid to the acromion (GA) by the distance from the glenoid to the lateral of the humeral head (GH) [Figure 1b]. The greater tuberosity angle (GTA) was measured as the angle between a parallel line through the humeral head center of rotation and a line connecting the upper border of the humeral head to the greater tuberosity's most superolateral edge [Figure 1c]. The lateral acromial angle (LAA) was determined by the intersection of a line parallel to the acromion undersurface and a second line parallel to the glenoid fossa [Figure 1d]. The total shoulder arthroplasty (TSA) was measured as the angle between a line connecting the glenoid's superior and inferior margins and the line connecting the humeral head to the glenoid's inferior margin [Figure 2a]. The reverse shoulder arthroplasty (RSA) was measured as the angle between a line connecting the supraspinatus fossa and the glenoid's inferior margin and the line connecting the humeral head to the glenoid's inferior margin [Figure 2b]. The RST angle was measured as the angle between a line connecting the supraspinatus fossa and the glenoid's inferior margin and the line connecting the glenoid's superior margin to the inferior margin of the glenoid [Figure 2c].

Statistical analysis

SPSS Inc, Chicago, IL, USA. All measurements, means, standard error mean (SEM), and minimum and maximum values were calculated. Moreover, they were tested for correlation to each other and sex, side, and group. "Kolmogorov-Smirnov" and "Shapiro–Wilk" tests were performed to determine whether the data were suitable for normal distribution. In the evaluation of parameters according to gender, the Mann–Whitney U-test was used for those who did not show typical distribution characteristics, and the independent *t*-test was used for those who did show. Differences between patient and control groups were analyzed using the independent *t*-test. Differences between acromion type and angles were analyzed using a one-way analysis of variance. All values were of mean ± SEM. $P < 0.05$ was considered statistically significant in all statistical analyses.

Results

Four hundred shoulders were studied in this paper. The mean age was 50 years (53 years in female and 48 years in male patients). When the acromion type was evaluated, Type 1 acromion was seen in 13.69%, Type 2 in 79.47%, and Type 3 in 6.84% of the rotator cuff patients, and Type 1 acromion was seen in 5.72%, Type 2 in 91.90%, and Type 3 in 2.38% of the control groups in our study. When we evaluated the angles according to the acromion type, LAA, GA, and TSA parameters were found to be significantly different according to the acromion types [Figure 3].

The LAA was significantly higher ($P = 0.001$) in individuals with Type 1 and Type 2 acromion than in individuals with Type 3 acromion. The distance from the GA was significantly lower ($P = 0.002$) in individuals

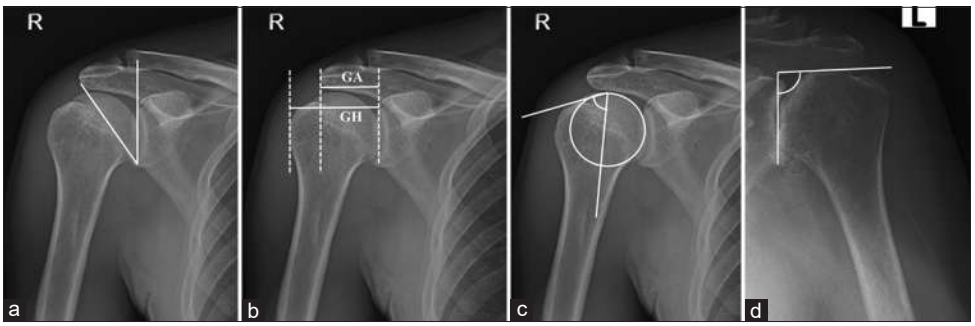

Figure 1: Measurements of CSA (a), AI (GA/GH) (b), GTA (c) and LAA (d). CSA: CSA, AI: Acromial index, GA: Glenoid acromion distance, GH: Glenoid humeral head, GTA: Greater tuberosity angle, LAA: Lateral acromial angle

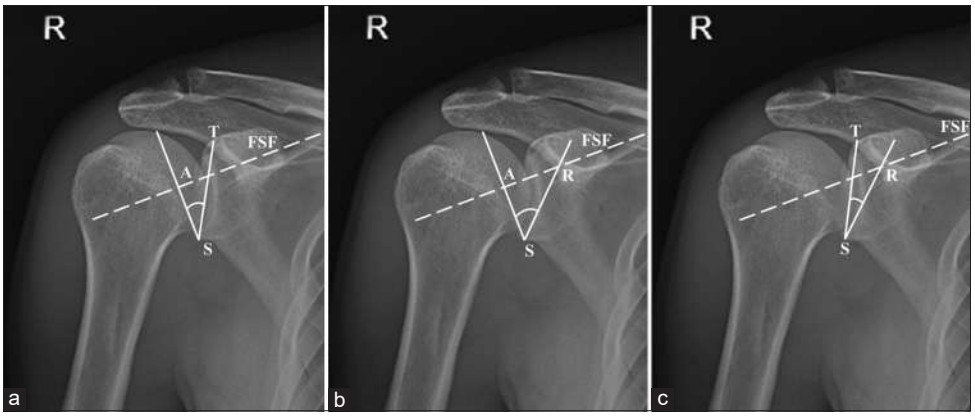

Figure 2: Measurements of TSA (a), RSA angle (b), and RST angle (c) FSF. TSA: Total shoulder arthroplasty, RSA: Reverse shoulder arthroplasty, FSF: Floor of the supraspinatus fossa

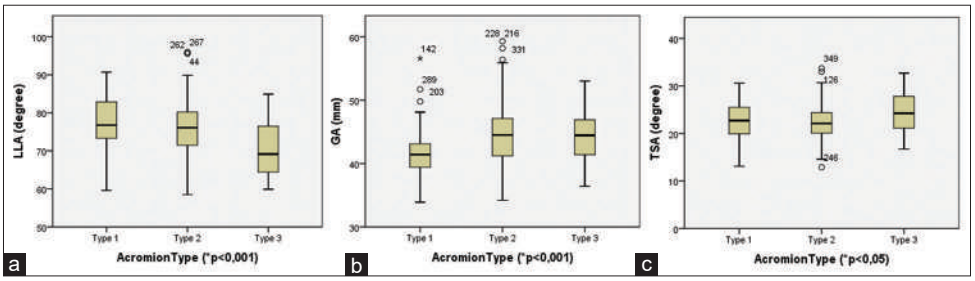

Figure 3: Statistically significant difference according to acromion types in the LAA (a), GA distance (b), and TSA angle TSA (c). LAA: Lateral acromial angle, GA: Glenoid-acromion, TSA: Total shoulder arthroplasty

with Type 1 acromion than in individuals with Type 2 and Type 3 acromion [Figure 3]. The total shoulder arthroplasty angle (TSA) was significantly higher (P = 0.004) in individuals with Type 3 acromion than in individuals with Type 1 and Type 2 acromion [Figure 3]. In the evaluation of parameters according to gender, it was seen that all measurements were significantly different between males and females [Table 1]. The mean values of the measurements according to gender and sides are listed in Table 1. According to syndromes, GH (P = 0.013), TSA (P = 0.000), RST (P = 0.015), and GTA (P = 0.000) were significantly different between the rotator cuff syndrome and control groups in evaluating parameters [Figure 4]. There was no statistically significant difference between the syndrome groups in AI, GA, RSA, CSA, and LAA measurements. According to syndromes, the mean values of the measurements are listed in Table 2.

Discussion

In this study, we tried to determine whether the angles and distances around the shoulder joint between the scapula and humerus are associated with gender, sides, and rotator cuff syndrome. Among the measurements we made, GH, TSA, RST, and GTA angles were statistically significant among the rotator cuff syndrome and control groups [Figure 4].

Bigliani *et al*. classified the acromion into three types with a progressive increase in impingement incidence from a Type 1 to Type 3 acromion. They stated that Type 3 acromion might impinge on the rotator cuff on the arm's elevation.[4] When the acromion shape was evaluated, the most common type seen was Type 2 acromion (79% in Group 1 and 92% in Group 2) in our study. Type 2 was reported as the most common acromion type: Banas,[5] Vahakari *et al*.,[6] and Balke *et al*.[3] reported Type 2 acromion in 51%, 81.3%, and 80% of cases, respectively. The ratio of Type 3 acromion was detected to be higher in the rotator cuff group (7%) than that in the control group (2%) in our study. The authors found a higher prevalence of rotator cuff tears in patients with a hooked acromion than in individuals with a curved or flat acromion.[7] The higher rate of Type 3 acromion in the rotator cuff syndrome group compared to the control group supported this information in our study.

The CSA has been reported for various degenerative shoulder problems which are significantly different from the corresponding angle in normal shoulders.[8] Our population had a CSA of 46.4°±0.61 in routine clinical radiographs, which is considerably higher than that of previous reports [Table 3].[8-19] In routine clinical radiographs, the CSA is subject to errors due to the viewing plane's orientation concerning the scapula.[25] Our investigation confirmed that the magnitude of the CSA depends on the viewing perspective of the X-ray beam. The literature reported that an abnormal CSA was a leading factor in

Table 1: Mean values of angles and measurements according to gender and sides

Measurement	Gender	*n*	Mean±SEM	Side	*n*	Mean±SEM
CSA	Male	200	45.98±0.48	Right	232	46.14±0.45
	Female	200	48.86±0.45	Left	168	49.20±0.48
LAA	Male	200	76.08±0.46	Right	232	76.49±0.45
	Female	200	75.55±0.48	Left	168	74.87±0.49
GA	Male	200	46.04±0.28	Right	232	45.26±0.28
	Female	200	42.23±0.26	Left	168	42.57±0.29
GH	Male	200	54.11±0.30	Right	232	51.30±0.35
	Female	200	47.38±0.26	Left	168	49.97±0.38
AI	Male	200	0.84±0.005	Right	232	0.88±0.005
	Female	200	0.88±0.005	Left	168	0.85±0.006
TSA	Male	200	21.39±0.22	Right	232	21.99±0.22
	Female	200	23.35±0.23	Left	168	22.89±0.24
RSA	Male	200	37.27±0.27	Right	232	37.08±0.21
	Female	200	37.85±0.18	Left	168	38.23±0.24
RST	Male	200	17.88±0.19	Right	232	17.24±0.21
	Female	200	16.93±0.23	Left	168	17.63±0.21
GTA	Male	200	87.35±0.48	Right	232	80.98±0.46
	Female	200	77.89±0.41	Left	168	84.88±0.66

$P<0.05$, differences between groups, (*n*, mean±SEM). *n*: Number of patients, SEM: Standard error mean, CSA: Critical shoulder angle, LAA: Lateral acromial angle, GA: Glenoid-acromion, GH: Glenoid-humeral head, AI: Acromial index, TSA: Total shoulder arthroplasty, RSA: Reverse shoulder arthroplasty, GTA; Greater tuberosity angle

Table 2: Mean values of angles and measurements according to syndrome

Measurement	Rotator cuff tears (210)	Control group (190)
CSA	47.57±0.47	47.27±0.48
LAA	75.32±0.46	76.36±0.49
GA	44.38±0.29	43.87±0.32
GH	51.37±0.35	50.06±0.39
AI	0.88±0.006	0.86±0.006
TSA	21.78±0.23	23.02±0.24
RSA	37.46±0.23	37.68±0.22
RST	17.77±0.19	17.01±0.24
GTA	84.95±0.53	80.05±0.53

$P<0.05$, differences between groups, (*n*, mean±SEM). *n*: Number of patients, SEM: Standard error mean, CSA: Critical shoulder angle, LAA: Lateral acromial angle, GA: Glenoid-acromion, GH: Glenoid-humeral head, AI: Acromial index, TSA: Total shoulder arthroplasty, RSA: Reverse shoulder arthroplasty, GTA; Greater tuberosity angle

developing rotator cuff tears.[8,25] According to our study, accurate measurement of the CSA is variable concerning the scapula's location. One study did not find a significant relationship between the CSA and the presence of rotator cuff syndrome.[19] The present study shows how highly sensitive the CSA is to radiograph the alignment of the scapula.

The morphological appearance of the acromion has been evaluated by many authors, as it is thought to be associated with various shoulder pathologies. AI is a criterion by which they determine acromion morphology. As stated in the literature, AI was lower in the control group than in the rotator cuff group in this study.[3,20,21] As our study result showed, Hamid *et al*. reported that AI was higher in females than males [Table 1].[21] We also evaluated GA (glenoid-acromion) and GH (glenoid-humerus) measurements in our study, different from the literature. The differences in the GH (P = 0.013) between the patients with rotator cuff syndrome and the control group were significant. GA was significantly lower (P = 0.002) in individuals with Type 1 acromion than in individuals with Type 2 and Type 3 acromion. A higher prevalence of rotator cuff syndrome in patients with a hooked acromion than in individuals with a curved or flat acromion was reported in the literature. Based on this, the fact that the distance between the glenoid and acromion is less in individuals with flat acromion type shows that this distance may also help in the diagnosis of rotator cuff syndrome. We concluded that GA and GH values, which were not taken into account in other studies, are helpful measurements for investigating the relationship between the humerus and the scapula.

In the present study, we evaluated LAA on routine radiographs. This angle is significantly different between genders in our study. The measurements of LAA in this study are consistent with the literature, and this angle was seen to be higher in the control group than that in the rotator cuff group [Table 3].[2,3,5] When we evaluated the relationship between acromion type and LAA, this angle was significantly lower in individuals with Type 3 acromion. The authors found a higher prevalence of rotator cuff syndrome in patients with a hooked acromion. So, we believe that a smaller LAA may cause pressure on the shoulder, and it can cause various pathology in the shoulder, such as impingement or rotator cuff syndrome.

Glenoid inclination (TSA, ß angle) has been defined and measured in many different ways.[7] The TSA angle is a modification of the ß angle, which provides a measure of the inclination of the glenoid surface and is useful for planning total shoulder arthroplasty.[22] In our study, we determined that the TSA (P = 0.000) was significantly lower in patients with rotator cuff syndrome than in the control groups. Also, TSA and RST (P = 0.014) angles were significantly different between the rotator cuff syndrome and control groups in this study. Boileau *et al*. and Shi *et al*. stated that TSA was a risk factor in the supraspinatus [Table 3].[22,23] Usually, the most rupture muscle is the supraspinatus muscle in rotator cuff syndrome. And, a higher prevalence of rotator cuff syndrome in patients with a hooked acromion was reported in the literature. And, we determined that TSA was significantly higher (P = 0.004) in individuals with Type 3 acromion in this study. Maurer *et al*. stated that the TSA between the glenoid fossa and the floor

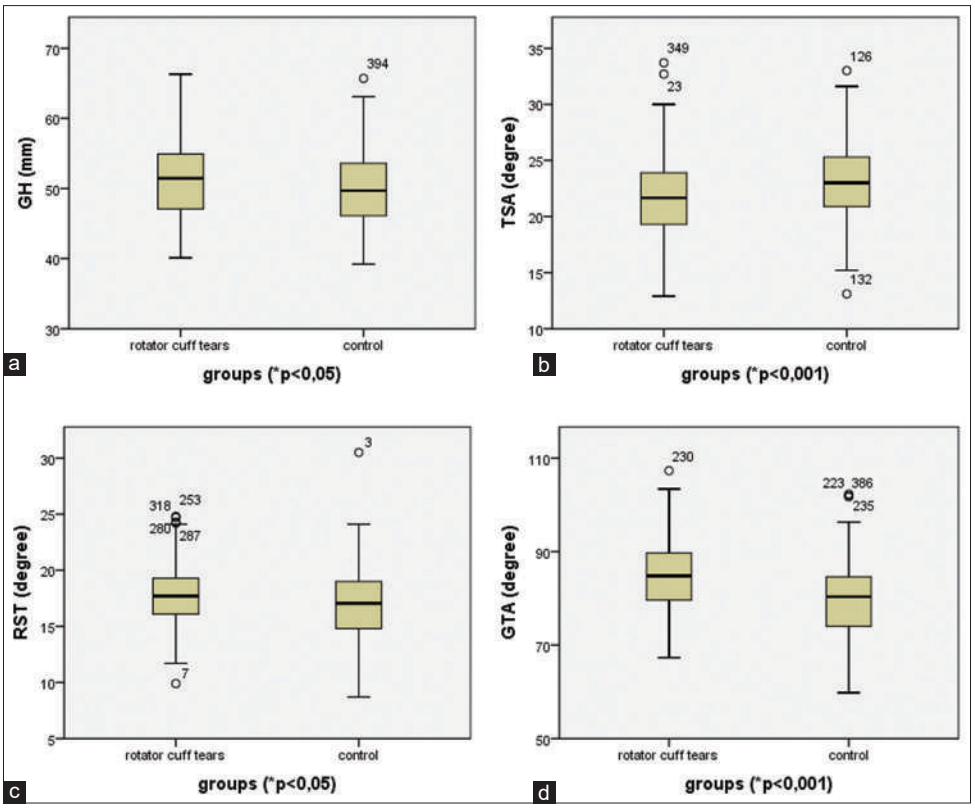

Figure 4: Statistically significant difference in the GH (a), TSA angle (b), reverse shoulder arthroplasty angle (RST) (c), and GTA (d) between the rotator cuff and control groups. TSA: Total shoulder arthroplasty, GH: Glenoid-humeral head, GTA: greater tuberosity angle

of the supraspinatus fossa was the most reproducible measurement method on conventional anteroposterior radiographs, providing good resistance to positional variability of the scapula.[26] From a surgical standpoint, the TSA is useful when planning a total shoulder arthroplasty implantation. Furthermore, although the TSA is appropriate to measure glenoid component inclination in total shoulder arthroplasty, it is not relevant to the reverse shoulder arthroplasty baseplate. Therefore, knowledge of the RSA is important for reverse shoulder arthroplasty operations.[22] We believe that these angles, which have been mentioned in very few articles yet, should be evaluated more.

Studies have shown that greater tuberosity malunion is associated with poor outcomes due to rotator cuff tension alteration and subacromial impingement, and rotator cuff tears.[24] Cunningham *et al*. reported that GTA values were significantly higher in patients with rotator cuff syndrome, compared with the control group. Consistent with this study, we found that GTA was significantly higher in patients with rotator cuff syndrome compared to the control group [Table 3 and Figure 4]. They stated that GTA could also guide treatment and serve as a postoperative control marker.[24] We believe that this angle, which has been defined quite recently and is mentioned in very few articles yet, should be evaluated more.

Limitations

The present study had some limitations. Despite our useful findings in this large study, we are aware that further research using prospectively collected data, including more detailed pathology definitions and broader ranges of shoulder diseases, is essential.

Conclusions

In this study, the importance of measurements and angles was evaluated in the diagnosis of shoulder diseases. We determined that overall the GH, TSA, RST, and GTA are associated with rotator cuff syndrome. Different from the literature, when we evaluated the relationship between acromion types and angles, we determined that LAA, GA, and TSA parameters were significantly different between acromion types. LAA was significantly higher (P = 0.001) in individuals with Type 1 and Type 2 acromion; GA was significantly lower (P = 0.002) in individuals with Type 1 acromion and TSA was significantly higher (P = 0.004) in individuals with Type 3 acromion. It has been stated in the literature that these parameters differ in rotator cuff syndrome. For this reason, we think that the relationship between acromion types and these parameters can contribute to the literature. And, we believe that our study will contribute to the literature in terms of gathering many angles that are important in shoulder pathologies in a single study.

Table 3: Comparison of CSA, LAA, AI, TSA, RSA, RST and GTA in rotator cuff patients and control patients between literatures

Literature	Angle	Rotator cuff tears	Control
Moor *et al*.[9]	CSA	38°	33.1°
Daggett *et al*.[10]	CSA	37.9°	-
Spiegl *et al*.[11]	CSA	37.3°	32.7°
Blonna *et al*.[8]	CSA	40°	34°
Suter *et al*.[12]	CSA	-	33.4°
Chalmers *et al*.[13]	CSA	34°	32°
Cherchi *et al*.[14]	CSA	36.4°	33.3°
Gomide *et al*.[15]	CSA	39.75°	33.59°
Peltz *et al*.[16]	CSA	36.9°	34.5°
Watanabe *et al*.[17]	CSA	34.4°	32.1°
Heuberer *et al*.[18]	CSA	36.3°	-
Bjarnison *et al*.[19]	CSA	33.9°	33.9°
Present study	CSA	47.98°	46.4°
Nyffeler *et al*.[20]	AI	0.73	0.64
Balke *et al*.[3]	AI	0.75	0.67
Hamid *et al*.[21]	AI	-	0.69
Present study	AI	0.88	0.86
Balke *et al*.[3]	LAA	77°	84°
Banas *et al*.[5]	LAA	-	78°
Li *et al*.[2]	LAA	-	78°
Present study	LAA	75°	76°
Boileau *et al*.[22]	TSA	-	16°
Shi *et al*.[23]	TSA	-	16°
Boileau *et al*.[22]	RSA	-	25°
Boileau *et al*.[22]	RST	-	9°
Present study	TSA	22°	23°
Present study	RSA	37°	38°
Present study	RST	18°	17°
Cunningham *et al*.[24]	GTA	73°	65°
Present study	GTA	85°	80°

CSA: Critical shoulder angle, LAA: Lateral acromial angle, AI: Acromial index, TSA: Total shoulder arthroplasty, RSA: Reverse shoulder arthroplasty, GTA; Greater tuberosity angle

Financial support and sponsorship

Nil.

Conflicts of interest

There are no conflicts of interest.

References

1. Khan Y, Nagy MT, Malal J, Waseem M. The painful shoulder: Shoulder impingement syndrome. Open Orthop J 2013;7:347-51.
2. Li X, Xu W, Hu N, Liang X, Huang W, Jiang D, *et al.* Relationship between acromial morphological variation and subacromial impingement: A three-dimensional analysis. PLoS One 2017;12:e0176193.
3. Balke M, Schmidt C, Dedy N, Banerjee M, Bouillon B, Liem D. Correlation of acromial morphology with impingement syndrome and rotator cuff tears. Acta Orthop 2013;84:178-83.
4. Bigliani LU, Ticker JB, Flatow EL, Soslowsky LJ, Mow VC. The relationship of acromial architecture to rotator cuff disease. Clin Sports Med 1991;10:823-38.
5. Banas MP, Miller RJ, Totterman S. Relationship between the lateral acromion angle and rotator cuff disease. J Shoulder Elbow Surg 1995;4:454-61.
6. Vähäkari M, Leppilahti J, Hyvönen P, Ristiniemi J, Päivänsalo M, Jalovaara P. Acromial shape in asymptomatic subjects: A study of 305 shoulders in different age groups. Acta Radiol 2010;51:202-6.
7. Nyffeler RW, Meyer DC. Acromion and glenoid shape: Why are they important predictive factors for the future of our shoulders? EFORT Open Rev 2017;2:141-50.
8. Blonna D, Giani A, Bellato E, Mattei L, Caló M, Rossi R, *et al*. Predominance of the critical shoulder angle in the pathogenesis of degenerative diseases of the shoulder. J Shoulder Elbow Surg 2016;25:1328-36.
9. Moor BK, Bouaicha S, Rothenfluh DA, Sukthankar A, Gerber C. Is there an association between the individual anatomy of the scapula and the development of rotator cuff tears or osteoarthritis of the glenohumeral joint?: A radiological study of the critical shoulder angle. Bone Joint J 2013;95-B: 935-41.
10. Daggett M, Werner B, Collin P, Gauci MO, Chaoui J, Walch G. Correlation between glenoid inclination and critical shoulder angle: A radiographic and computed tomography study. J Shoulder Elbow Surg 2015;24:1948-53.
11. Spiegl UJ, Horan MP, Smith SW, Ho CP, Millett PJ. The critical shoulder angle is associated with rotator cuff tears and shoulder osteoarthritis and is better assessed with radiographs over MRI. Knee Surg Sports Traumatol Arthrosc 2016;24:2244-51.
12. Suter T, Gerber Popp A, Zhang Y, Zhang C, Tashjian RZ, Henninger HB. The influence of radiographic viewing perspective and demographics on the critical shoulder angle. J Shoulder Elbow Surg 2015;24:e149-58.
13. Chalmers PN, Beck L, Granger E, Henninger H, Tashjian RZ. Superior glenoid inclination and rotator cuff tears. J Shoulder Elbow Surg 2018;27:1444-50.
14. Cherchi L, Ciornohac JF, Godet J, Clavert P, Kempf JF. Critical shoulder angle: Measurement reproducibility and correlation with rotator cuff tendon tears. Orthop Traumatol Surg Res 2016;102:559-62.
15. Gomide LC, Carmo TC, Bergo GH, Oliveira GA, Macedo IS. Relationship between the critical shoulder angle and the development of rotator cuff lesions: A retrospective epidemiological study. Rev Bras Ortop 2017;52:423-7.
16. Peltz CD, Divine G, Drake A, Ramo NL, Zauel R, Moutzouros V, *et al.* Associations between *in-vivo* glenohumeral joint motion and morphology. J Biomech 2015;48:3252-7.
17. Watanabe A, Ono Q, Nishigami T, Hirooka T, Machida H. Differences in risk factors for rotator cuff tears between elderly patients and young patients. Acta Med Okayama 2018;72:67-72.
18. Heuberer PR, Plachel F, Willinger L, Moroder P, Laky B, Pauzenberger L, *et al.* Critical shoulder angle combined with age predict five shoulder pathologies: A retrospective analysis of 1000 cases. BMC Musculoskelet Disord 2017;18:259.
19. Bjarnison AO, Sørensen TJ, Kallemose T, Barfod KW. The critical shoulder angle is associated with osteoarthritis in the shoulder but not rotator cuff tears: A retrospective case-control study. J Shoulder Elbow Surg 2017;26:2097-102.
20. Nyffeler RW, Werner CM, Sukthankar A, Schmid MR, Gerber C. Association of a large lateral extension of the acromion with rotator cuff tears. J Bone Joint Surg Am 2006;88:800-5.
21. Hamid N, Omid R, Yamaguchi K, Steger-May K, Stobbs G, Keener JD. Relationship of radiographic acromial characteristics

and rotator cuff disease: A prospective investigation of clinical, radiographic, and sonographic findings. J Shoulder Elbow Surg 2012;21:1289-98.

22. Boileau P, Gauci MO, Wagner ER, Clowez G, Chaoui J, Chelli M, *et al.* The reverse shoulder arthroplasty angle: A new measurement of glenoid inclination for reverse shoulder arthroplasty. J Shoulder Elbow Surg 2019;28:1281-90.
23. Shi X, Xu Y, Dai B, Li W, He Z. Effect of different geometrical structure of scapula on functional recovery after shoulder arthroscopy operation. J Orthop Surg Res 2019;14:312.
24. Cunningham G, Nicodème-Paulin E, Smith MM, Holzer N, Cass B, Young AA. The greater tuberosity angle: A new predictor for rotator cuff tear. J Shoulder Elbow Surg 2018;27:1415-21.
25. Zaid MB, Young NM, Pedoia V, Feeley BT, Ma CB, Lansdown DA. Anatomic shoulder parameters and their relationship to the presence of degenerative rotator cuff tears and glenohumeral osteoarthritis: A systematic review and meta-analysis. J Shoulder Elbow Surg 2019;28:2457-66.
26. Maurer A, Fucentese SF, Pfirrmann CW, Wirth SH, Djahangiri A, Jost B, *et al.* Assessment of glenoid inclination on routine clinical radiographs and computed tomography examinations of the shoulder. J Shoulder Elbow Surg 2012;21:1096-103.

Original Article

Students' Approaches to Learning Anatomy: The Road to Better Teaching and Learning

Mohamed Al Mushaiqri, Adnan Albaloshi[1], Srijit Das

Department of Human and Clinical Anatomy, [1]College of Medicine and Health Sciences, Sultan Qaboos University, Muscat, Sultanate of Oman

Abstract

Introduction: The quality of medical and nursing student's anatomical knowledge and their experience in learning anatomy assists them in their health-care professions and it is largely influenced by their approach to learning. The main aim of this study was to investigate medical and nursing students' approach to learning anatomy at Sultan Qaboos University, Oman. **Material and Methods:** This survey-based cross-sectional study was conducted among 250 students. The Study Process Questionnaire was used to measure students approach to learning anatomy. The association between the approach to learning anatomy and demographic information such as gender, previous anatomical knowledge, and academic performance was also analyzed. **Results:** Of the 250 distributed questionnaires, 205 completed questionnaires were obtained with an 82% response rate. The analysis revealed that the deep approach (DA) mean score was significantly higher than the surface approach (SA) mean score for medical and nursing students, collectively (34.81 vs. 28.62, $P < 0.05$), medical students alone (34.96 vs. 26.83, $P < 0.05$), and nursing students alone (34.62 vs. 30.62, $P < 0.05$). There was no association between the approach to learning anatomy and gender among medical students nor nursing students. There was a positive correlation between the DA score and both the overall academic performance ($r = 0.33$, $P < 0.01$) and the performance in a previous anatomy course ($r = 0.33$, $P < 0.01$). **Discussion and Conclusion:** The results provide important feedback to anatomy teachers and students for effective teaching and learning anatomy. The study also provides baseline data for future research on factors influencing students' approaches to learning anatomy.

Keywords: *Academic performance, anatomy, approach to learning, medicine, nursing*

Introduction

Learning is "*a process that leads to change, which occurs as a result of experience and increases the potential for improved performance and future learning.*" However, learning is not "*something done to students, but rather something students themselves do.*"[1] In the 21st century, learning has changed much with the implementation and use of new technologies, online resources, and new methods. Learning is difficult and more challenging in the medical profession.

Students who choose medical career are expected to undergo rigorous training procedures and it is difficult to master all the subjects in the medical curriculum. Research studies have reported the stress, anxiety, exhaustion, and burnout in medical students and the challenges posed by medical schools.[2-4] Interestingly, the stress and burnout were found to be present in 50%–60% of the medical students and it was found to be higher in medical students compared to similar aged individuals in the general population.[2,4] The psychological stress was also reported to be associated to poor learning outcomes and lapses in the profession.[4]

Anatomy is regarded as a fundamental subject for clinical practice and all health care professionals must have a sound knowledge of anatomy.[5] Anatomy is considered to be a dull subject that requires intensive labor, is sometimes learned through surface learning practices and rote memorization.[6,7] The subject is considered to be vast and time frame for covering anatomy course is too short. Many students find it difficult to learn and understand anatomy. Learning anatomy is always a challenge for the students, who have a transition from the secondary to tertiary education in medical schools. It has been noticed that many students who fared well during their secondary stage, faltered in the medical schooling stage. Hence, the students need to adapt to different strategies

How to cite this article: Al Mushaiqri M, Albaloshi A, Das S. Students' approaches to learning anatomy: The road to better teaching and learning. J Anat Soc India 2023;72:29-36.

Article Info

Received: 25 April 2022
Revised: 13 September 2022
Accepted: 15 September 2022
Available online: 24 March 2023

Address for correspondence:
Dr. Mohamed Al Mushaiqri, Department of Human and Clinical Anatomy, College of Medicine and Health Sciences, Sultan Qaboos University, Al Khoud, Muscat 123, Sultanate of Oman.
E-mail: mohamed@squ.edu.om

Access this article online

Website: www.jasi.org.in
DOI: 10.4103/jasi.jasi_67_22
Quick Response Code:

and techniques, to learn anatomy. Many students struggled to learn anatomy and thereby resorted to memorizing the subject.

Students often pass their examination but fail to solve a clinical problem later during their clinical clerkship period.[8] This has led to many clinical teachers being upset with the students with regard to their knowledge of anatomy gained in preclinical years. Many medical schools have even started refresher courses in anatomy for postgraduate training period as students tend to forget anatomy in later years. Researchers also stressed the importance of anatomy knowledge for building a strong foundation for future clinical exposure and professional practice.[9,10]

The anatomy subject provides a suitable platform for "authentic learning."[8] Authentic learning is seen in daily teaching and learning activities that take place in the classrooms and lecture theatres of anatomy.[8] According to the same researchers, all anatomy teachers need to make sure that their methods are enriched with intrinsic and instrumental value which may help the student in clinical setting. Authentic learning has gained much attention during recent times. Anatomy teachers also need to expose to innovative approaches to improve their teaching. Already, the researchers have identified the changes in different components of anatomy.[11]

Student's anatomical knowledge and experiences in learning anatomy may assist them in their health-care profession. Outcomes of their careers are related to the effective learning and application of anatomy in clinical practice.[12] However, the study of human anatomy requires memorization of thousands of facts about the human body structures and often students are required to recall the information for specific assessments whether in their educational life or health-care clinical practice.[13] Moreover, there has been a trend of decreasing time available for the anatomy course in medical curricula which means that students need to learn the already overwhelming amount of anatomy information in a compressed timeframe.[14] These factors alerted the anatomy faculty about the possibility, that a surface learning approach is likely to be adopted by the students in such a learning context. Accordingly, the topic of students' approach to learning anatomy has attracted researches involved with anatomy teaching.

Students' approach to learning is the concept of how students learn and study in a specific context. It was initially established by educational psychologists.[15] Marton and Saljo (1976), determined the process of learning based on students' learning experience of reading an article, and then interviewed them to estimate their level of understanding.[15] The outcomes of that study lead to identification of two levels of processing, i.e. "deep" and "surface." These processing modes greatly assisted educational systems in understanding how students experience the learning.[12,16]

Researchers changed the term "process" to "approach" which they preferred for being the best in describing how students go about learning.[15,17] Deep approach (DA) students were found to be active learners. They interact, engage, and show personal interest in a subject. They also tend to relate new ideas with previous knowledge and have an intrinsic intention to understand the subject in a meaningful and fulfilling way, which yields greater levels of effective learning results. In contrast, surface approach (SA) students tend to memorize and prefer rote learning without understanding the meaning of the material. Their main intention is to pass examinations of a specific subject with the minimum effort possible.[18-21]

Further research on learning approaches identified a third level known as "achieving or strategic."[22] Strategic or achieving students adopt both deep and SAs to complete a task with the intention of achieving the highest grades. They are highly competitive and have good time management skills.[23] Further investigations refined and characterized student's approach to learning in three different categories "deep," "surface," and "achieving/or strategic."

Many researchers believe that achieving the learning outcomes is largely influenced by the student's learning approaches, which reflect in the path students follow toward fulfilling specific study tasks.[16] Learning outcomes are affected by personal characteristics of the students and circumstantial factors. Personal characteristics include personality, locus of control, ability, background, conceptions of learning, attitudes, and general experiences. On the other hand, circumstantial factors include the learning context, nature of the task, time pressures, method of teaching, assessment, and perceptions of institutional requirements.[24]

Smith and Mathias from the University of Southampton found that among 243 medical students, 47%, 39%, and 14% of students followed deep, strategic, and SAs while learning anatomy, respectively.[12] Moreover, it was also found that DA was followed by male students and strategic approach by female students.[12] In another study, the same researchers found a clear relationship between anatomy activities involving human cadavers and student approach to learning anatomy.[12]

A study from Ghana reported that majority of the students adopted a DA while fewer students adopted SA to learning anatomy. However, there was no significant relationship between students' approaches to learning and gender.[25]

Although many studies were conducted on student's approach to learning anatomy, an extant search of literature showed a paucity of studies on SA and DA from the Middle-east region, Arab world, and Oman, specifically. Hence, the present study was aimed at filling this gap through investigating students' approaches to learning anatomy at Sultan Qaboos University (SQU), Oman. The

results of the present study may help anatomy teachers improve the quality of learning outcomes and encourage deep learning through educating–learning process.

Material and Methods

Study setting and participants

This was a survey-based cross-sectional study conducted at the College of Medicine and Health Sciences, SQU, Sultanate of Oman, during fall semester of the academic year 2018–2019. The medical students and nursing students enrolled in courses that had the most significant anatomy content and offered in Fall semester of 2018 were included in this study. For medical students, one course was chosen called "Structure-Function relationship." For nursing students, two courses were chosen; "Anatomy and Physiology-I" and "Anatomy and Physiology II." Medical students learn anatomy through didactic lectures and practical sessions that include cadavers, prosections, plastic models, radiological images, and surface anatomy. Nursing students learn anatomy through didactic lectures and practical sessions that include plastic models only.

Ethical approval was obtained from the Medical Research and Ethics Committee of the College of Medicine and Health Science at SQU. The participants were informed about the purpose of the study. Their names in questionnaire were kept anonymous to maintain the confidentiality, so that they could fill in the questionnaire within adequate time.

Instruments

The instrument to collect the data was a survey-based questionnaire, which was divided into two sections. First section of the questionnaire included demographic information of the students, i.e. (i) college, (ii) cohort, (iii) gender, (iv) current course, (v) cumulative grade point average score, as an indicative of overall academic performance, and (vi) grade in Academic English for Medicine or Academic English for Nursing, as an indicative of the English language skills level.

The second section was one of the best two designed inventories used to measure students' approach to learning, the study process questionnaire (SPQ).[20,26] It is a widely used self-reported questionnaire for investigating higher education students' approach to learning in general and allows researchers to differentiate between deep, surface, and strategic learning approaches of a specific subject in the study program.[24] Diverse forms of SPQ have been utilized as a part of the study for various purposes. Based on earlier studies, the questionnaire was validated and based on the Cronbach alpha test, the questionnaire was considered to be reliable.

Considering the general nature of SPQ, the word "anatomy" was inserted into the items as appropriate to make sure that the students' responses referred only to the anatomy content of the courses and not the other disciplines' content. This section included 20 questionnaire items, which were planned to evoke student responses as to how they approach learning Anatomy. Responses were given utilizing a 5-point Likert-type scale extending from "A-this item will always or almost always be true" to "E-this item will never or rarely be true."

The questionnaire also included a consent form on the first page describing the study, its goal, and invitation to students to participate in the study. The questionnaire was distributed to the participants in hard copy version during the middle of the Fall 2018 semester. They were requested to fill in the questionnaire and return it within 2 weeks.

Statistical analysis

The collected data were entered and analyzed using the Statistical Package for Social Sciences (SPSS) software version 23 (IBM Corporation, NY, USA). This included the data collected through the first part of the questionnaire dealing with students' demographics and the data obtained from the SPQ. Demographic data were analyzed descriptively and presented as frequency and percentage distributions of variables and mean scores. Inferential statistical analysis in the form of Student's *t*-test and correlation tests was also used to test for significant differences in certain variables among groups. Data were presented in the form of bar charts and frequency tables. Scatted dot graphs and correlation tables were used to present correlation test data. A $P \leq 0.05$ was considered to be statistically significant.

Results

Out of a total of 250 students targeted for the study, only 205 students completed the questionnaire with a response rate of 82%. Female students comprised the majority of medical and nursing students with a percentage of 63% (n = 68) and 78.4% (n = 76), respectively [Table 1].

Medical students' demographic data

Female students demonstrated better academic performance in general, as reflected by the mean grade point average (GPA) (2.94 vs. 3.36, $P < 0.05$), and the mean General Education Diploma grade (93.09 vs. 96.94, $P < 0.001$). They also performed better in previous

Table 1: Demographic data of participants and their distribution among gender groups and colleges

	College of Medicine	College of Nursing	Total
Male	*n*=40	*n*=21	*n*=61
	Percent=37%	Percent=21.6%	Percent=29.8%
Female	*n*=68	*n*=76	*n*=144
	Percent=63%	Percent=78.4%	Percent=70.2%
Total	*n*=108	*n*=97	*n*=205
	Percent=100%	Percent=100%	Percent=100%

anatomy courses as reflected by the mean grade in that course (3.02 vs. 3.35/4.0, $P < 0.05$). Female students also had a significantly higher English language skill level as reflected by the grade in English for Medicine course [2.94 vs. 3.42/4.0, $P < 0.001$ Table 2].

Nursing students' demographic data

Females showed similar findings to that of medical students, in which they demonstrated better academic performance in general as reflected by the mean GPA (2.35 vs. 3.13/4.0, $P < 0.05$), and the mean general education diploma (87.14 vs. 93.50/100, $P < 0.001$). Although female students' findings were lower in mean number of foundation semesters (2.50 vs. 1.23/4.0 $P < 0.001$), the mean grade in English course was not significant [Table 3].

Approach to learning anatomy

Nursing and medical students

Medical and nursing students at SQU significantly adopt DA to learning anatomy. The mean score of the DA and the SA obtained from SPQ was 34.81 and 28.62, respectively ($P < 0.05$) [Figure 1].

There were no significant differences in the DA score or SA score among genders [Figure 2].

Medical students

When focusing on medical students alone, they also had a significant higher DA mean score (34.96) compared to SA mean score (26.83) [Figure 3].

There were not any significant differences in the DA mean score or SA mean score among genders, although both male and female students appeared to have higher DA mean scores than SA mean scores [Figure 4].

The relationship between the mean scores of DA and SA and the general academic performance and performance in anatomy courses was investigated using the Pearson correlation coefficient. There was a significant positive correlation between students' DA mean score and their GPA ($r = 0.33$, $P > 0.01$). There was also a significant negative correlation between students, SA mean score, and their GPA ($r = -0.22$, $P < 0.05$).

There was also a significant positive correlation between students' DA mean score and their grade in a previous anatomy course ($r = 0.33$, $P > 0.01$). A negative correlation

Table 2: Medical student's academic performance indicators

	Male	Female	*P*	All students
Mean GPA score	2.94	3.36	<0.05	3.21
Mean General Education Diploma grade (out of 100)	93.09	96.94	<0.001	95.53
Mean grade in previous anatomy course (out of 4.00)	3.02	3.35	<0.05	3.32
Mean Grade in Academic English for Medicine course (out of 4.00)	2.94	3.42	<0.001	3.24

GPA: Grade point average

Table 3: Nursing student's academic performance indicators

	Male	Female	*P*	All students
Mean GPA score	2.35	3.13	<0.05	2.96
Mean General Education Diploma grade (out of 100)	87.14	93.50	<0.001	92.12
Mean Grade in Academic English for Nursing course (out of 4.00)	2.53	2.92	>0.05	2.84

GPA: Grade point average

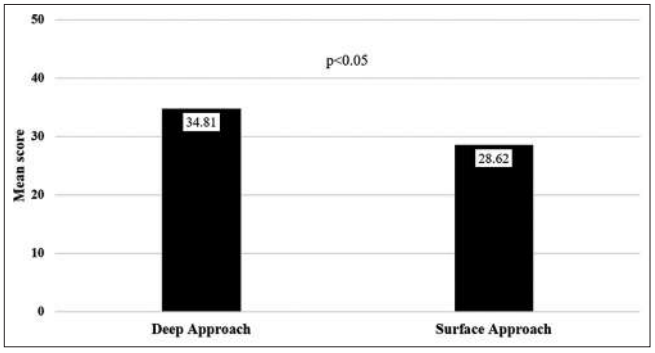

Figure 1: Overall medical and nursing students approach to learning anatomy

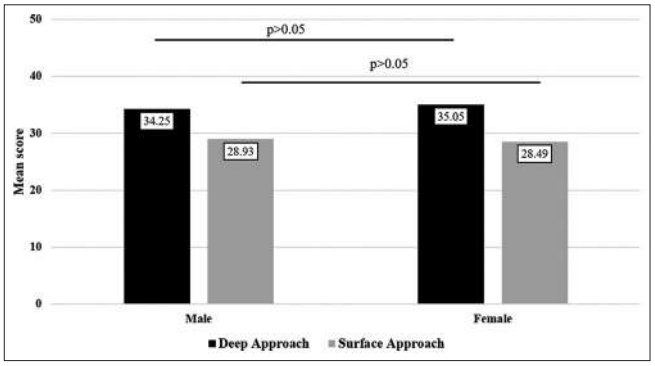

Figure 2: Overall medical and nursing students approach to learning anatomy according to gender

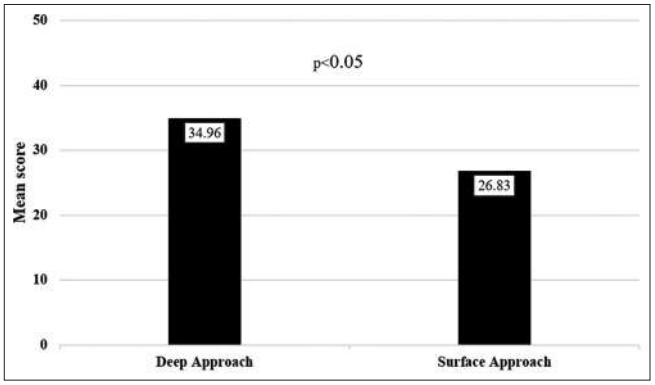

Figure 3: **Medical students approach to learning anatomy**

was also found between students' SA mean score and their grade in that course, through no significant ($r = -0.17$, $P > 0.05$).

Moreover, there was also a significant positive correlation between SA mean score and number of semesters student spent in the foundation program ($r = 0.202$, $P < 0.05$).

Nursing students

Overall nursing students had a significantly higher DA mean score than SA mean score (34.65 compared to 30.62, $P < 0.05$) [Figure 5].

Moreover, male students had a higher SA mean score than female students (33.52 compared to 29.82, $P < 0.05$). However, there was no significant differences in DA mean score among genders [Figure 6].

Pearson correlation coefficient showed no significant relationships between nursing students approach to learning anatomy and any other demographic variable.

When analyzing nursing students approached to learning anatomy in the two included courses separately, it was found that only students of "Anatomy and Physiology I" had a significantly higher DA mean score than SA mean score (36.94 compared to 30.35, $P < 0.001$). No such significant difference was found in the "Anatomy and Physiology II" course [Figure 7].

Discussion

The results of the present study presented a few interesting findings related to SQU students' approaches to learning anatomy. To start with, the response rate in this study was quite high. Students were approached directly and individually, which may explain the reason why the response rate was high. The higher representation of female students could be due to admission criteria or preference of Omani females for the medical and nursing profession. Interestingly, nursing has become one of the fastest-growing professions in Oman.[27] As per earlier reports, even from other parts of the world, one in ten registered nurses were found to be males and many thought nursing professions as feminine one.[28] A past study found that the number and percentage of females in the medical profession and the density of doctors and nurses per population in Oman has also increased progressively.[29] Hence, the more number of female students in medicine and nursing in Oman could be a well-accepted fact.

In the present study, DA was the dominant approach to learning anatomy among all medical and nursing students. It was also the dominant approach among medical and nursing students, separately. These results are similar to earlier findings.[12,30] Both studies were conducted at the University of Southampton in the United Kingdom. The medical program at this university is system-based and utilizes a mixture of problem-based and case-based

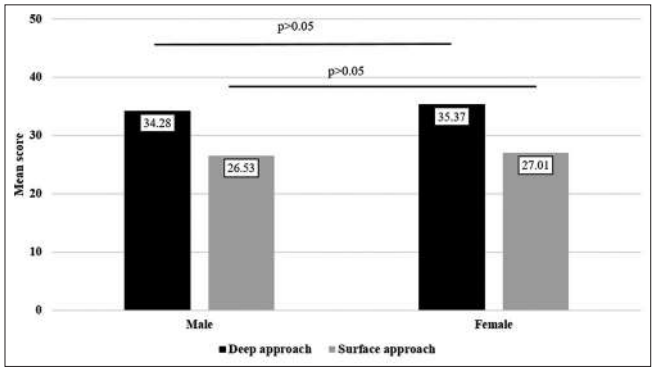

Figure 4: Medical students approach to learning anatomy according to gender

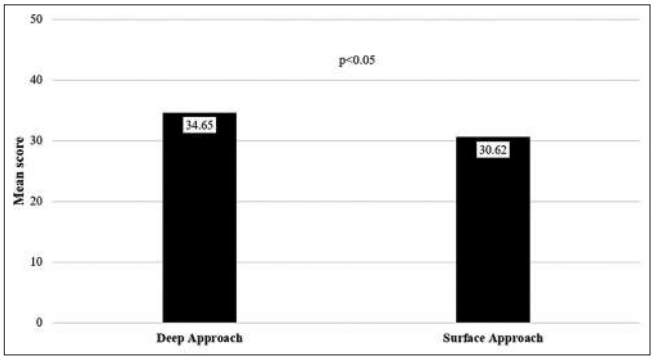

Figure 5: Nursing students approach to learning anatomy

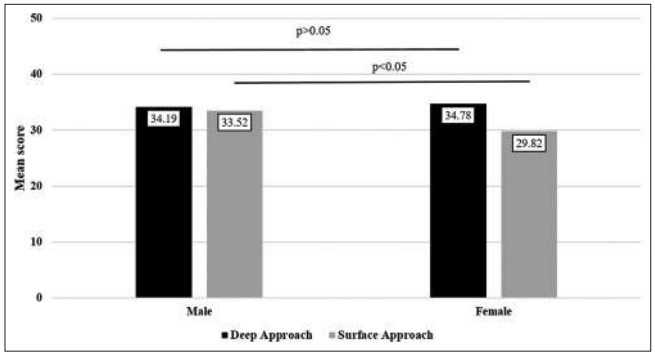

Figure 6: Nursing students approach to learning anatomy according to gender

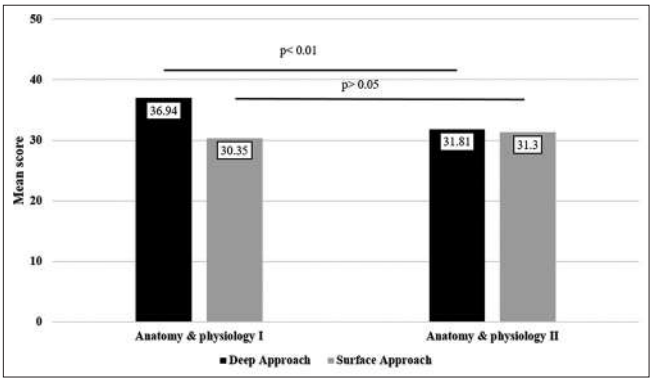

Figure 7: Nursing students approach to learning anatomy in two different courses

learning. This program is similar to the MD program at SQU and therefore such similarity in the findings of studies conducted in these two universities is expected. Moreover, such link may also apply to nursing students at SQU, who study anatomy in a system-based approach, although there was no component between problem-based learning (PBL) and case-based learning. The association between PBL and DA to learning in the context of medical education has already been reported in the literature.[25] PBL enhances self-regulated learning. An earlier study by Pawlina *et al*. reported that medical and dental students generated much interest with PBL involving gross anatomy dissection. Interestingly, the same study stated that if the faculty resorts to discussions and more probing of student's knowledge through PBL sessions, they may even improve their teaching skills.[31]

Despite the apparent higher academic performance of female students, as reflected by the demographic data, there were no significant differences in the DA to anatomy learning among genders. Interestingly, there are contradictory findings in the literature regarding this issue. While Mogr and Malba did not find any differences between genders,[25] Smith and Mathias reported that male students favored DA.[30] Earlier studies in medical science showed that males tended to perform better than females in completing any task that involved the usage of visual-spatial manipulation of the instruments involved in laparoscopy or endoscopy.[32] There are reports of females using specific learning strategies and goal structures.[33,34] The results of the present study support the fact, that approach to learning is not an internal characteristic of the student that applies to all learning contexts and situations. Instead, it is how the students learn in that specific course under that specific learning environment. The educational environment for learning is considered to be one of the most important determinants of an effective implementation of any curriculum in any institution and the student's perception of such an environment increases the quality of medical education.[35,36] The learning environment in any institution also includes the educational, physical, social, and psychological aspects.[37] The learning environment also determines how and why students should learn and the enthusiasm and effectiveness are influenced, accordingly.[38] A recent research study found ranking category of students' learning institutions determines the intrinsic and extrinsic motivation of toward medicine.[39] Furthermore, the approach to learning in any course could be predicted based on the academic performance of the students in other courses.

Another significant finding in the present study was that the DA mean score positively correlated with both the GPA and the grade in a previous anatomy course. The correlation with the GPA probably indicates that those students who adopt a DA to learning anatomy also adopt the same approach to other courses, which resulted in improving their overall academic performance. The DA to learning adds more detailed information to the existing level of knowledge. In the DA, the student is more interested in the task, derives enjoyment from it, searches for more, personalizes the task, integrates aspects of the task, and tries to create hypothesis.[40]

The positive correlation between the DA mean score and the grade in previous anatomy course is supported by literature linking the approach to leaning anatomy to previous experience in anatomy. Notebaert reported that students with no previous experience in anatomy had a significantly higher SA score than those with some previous experience.[41] According to the same study, students thought that anatomy was concerned more about memorizing structures and remembering terminologies. Hence, instructional techniques that support DA to learning are needed to change the students' perception.[41]

With regard to nursing students, only students of the "Anatomy and Physiology I" course significantly adopted a DA. This may be explained by the implementing a different teaching environments and styles than that of the "Anatomy and Physiology II" course. These two courses were taught by two different instructors. The students of "Anatomy and Physiology II" learned anatomy through didactic lectures and practical demonstrations, only. The assessment included written in-course examinations, a practical spotter examination, and a final written examination. The students of "Anatomy and Physiology I" course had additional interactive tasks during the lectures and short quizzes before each practical that covers the content of the previous practical. Therefore, the interactive learning tasks and the more frequent assessments could have been the drive behind adopting a DA by those students.

A positive teacher–student relationship was reported to influence students' engagement in learning.[42] The educators' enthusiasm and support may have a positive impact on the nursing student's learning.[43] All the nursing students' engagement in learning and the educators' approach to develop the cognitive skills may be useful for nursing students. Many previous studies proved that approaches to learning anatomy are temporary, due to learning and teaching approaches changing continuously thus students approach to learning depend on the situation and are not permanent.[23] The present study being a cross-sectional may not provide adequate information on students' approach to learning anatomy after being assessed at one point of time.

DA for learning may involve critical thinking and problem-solving attitude. Deep learning may be possible with artificial machines and robots. During recent times, artificial intelligence (AI) has drawn much attention. The AI aspect has been included in many medical subjects including anatomy. It has been a fact of debate if AI could really assist in deep learning. Few researchers felt that AI

may be still in its infancy state.[44] Few components such as human touch, discipline-based kills, to serve as a role model in profession and mentoring students may not be achievable through AI.[44]

Limitations

Longitudinal studies may be needed in future. Studies with a bigger sample size may be planned and replicated in other parts of the world, as well. There is a need for future research studies to investigate students' approaches to learning anatomy throughout the medical program. One aspect of interest in this regard is the impact of integration on medical students' approaches to learning anatomy.

Conclusion

To the best of our knowledge, this may be the first study of its kind to report on students' approaches to learning anatomy from the Middle-east, Arab World, particularly from Oman. The study found that medical and nursing students at SQU adopt a DA to learning anatomy. The DA was found to be positively correlated with the academic performance in general and with the performance in the previous anatomy course. The outcome of this study may be useful for anatomy teachers at SQU in helping them to implement a learning environment that promotes deep learning approach. The study also provided a baseline information for the future studies on factors affecting students' approach to learning anatomy.

Financial support and sponsorship

Nil.

Conflicts of interest

There are no conflicts of interest.

References

1. Ambrose SA, Bridges MW, DiPietro M, Lovet MC, Norman MK. How Learning Works: Seven Research-Based Principles for Smart Teaching; 2010. Available from: https://doi.org/10.14434/josotl.v14i1.4219. [Last accessed on 2021 Jul 15].
2. Villwock JA, Sobin LB, Koester LA, Harris TM. Impostor syndrome and burnout among American medical students: A pilot study. Int J Med Educ 2016;7:364-9.
3. Babenko O, Daniels LM, Ross S, White J, Oswald A. Medical student well-being and lifelong learning: A motivational perspective. Educ Health (Abingdon) 2019;32:25-32.
4. Dyrbye LN, Thomas MR, Shanafelt TD. Systematic review of depression, anxiety, and other indicators of psychological distress among U.S. and Canadian medical students. Acad Med 2006;81:354-73.
5. Cottam WW. Adequacy of medical school gross anatomy education as perceived by certain postgraduate residency programs and anatomy course directors. Clin Anat 1999;12:55-65.
6. Biggs J. Constructing learning by aligning teaching: Constructive alignment. In: Teaching for Quality Learning at University: What the Student Does. 2nd ed. Buckingham: SRHE and Open University Press; 2003.
7. Hopkins R, Regehr G, Wilson TD. Exploring the changing learning environment of the gross anatomy lab. Acad Med 2011;86:883-8.
8. Pawlina W, Drake RL. Authentic learning in anatomy: A primer on pragmatism. Anat Sci Educ 2016;9:5-7.
9. Smith CF, Finn GM, Stewart J, McHanwell S. Anatomical Society core regional anatomy syllabus for undergraduate medicine: The Delphi process. J Anat 2016;228:2-14.
10. Tubbs RS, Sorenson EP, Sharma A, Benninger B, Norton N, Loukas M, *et al.* The development of a core syllabus for the teaching of head and neck anatomy to medical students. Clin Anat 2014;27:321-30.
11. Drake RL, McBride JM, Lachman N, Pawlina W. Medical education in the anatomical sciences: The winds of change continue to blow. Anat Sci Educ 2009;2:253-9.
12. Smith CF, Mathias HS. Medical students' approaches to learning anatomy: Students' experiences and relations to the learning environment. Clin Anat 2010;23:106-14.
13. Miller SA, Perrotti W, Silverthorn DU, Dalley AF, Rarey KE. From college to clinic: Reasoning over memorization is key for understanding anatomy. Anat Rec 2002;269:69-80.
14. Collins JP. Modern approaches to teaching and learning anatomy. BMJ 2008;337:a1310.
15. Marton F, Saljo R. Approaches to learning. In: Marton F, Hounsell D, Entwistle NJ, editors. The Experience of Learning: Implications for Teaching and Studying in Higher Education. 2nd ed. Edinburgh: Scottish Academic Press; 1997. p. 39-58.
16. Zain ZM, Mala IN, Noordin F, Abdullah Z. Assessing student approaches to learning: A case of business students at the faculty of business management, UiTM. Procedia Soc Behav Sci 2013;90:904-13.
17. Entwistle N, Hanley M, Hounsell D. Identifying distinctive approaches to studying. High Educ 1979;8:365-80.
18. Newble DI, Clarke RM. The approaches to learning of students in a traditional and in an innovative problem-based medical school. Med Educ 1986;20:267-73.
19. Newble DI, Entwistle NJ. Learning styles and approaches: Implications for medical education. Med Educ 1986;20:162-75.
20. Biggs J. Student Approaches to Learning and Studying. Research Monograph, Australian Education Research and Development, 153. Available from: https://eric.ed.gov/?id=ED308201. [Last accessed on 2021 Jul 25].
21. Trigwell K, Prosser M. Improving the quality of student learning: The influence of learning context and student approaches to learning on learning outcomes. High Educ 1991;22:251-66.
22. Biggs J. Teaching for Quality Learning at University. 2nd ed. Buckingham: Society for Research into Higher Education and Open University Press; 2003.
23. Biggs JB. Individual and group differences in study processes. Br J Educ Psychol 1978;48:266-79.
24. Snelgrove SR. Approaches to learning of student nurses. Nurse Educ Today 2004;24:605-14.
25. Mogr V, Malba A. Approaches to learning among Ghanaian students following a PBL-based medical. Educ Med J 2015;7:38-45.
26. Biggs J. Study Process Questionnaire Manual. Student Approaches to Learning and Studying, Australian Education Research and Development, 53. Available from: http://files.eric.ed.gov/fulltext/ED308200.pdf. [Last accessed on 2021 Jul 25].
27. Professional Nursing in Oman. Available from: https://minoritynurse.com/professional-nursing-in-oman/. [Last accessed on 2021 Jul 25].
28. Why are There so Few Men in Nursing? Nursing Times; 2008. Available from: https://www.nursingtimes.net/archive/

why-are-theresofew-men-in-nursing-03-03-2008. [Last accessed on 2021 Jul 25].
29. Mohamed NA, Abdulhadi NN, Al-Maniri AA, Al-Lawati NR, Al-Qasmi AM. The trend of feminization of doctors' workforce in Oman: Is it a phenomenon that could rouse the health system? Hum Resour Health 2018;16:19.
30. Smith CF, Mathias H. An investigation into medical students' approaches to anatomy learning in a systems-based prosection course. Clin Anat 2007;20:843-8.
31. Pawlina W, Romrell LJ, Rarey KE, Larkin LH. Problem-based learning with gross anatomy specimens: One-year trial. Clin Anat 1991;4:298-306.
32. White MT, Welch K. Does gender predict performance of novices undergoing Fundamentals of Laparoscopic Surgery (FLS) training? Am J Surg 2012;203:397-400.
33. Pokay P, Blumenfeld Phyllis C. Predicting achievement early and late in the semester: The role of motivation and use of learning strategies. J Educ Psychol 1990;82:41-50.
34. Patrick H, Ryan AM, Pintrich PR. The differential impact of extrinsic and mastery goal orientations on males' and females' self-regulated learning. Learn Individ Differ 1999;11:15371.
35. Shah DK, Piryani S, Piryani RM, Islam MN, Jha RK, Deo GP. Medical students' perceptions of their learning environment during clinical years at Chitwan Medical College in Nepal. Adv Med Educ Pract 2019;10:555-62.
36. Ostapczuk MS, Hugger A, de Bruin J, Ritz-Timme S, Rotthoff T. DREEM on, dentists! Students' perceptions of the educational environment in a German dental school as measured by the Dundee Ready Education Environment Measure. Eur J Dent Educ 2012;16:67-77.
37. Kennedy C, Lilley P, Kiss L, Littvay L, Harden RM. 2017, Curriculum Trends in Medical Education in Europe in the 21st Century. Association for Medical Education in Europe Conference; 2013. Available from: http://www.medine2.com/Public/docs/outputs/wp5/DV5.18.1_CURRICULUM_TRENDS_FINL_REPORT.pdf. [Last accessed on 2021 Jul 27].
38. Ahmed Y, Taha MH, Al-Neel S, Gaffar AM. Students' perception of the learning environment and its relation to their study year and performance in Sudan. Int J Med Educ 2018;9:145-50.
39. Wu H, Li S, Zheng J, Guo J. Medical students' motivation and academic performance: The mediating roles of self-efficacy and learning engagement. Med Educ Online 2020;25:1742964.
40. Johnson SN. Cognitive Cognitive Processes in Under Undergraduate Anatomy and Physiology. Physiology Courses. Available from: https://tigerprints.clemson.edu/cgi/viewcontent.cgi?article=3500&context=all_dissertations. [Last accessed on 2021 Jul 25].
41. Notebaert AJ. Student perceptions about learning anatomy. Iowa Research Online; 2009. Available from: https://ir.uiowa.edu/etd/312/. [Last accessed on 2021 Jul 27].
42. van Uden JM, Rietzen H, Pieters JM. Engaging students: The role of teacher beliefs and interpersonal teacher behavior in fostering student engagement in vocational education. Teach Teach Educ 2014;37:21-32.
43. Takase M, Niitani M, Imai T. What educators could do to facilitate students' use of a deep approach to learning: A multisite cross-sectional design. Nurse Educ Today 2020;89:104422.
44. Chan LK, Pawlina W. Artificial intelligence or natural stupidity? Deep learning or superficial teaching? Anat Sci Educ 2020;13:5-7.

Original Article

Extra Virgin Olive Oil Prevents Renal Histopathological Damage in Arsenic Exposed Albino Rats

Abstract

Introduction: To study the protective effect of extra virgin olive oil (EVOO) on histopathological changes induced by arsenic in the kidneys of albino rats. Randomized control trial. November 1, 2017–November 30, 2017 at National Institute of Health. **Material and Methods:** Forty-five male adult albino rats were placed in three cages having 15 rats each. Distilled water was given to the rats of control Group I for 30 days. The dose of sodium arsenite given to rats was 40 mg per kg per day dissolved in drinking water for 30 days. Olive oil of 0.2 ml per day was only given to Group III rats for 30 days along with sodium arsenite. In dissection was done after 30 days and their kidneys were approached and dissected out for histological changes. **Results:** EVOO has ameliorated the microscopic quantitative and qualitative histological changes induced by arsenic on both kidneys of albino rats. Olive oil had significantly prevented the increase in the diameter of the proximal convoluted tubule (PCT). **Discussion and Conclusion:** The present study demonstrates that EVOO prevents the quantitative and qualitative histological changes caused by arsenic on kidneys which include the diameter of PCT and distal convoluted tubule, the diameter of glomeruli, width of bowman's space, and loss of brush border.

Keywords: *Drinking water, kidney tubules, leukocytes, male rats, olive oil, sodium arsenite*

Minahil Haq, Shabana Ali[1], Hira Waqas Cheemal[1], Huma Beenish[1], Naseeruddin Sheikh[1], Hassan Mumtaz[2]

Departments of Anatomy Islamic International Medical College, Rawalpindi, Pakistan, [1]Department of Forensic Medicine, Rawalpindi Medical College, Rawalpindi, Pakistan, [2]Public Health Scholar, Health Services Academy, Pakistan

Introduction

The beneficial effects of olive oil are mainly due to its high oleic acid content. Its strong antioxidant properties are due to the presence of phenolic components. The kidney performs its vital role in the infiltration of blood and excretion of waste compounds through the various parts of its nephron.[1] It has various parts which including the Bowman's capsule which surrounds the glomerulus. Filtration of blood takes place in the medulla through a loop of Henle and collecting tubules, both of which are found in the medulla.[2] Among various metalloids which affect the organs of the human body, arsenic is a naturally occurring metalloid. It is the most predominant global environmental toxin which causes oxidative damage to the kidney. Arsenic in drinking water causes proteinuria, albuminuria, and chronic kidney disease (CKD) which is determined by decreased glomerular filtration rate.[3] The renal biopsies of patients who are exposed to arsenic showed acute tubular necrosis causing acute renal failure. Some patients may develop renal cortical necrosis (RCN), diffuse interstitial fibrosis which ultimately leads to CKD.[4] Arsenic in drinking water is about 200–300 µg per l. This causes a high mortality rate due to diabetes mellitus, kidney disease, and cardiovascular diseases. The inorganic arsenic is distributed throughout the body and is taken up by the cells in tissues.[5]

It is present in water, soil, and even in some types of food.[4] As a result of arsenic contamination from industrial operations and groundwater overdrawn for irrigation, drinking water is the primary source of arsenic exposure to living organisms (0.01–3.7 mg/l).[6] Arsenic contaminated groundwater is extensively utilized both for irrigation and drinking nearly in all areas of Pakistan. The groundwater of 32 districts of Punjab is contaminated with a toxic level of arsenic. According to the World Health Organization (WHO), drinking water should be having a cutoff value for arsenic to be <10 µg/l.[7] A nationwide survey of drinking water conducted in 35 of 104 districts show that only 9% of samples have arsenic levels meeting the WHO standard of 10 ppb. In Sindh, the arsenic level in

How to cite this article: Haq M, Ali S, Cheemal HW, Beenish H, Sheikh N, Mumtaz H. Extra virgin olive oil prevents renal histopathological damage in arsenic exposed albino rats. J Anat Soc India 2023;72:37-42.

Article Info

Received: 24 November 2021
Revised: 08 February 2022
Accepted: 25 July 2022
Available online: 24 March 2023

Address for correspondence:
Dr. Hira Waqas Cheemal, Department of Anatomy, Islamic International Medical College, Riphah International University, Islamabad, Pakistan. E-mail: hirawaqas.cheema@riphah.edu.pk

Access this article online

Website: www.jasi.org.in
DOI: 10.4103/jasi.jasi_190_21
Quick Response Code:

groundwater is 96 μg per l and 157 μg per l in surface water.[8]

In Pakistan, an important cause of CKD is the occurrence of arsenic and heavy metals in the feed of poultry chicken. Therefore, arsenic can be transmitted to the human body by eating chicken.[1,9] The increased production of reactive oxygen species (ROS) by arsenic causes raised lipid peroxidation in the hepatic and renal tissue. The activity of antioxidant enzymes such as superoxide dismutase and catalase is decreased leading to reduced glutathione content in the kidney.[10,11] Distortion of cortical cellular architecture, tubular atrophy, and necrosis along with densely packed red blood cells in the glomerulus as well as both degenerative and atrophic changes have been reported. The RCN involves both tubules and interstitium.[12]

Antioxidants such as olive oil may reduce the effect of arsenic on the kidney.[3] Olive oil possesses great health benefits such as the prevention of coronary heart disease, cancers, and modification in immune responses. It has anti-apoptotic, anti-inflammatory, and anti-oxidative properties as it protects the tissues against damage caused by oxidative stress.[13] There is the ability of extra virgin olive oil (EVOO) to alter the cell membrane structure and to reduce oxidative injury of compounds.[14]

The antioxidant effect of EVOO depends upon the amount of oleuropein and tyrosol.[15] The use of olive oil has also improved renal histoarchitecture including glomerular fragmentation, enlargement of Bowman's space, hemorrhage, infiltration of leukocytes, and tubular dilation caused by acrylamide[16] based on its properties, olive oil may be effective in protecting kidneys from arsenic-induced histological changes. In Pakistan, epidemiological data show that CKD is progressively increasing due to arsenic use[17] while its awareness is very poor among common as well as medical officers and pg trainees.[18]

The objective of our study is to determine the association of high levels of arsenic in the body with kidney damage and also find out the ameliorative effect of EVOO.

Material and Methods

The study was conducted at the Islamic International Medical College after approval from the ethical review committee. The duration of the study was 4 weeks from November 1, 2017 to November 30, 2017. Forty-five adult male albino rats, 250–300 g, were procured. All rats included were 2–4 months of age and those with any obvious congenital anomaly and female rats were excluded to avoid their mating with males. Under the supervision of animal house National Institute of Health, rats were kept in a well-ventilated room with alternating 12 h light and dark cycle at 20°C–26°C temperature. They were kept in three cages 15 rats per cage in a controlled standard living environment suitable to their class with an adjusted diet. Rats in the control group consumed distilled water as drinking water for 4 weeks. Group II rats consumed sodium arsenite (40 mg/kg) for 4 weeks, while rats in Group III sodium arsenite (40 mg/kg) along with olive oil 0.2 ml/day for 4 weeks. After 4 weeks, all rats were euthanized and their kidneys were dissected. H and E staining of control and experimental groups was done. Renal corpuscle, tubule, and interstitium were observed in the renal cortex of each slide at four different fields and the mean of all readings was taken as a single reading. The diameter of renal glomerulus and width of Bowman's space was measured by method,[19] as shown in Figure 1.

The following histological parameters were observed in the slides in detail under ×10 and ×40 power of light microscope by using image J software. n kidneys of the experimental group.

The diameter of proximal and distal convoluted tubule (DCT) was noted in renal tubule, whereas width of Bowman's space and the diameter of the glomerulus were noted in the renal corpuscle.

After accomplishment of 4 weeks duration of the experiment, rats were anesthetized with chloroform and dissected.

After fixation and embedding, eosin and hematoxylin stains were used for the histological section.

Results

The leukocyte or white blood cell which includes plasma cells, lymphocytes, neutrophils, and macrophages was counted in four areas of one slide. No leukocytes are found in control Group I, whereas the count of leukocytes in Group II and Group III was 32 and 13, respectively. As *P* value in the comparison of Groups I and III are 0.375 which is ≥0.05, so it is insignificant. The mean width of Bowman's space was 21.84 um in Group II, which was increased due to the use of arsenic as compared to

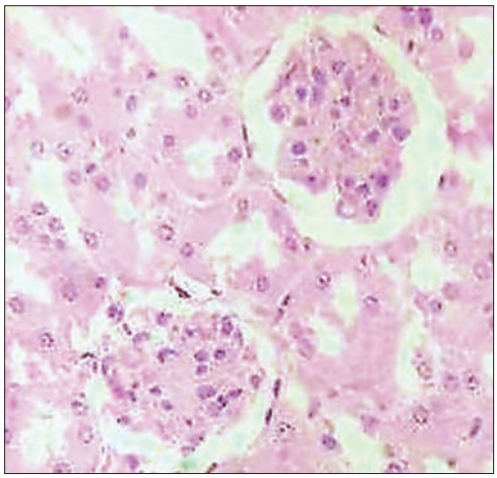

Figure 1: Shows the method used for the determination of glomerular radius and width of Bowman capsule with the help of triangle drawn

control Group I. The use of olive oil in Group III has significantly prevented the increase in width of Bowman's space as it was 12.55 um. As the *P* value in comparison of Groups I and III are 0.330 which is ≥0.05, this shows that difference of mean width of Bowman space between these two groups is insignificant showing that olive oil has significantly decreased leukocyte count. It is shown in [Table 1 and Figure 2].

The mean diameter of the glomerulus in Group I was 104.72 um which was decreased to 80.86um in Group II due to the use of arsenic as Bowman's space was enlarged. The use of olive oil in Group III prevented the decrease in glomerular diameter which was found to be 93.5 um. The *P* value for the comparison of Groups II and III was found to be 0.23 (≥0.05); therefore, it is statistically insignificant. This proves that olive oil has not significantly improved the decrease in the diameter of glomeruli caused by arsenic in Group III [Table 2 and Figure 2].

The mean diameter of proximal convoluted tubule (PCT) in Group I was 30.94um which was increased to 49.11um in Group II due to the use of arsenic which caused loss of brush border. The use of olive oil in Group III prevented the increase in PCT diameter which was found to be 35.95um. The *P* value for the comparison of all groups is <0.05 which is highly significant. This proves that olive oil has significantly prevented the increase in diameter of PCT caused by arsenic in Group III [Table 3 and Figure 2].

The mean diameter of DCT in Group I was 52.19 μm which was increased to 96.16um in group II due to the use of arsenic. The use of olive oil in Group III prevented the increase in DCT diameter which was found to be 66.04 μm. The *P* value for the comparison of all groups is 0.000 which is highly significant. This proves that olive oil has significantly improved the increase in diameter of DCT caused by arsenic in Group III [Table 3 and Figure 2].

All the rats in the control group showed a brush border of PCT. 87% of experimental animals in Group II showed loss of brush border of PCT. In Group III, only 5% of rats showed loss of brush border in PCT, whereas 10% showed the presence of brush border in PCT. In this way, olive oil has significantly decreased the number of rats in Group III showing loss of brush border of PCT. *P* = 0.000 as shown in Figure 3.

Discussion

The arsenic concentration in drinking water of various regions of Pakistan including KPK, Rahimyarkhan, and Bahawalpur is 1.56 μg/l. 10 to 50 μg/l, and 0–10 μg/l.[20] In district Multan,

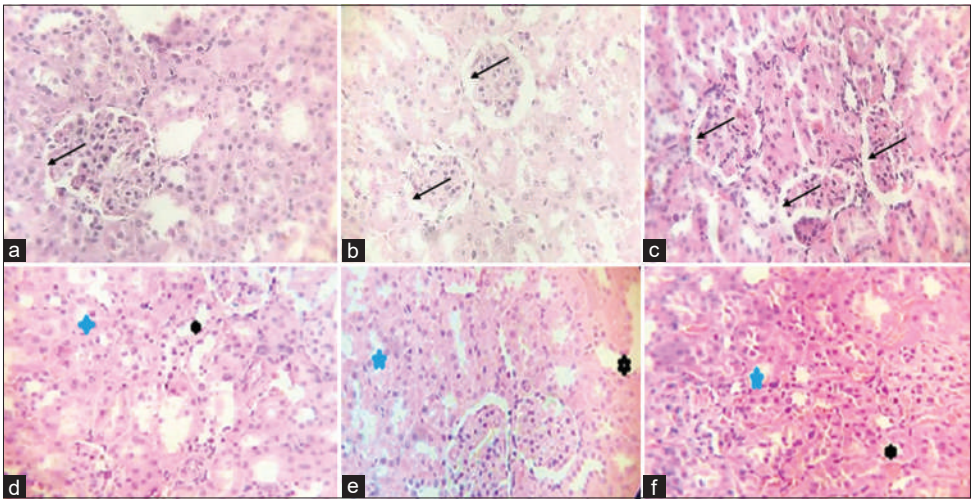

Figure 2: (a) Shows the change in the urinary space (μm) indicated by arrows and (b) shows the change in diameter of PCT and DCT indicated by stars Figure shows (c) olive oil group with decreased bowman's space (d) control group, (e) arsenic group and (f) olive oil and arsenic group. Blue stars for the lumen of PCT while black stars for the lumen of DCT (a = control group, b = Arsenic group, c = Arsenic with olive oil group). PCT: Proximal convoluted tubule. DCT: Distal convoluted tubule

Table 1: Group wise distribution and multiple comparisons of mean leukocyte count in the renal interstitium of control and experimental groups of albino rats

Groups	Mean	SEM	*P*	Comparison	Mean difference	*P*
Group I control	0	0.00	0.000	I versus II	0.317	0.000
Group II experimental arsenic	32	1.84		I versus III	0.043	0.375
Group III experimental arsenic and olive oil	13	0.883		II versus III	0.274	0.000
P	0.000*					

**p* value is 0.000, SEM: Standard error of the mean

Table 2: Group wise distribution and multiple comparisons of a width of Bowman's space and diameter of the glomerulus in the renal interstitium of control and experimental groups of albino rats

Groups	Parameters	Mean	SEM	Comparison	Mean difference	*P*
Group I control	Width of Bowman's space	11.36	0.36	I versus II	10.48	0.000
	Diameter of glomerulus	104.72	3.33		11.92	0.008
Group II experimental arsenic	Width of Bowman's space	21.84	0.795	I versus III	1.196	0.330
	Diameter of glomerulus	80.86	1.307		5.608	0.311
Group III experimental arsenic and olive oil	Width of Bowman's space	12.55	0.51	II versus III	9.288	0.000
	Diameter of glomerulus	93.5	2.95		6.318	0.23
P		0.000*				

**p* value is 0.000, SEM: Standard error of the mean

Table 3: Group wise distribution and multiple comparisons of the diameter of proximal convoluted tubule and distal convoluted tubule in the renal cortex of control and experimental groups pf albino rats

Groups	Parameters	Mean	SEM	Comparison	Mean difference	*P*
Group I control	PCT diameter	30.94	0.921	I versus II	18.17	0.000
	DCT	52.19	1.603		43.96	0.000
Group II experimental arsenic	PCT	49.11	1.62	I versus III	5.011	0.014
	DCT	96.16	2.31		13.85	0.000
Group III experimental arsenic and olive oil	PCT	35.95	0.924	II versus III	13.15	0.000
	DCT	66.04	2.30		30.11	0.000
P		0.000*				

**p* value is 0.000, PCT: Proximal convoluted tubule, DCT: Distal convoluted tubule, SEM: Standard error of the mean

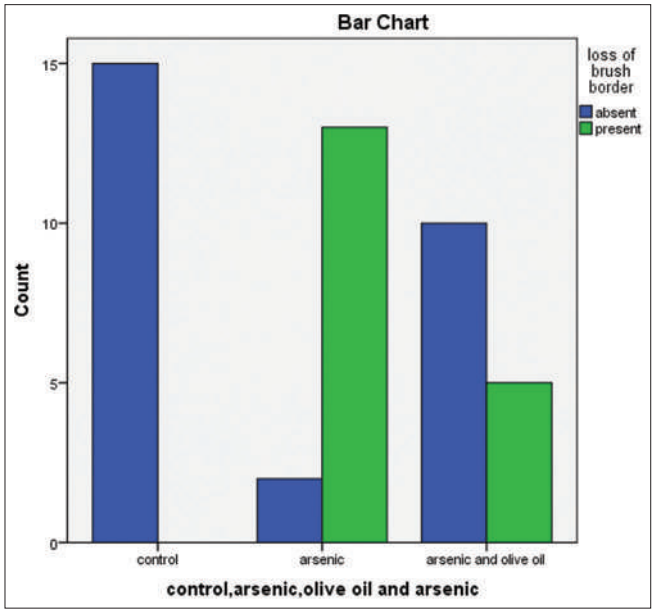

Figure 3: Shows the percentage of rats showing the presence and absence of loss of brush border

DG Khan, Jhang, Leiah, Mianwali, and Muzaffargarh, it is reported between 10 and 50 µg/l.[21] Among natural antioxidants, owing to a protective effect against heavy metals-induced toxicity especially when ROS are involved, olive oil is an integral ingredient. Virgin olive oil (VOO) is a good source of phytochemicals including polyphenolic compounds which have a protective effect on the kidney.[22]

In our study, leukocytes were counted in the renal parenchyma. The mean leukocyte count in Group II was found to be 32, whereas in Group III, it was reduced to 13. The leukocytes are infiltrated in the regions of RCN. RCN is either diffuse cortical necrosis or patchy cortical necrosis depending upon the area of the cortex involved. A study conducted by Alforkan from China in 2019 showed an increase in the number of inflammatory cells in the interstitium of the renal cortex of sodium arsenite-treated rats. Sodium arsenite was given in distilled water in different doses of 10, 30, and 50 ppm for 90 days.[23] In a study conducted by Hewa in 2016, mice were treated with hard water containing arsenic above 0.01 mg for 28 weeks. This long study showed CKD with increased mononuclear infiltrate in the kidney as compared to groups that were given hard water with 0.01 mg per l of arsenic. This range is acceptable according to WHO.[19]

In another study by Kharroubi *et al*.,[27] conducted in 2014 in Berlin, sodium arsenite of 1 and 10 mg per liter was given for 45 and 90 days and showed lymphocytes infiltration which was increased with increased duration of the study. In a study conducted by Ghorbel *et al*.,[16] the use of EVOO of 300 ul for 21 days has significantly reduced leukocyte count in renal interstitium caused by 40 mg per kg of arsenic.[24] Said Elshama in 2016 proved that the use of 100 mg per kg per day naringin and 1.25 ml per kg per day olive oil have renoprotective properties. Both caused a significant decrease in inflammatory cell infiltrates in rats which were treated with 25 mg per kg of cyclosporine.[16] Similarly, in the study conducted by Eman Taha Mohammad from Egypt in 2014, 5 mg/kg of $CdCl_2$ was used orally for 4 weeks. 0.5 ml per kg of VOO

markedly decreased the inflammatory cells infiltrate in rats.[25]

In a recent study, an increase in Bowman's space diameter was caused by 40 mg per l of Arsenic for 4 weeks. In comparison to this study, Kharroubi *et al*. in 2014 used sodium arsenite for 45 and 90 days in a dose of 10 mg per l, this showed expansion in space between glomeruli and Bowman's capsule.[26] In contrast to this study, another study conducted by Kumar *et al*.,[28] of India in June 2016, mice were administered with only 6 mg per kg of Arsenic for 4 weeks followed by lactobacillus for 8 weeks. The Bowman's space was diminished. This was due to the dilation of glomeruli in the early stage of inflammation.[27] In one of the other studies conducted by Zongyuan of China in which arsenic was given in the low dose of 4 mg per kg for 60 days in drinking water, it caused hyperemia and dilation of glomeruli resulting in diminished Bowman's space.[28]

Jemai *et al*. conducted a study in May 2015 in which treatment with olive leaf extracts markedly improved collapsed glomerular tuft causing Bowman's space diameter almost the same as that of control rats.[31] Similarly, a study by Eman taha from Egypt in 2014 used 0.5 ml per kg of VOO orally which significantly reduced dilation of Bowman's space caused by an oral dose of 5 mg per kg of $CdCl_2$ for 4 weeks in rats.[29] Said Elshama in 2016 proved that use of 100 mg per kg per day naringin and 1.25 ml per kg per day olive oil significantly decreased dilation of Bowman's space caused by 25 mg per kg of cyclosporine.[26]

In our study, the use of 40 mg per kg of arsenic increased the diameter of PCT due to loss of brush border and also increased the diameter of DCT along with degeneration of epithelium. A similar study conducted by Kharroubi *et al*. in 2014 in which 10 mg per l of sodium arsenite was given for 45 and 90 days produced similar results of an increase in diameter of PCT and DCT.[27] In contrast to this, a study conducted by Zongyuan *et al*. of China in which mice were exposed to only 4 mg per l of arsenic in drinking water for 60 days, arsenic caused swelling of epithelial cells of PCT and DCT which caused a decrease in diameter. This is the early stage of inflammation. If a toxic level of arsenic is used as in our study, it caused degeneration of cells of DCT resulting in dilation of diameter.[2]

In a study carried by Azab elsaied of Libya in 2017, pretreatment with olive leaf extract in 3 groups with a dose of 25, 50, and 100 mg per kg reduced significantly tubular necrosis and diameter of PCT. These histopathological alterations were caused by CCl_4.[30] Said Elshama in 2016 showed that the use of 100 mg per kg per day naringin and 1.25 ml per kg per day olive oil significantly improved the cellular atrophy of PCT and DCT caused by 25 mg per kg of cyclosporin.[26] Ghorbel *et al*. from Tunisia in 2017 conducted one experimental study in which they used 300 ul of EVOO. It significantly reduced tubular dilation of PCT and DCT.[16]

Conclusion

The present study demonstrates that EVOO prevents the quantitative and qualitative histological changes caused by arsenic on kidneys which include the diameter of PCT and DCT, the diameter of glomeruli, width of Bowman's space, and loss of brush border.

Financial support and sponsorship

Nil.

Conflicts of interest

There are no conflicts of interest.

References

1. Kidney Anatomy, Parts & Function, Renal Cortex, Capsule, Nephron, Calyx, Pyramids (healthpages.org). 2018. p. 1-10. Available from: https://ntp.niehs.nih.gov/nnl/urinary/kidney/kidney-introduction-pdf_508.pdf.
2. Schmidler C. Kidney Anatomy and Function. Available from: http://healthpages.org. [Last accessed on 2022 Jun 27].
3. Zhang Q, Liu Y, Wang H, Ma L, Xia H, Niu J. Preventive Effects of Taurine and Vitamin C on Renal DNA Damage of Mice Exposed to Arsenic. 2009;9:169-72.
4. Robles-Osorio ML, Sabath-Silva E, Sabath E. Arsenic-mediated nephrotoxicity. Ren Fail 2015;37:542-7.
5. Karabulut G, Barlas N. Genotoxic, histologic, immunohistochemical, morphometric and hormonal effects of di-(2-ethylhexyl)-phthalate (DEHP) on reproductive systems in pre-pubertal male rats. Toxicol Res (Camb). 2018;7:859-73.
6. Nakbi A, Tayeb W, Dabbou S, Issaoui M, Grissa AK, Attia N, *et al.* Dietary olive oil effect on antioxidant status and fatty acid profile in the erythrocyte of 2,4-D- exposed rats. Lipids Health Dis 2010;9:89.
7. Singh S, Rana SV. Amelioration of arsenic toxicity by L-Ascorbic acid in laboratory rat. J Environ Biol 2007;28:377-84.
8. Naseem S, McArthur JM. Arsenic and other water-quality issues affecting groundwater, Indus alluvial plain, Pakistan. Hydrol Process 2018;32:1235-53.
9. Imtiaz S, Alam A, Salman B. The role of the poultry industry on kidney and genitourinary health in Pakistan. Pak J Med Sci 2020;36:S67-74.
10. Peters BA, Hall MN, Liu X, Neugut YD, Pilsner JR, Levy D, *et al.* Creatinine, arsenic metabolism, and renal function in an arsenic-exposed population in Bangladesh. PLoS One 2014;9:e113760.
11. Ahmad T, Kahlown MA, Tahir A, Rashid H. Arsenic an Emerging Issue: Experiences from Pakistan. Vol. 2. 30th WEDC International Conference Vientiane, Lao PDR; 2004. p. 459-66.
12. Khattak SA, Polya D, Ali L. Arsenic exposure assessment from ground water sources in Peshawar Basin of Khyber Pakhtunkwa, Pakistan. J Himalayan Earth Sci 2016;49:68-76.
13. Bhattacharya S. Medicinal plants and natural products in amelioration of arsenic toxicity: A short review. Pharm Biol 2017;55:349-54.
14. Fitó M, de la Torre R, Farré-Albaladejo M, Khymenetz O, Marrugat J, Covas MI. Bioavailability and antioxidant effects of olive oil phenolic compounds in humans: A review. Ann Ist

Super Sanita 2007;43:375-81.
15. Restuccia D, Spizzirri UG, Chiricosta S, Puoci F, Altimari I, Picci N. Antioxidant properties of extra virgin olive oil from cerasuola cv olive fruit: Effect of stone removalal. Ital J Food Sci 2011;23:62-71.
16. Ghorbel I, Elwej A, Fendri N, Mnif H, Jamoussi K, Boudawara T, *et al.* Olive oil abrogates acrylamide induced nephrotoxicity by modulating biochemical and histological changes in rats. Ren Fail 2017;39:236-45.
17. Ullah K, Butt G, Masroor I, Kanwal K, Kifayat F. Epidemiology of chronic kidney disease in a Pakistani population. Saudi J Kidney Dis Transpl 2015;26:1307-10.
18. Anees M, Ibrahim M, Adhmi SU, Nazir M. Comparison of awareness about nephrology and kidney diseases amongst doctors in institutes with and without nephrology departments. Pak J Med Sci 2014;30:891-4.
19. Kotyk T, Dey N, Ashour AS, Balas-Timar D, Chakraborty S, Ashour AS, *et al.* Measurement of glomerulus diameter and Bowman's space width of renal albino rats. Comput Methods Programs Biomed 2016;126:143-53.
20. Kitchin KT. Recent advances in arsenic carcinogenesis: Modes of action, animal model systems, and methylated arsenic metabolites. Toxicol Appl Pharmacol 2001;172:249-61.
21. Saha JC, Dikshit AK, Bandyopadhyay M, Saha KC. A review of arsenic poisoning and its effects on human health. Crit Rev Environ Sci Technol 1999;29:281-313.
22. Toor IA, Tahir SN. Study of arsenic concentration levels in Pakistani drinking water. Polish J Environ Stud 2009;18:907-12.
23. Al-Forkan M, Islam S, Akter R, Shameen Alam S, Khaleda L, Rahman Z, *et al*. A sub-chronic exposure study of arsenic on hematological parameters, liver enzyme activities, histological studies and accumulation pattern of arsenic in organs of Wistar albino rats. J Cytol Histol 2016;S5:1-7.
24. Wasana HM, Perera GD, Gunawardena PS, Fernando PS, Bandara J. WHO water quality standards Vs. Synergic effect(s) of fluoride, heavy metals and hardness in drinking water on kidney tissues. Sci Rep 2017;7:42516.
25. Mohammed HA, Okail HA, Ibrahim MA, Emam NM. Influences of olive leaf extract in the kidney of diabetic pregnant mice and their offspring. J Basic Appl Zool 2018;79:3.
26. Pineda J, Herrera A, Antonio MT. Comparison between hepatic and renal effects in rats treated with arsenic and/or antioxidants during gestation and lactation. J Trace Elem Med Biol 2013;27:236-41.
27. Kharroubi W, Dhibi M, Haouas Z, Chreif I, Neffati F, Hammami M, *et al.* Effects of sodium arsenate exposure on liver fatty acid profiles and oxidative stress in rats. Environ Sci Pollut Res Int 2014;21:1648-57.
28. Kumar R, Kumari R, Kumar A, Kumar Ravi V, Ali M. *In vivo* elimination of arsenic through lactobacillus sporogenes. Int J Adv Res 2016;4:1723-8.
29. Mohammed E, Hashem K, Rheim M. Biochemical study on the impact of nigella sativa and virgin olive oils on cadmium-induced nephrotoxicity and neurotoxicity in rats. J Invest Biochem 2014;3:71-8. https://doi.org/10.5455/jib.20140716041908.
30. Azab AE, Albasha MO, Elsayed AS. Prevention of nephropathy by some natural sources of antioxidants. Yangtze Med 2017;1:235-66.
31. Jemai H, Bouaziz M, Fki I, Feki AE, Sayadi S. Hypolipidimic and antioxidant activities of oleuropein and its hydrolysis derivative-rich extracts from Chemlali olive leaves. Chem Biol Interact 2008;176:88–98.

Original Article

An Alternative Route for Petroclival Tumors: Without Mastoidectomy and Superior Petrosal Sinus Ligation: A Cadaveric Study

Abstract

Objective: Retrosigmoid approach and presigmoid approach and its derivatives including retrolabyrinthine, translabyrinthine, and transpetrosal approaches have long been used for reaching posterior and middle cranial fossa. In neurosurgery perspective, many types of tumors arise extradurally and surgical resection of these tumors is still challenging. We aimed to describe a modified way to approach posterior and middle fossa to contribute to the surgical management of petroclival tumors with posterior extension. **Methods:** Modified sigmoid approaches were performed bilaterally in 5 fresh adult cadaver heads. **Results:** In this approach, it was possible to reach the middle and posterior fossa with a single craniotomy. Temporal dura matter was dissected from the temporal bone with extradural gentle dissection. In addition, sigmoid sinus and superior petrosal sinus (SPS) were dissected off from the petrous bone meticulously. Subsequently, the posterolateral superior arcuate petrosectomy was performed with high-speed surgical drill extradurally by protecting the semicircular canal, labyrinthine channel, and cochlea. Dura matter was elevated for 1.5 cm with retractor above the mastoid bone. Dura was opened from an alternative area of Trautmann's triangle. After having exposed and opened the dura, posterior fossa was reached at the level of 7.−8. cranial nerves. **Conclusion:** We described an alternative route which seems to be a feasible way to reach posterior and middle fossa without mastoidectomy and SPS ligation. Notably, this technique can be applicable to petroclival tumor surgery after more anatomic studies with cadaveric specimens.

Keywords: *Extradural sigmoid approach, petroclival tumors, without mastoidectomy, without superior petrosal sinus ligation*

Muhammet Arif Özbek, Ahmet Tulgar Başak[1]

Department of Neurosurgery, Istanbul Medipol University, [1]Department of Neurosurgery, American Hospital, Istanbul, Turkey

Introduction

In neurosurgical practice, petroclival region is quite challenging in terms of microneurosurgical technique. Petroclival tumors usually extend into both the middle and posterior fossa and thereby they pose a significant challenge to the neurosurgeons.[1] Their large size at presentation and proximity to the critical neurovascular structures further complicate the surgical management. The surgical corridor in common use is very deep and narrow, thus rendering current approaches spatially being limited. There are variety of skull base approaches including middle fossa (Kawase and extended middle fossa), retrosigmoid, retrosigmoid intradural suprameatal approach, and combined subtemporal–presigmoid and transpetrosal approaches for the purpose of access to the petroclival region.[1,2]

In accordance with the requirements, classical skull base approaches could be modified or be used in combination. However, the surgeon needs to consider many factors to determine which of these approaches is appropriate for the patient. The general condition, age, current neurological deficits, normal vascular anatomy, planned treatment (palliative/radical), prediction and histopathology of lesion, compartment (s) (intradural/extradural/intra-extradural), extension (midline/lateral extension), tumor size, its relationship with neurovascular structures, experience and the preference of the surgeon are important. Although surgical approaches to this region have been applied for many years, mortality and morbidity rates were quite high. Microneurosurgical experience indicates that the most important reasons for high morbidity and mortality are the difficult and inadequate surgical access to the region, mostly because of giant size of the tumors at diagnosis and suboptimal radiologic evaluation of the relationship between tumor and neurovascular structures.[3-5]

How to cite this article: Özbek MA, Başak AT. An alternative route for petroclival tumors: Without mastoidectomy and superior petrosal sinus ligation: A cadaveric study. J Anat Soc India 2023;72:43-7.

Article Info

Received: 25 January 2021
Revised: 01 December 2021
Accepted: 30 September 2022
Available online: 24 March 2023

Address for correspondence:
Dr. Ahmet Tulgar Başak, Koç Üniversitesi Hastanesi, Davutpaşa Caddesi No: 4, 34010, Topkapi, Istanbul, Turkey.
E-mail: basak_ahmet@hotmail.com

Access this article online

Website: www.jasi.org.in
DOI: 10.4103/jasi.jasi_18_21
Quick Response Code:

Methods

In this study, 5 fresh cadaver heads were harvested. The heads were embalmed in 10% formaldehyde solution and dissected bilaterally so that a total of 10 sides were used. Vessels were not cannulated and not injected with colored latex solution.

Cadaveric heads were placed first in right then left lateral position. Heads were fixed in a headholder (Doro, QR3, USA) and entrenched in lateral decubitus position *(*the zygomatic arch parallel to the floor with the vertex facing the floor, and the mastoid as the highest point). Central temporo-occipital reversed U-shaped skin incision was fashioned around the ear to expose anatomical landmarks clearly. Skin incision was performed starting about 1 cm anterior to the tragus on the root of zygoma and extending posterior to expose the posterior fossa. The superficial and deep temporal fascia was opened and the temporal muscle was then dissected forward from the skull [Figure 1]. A previously described modified temporo-occipital craniotomy was performed.[6,7] For preparation of the temporo-occipital bone flap, burr holes were marked and drilled with Midas Rex Legend high-speed drill (Medtronic, USA). The first burr hole was positioned at the level of zygoma to flush with the floor of the middle fossa dura. The second burr hole was placed 3 cm above the first burr hole. The third burr hole was placed at the occipitomastoid suture 1.5 cm below the asterion, and the fourth burr hole was positioned 2 cm above asterion and above the squamous portion of the occipital bone [Figure 1]. The burr holes were connected with the high-speed drill. A sizeable (4 cm × 8 cm) temporo-occipital craniotomy flap was elevated to expose both the middle and the posterior fossa.

Middle fossa

Middle cranial fossa dura was dissected off from the temporal base from posterior to anterior and elevated gently from middle cranial fossa. The middle meningeal artery was identified at the foramen spinosum. Mandibular nerve (V3) and maxillary nerve (V2) on the floor of middle cranial fossa were identified near the ventrolateral wall of the Meckel's cave. Dorsolateral wall of the Meckel's cave was occupied by superior petrosal sinus (SPS). From this step on, the greater superficial petrosal nerve was dissected and Kawase triangle was exposed. The drilling was limited to this triangle to expose the supratentorial ventral brain stem area.

Posterior fossa

Extradural dissection of sigmoid sinus, superior petrosal sinus, and posterolateral superior arcuate petrosectomy and dural opening

Following the elevation of the craniotomy flap, the transverse sinus, sigmoid sinus (SS) junction was identified. SS was dissected gently from the groove in the mastoid bone with blunt dural dissection. SS dissection was proceeded up to its anatomical limits. After dissection of SS, squamous part of occipital bone was drilled up to the superior border of the mastoid bone. The appearance of mastoid air cells was considered as an anatomical limit. Then, SPS was dissected from SPS groove of petrous bone from lateral to medial. SPS dissection limit was the subarcuate fossa level in the groove of the petrous bone [Figure 2]. The integrity of both sinuses was preserved. The posterior fossa dura was elevated up to 1.5 cm. The posterior wall of the petrous bone was drilled extradurally with high-speed diamond drill. Drilling area; Its inferior border is the subarquat fossa, and its medial border is deep part of posterior semicircular canal. Drilling was started from the groove of SPS from superiorly and continued inferiorly (posterolateral subarcuate petrosectomy) [Figure 3]. Hence, we obtained a rhomboid shaped area. This rhomboid bone cavity was bounded by the dissected part of the SS posteriorly, the subarcuate

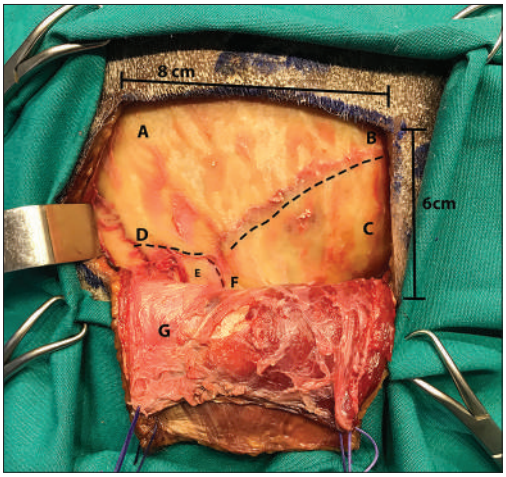

Figure 1: Skin incision. (A) Parietal bone. (B) Squamous suture. (C) Temporal bone. (D) Parietomastoid suture. (E) Mastoid bone. (F) Mastoid part of temporal bone. (G) Temporal muscle

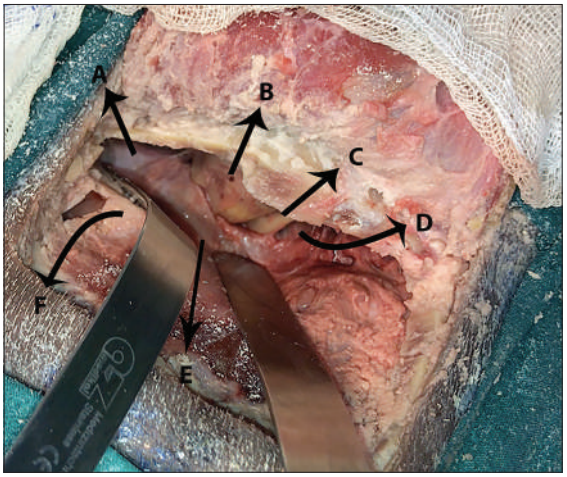

Figure 2: Extradural approach. (A) Middle fossa. (B) Petrous bone. (C) Groove of superior petrosal sinus. (D) Posterior cranial fossa after extradural dissection. (E) Superior petrosal sinus. (F) Dura mater

fossa inferomedially, posterior semicircular canal in petrous bone medially, and the posterior petrosectomy area superolaterally [Figures 4 and 5]. This area was greater than that obtained with the posterior intradural petrous apicectomy. Another novel modification was dural opening which was placed at the level of subarcuate fossa with a linear incision. This is an alternative dural opening to the opening in Trautmann's triangle. After dural opening, facial nerve (CN. VII) and vestibulocochlear nerve (CN. VIII) were exposed at the level of the internal acoustic canal. In addition, infratentorial brain stem and tentorium were visualized medially and superiorly, respectively.

Discussion

The petroclival region is a critical area that harbors vital neurovascular structures and it has anatomical limitations to access. Therefore, the microsurgical resection of the lesions in this area always posed great problems until today. Fortunately, advances in neuroimaging provided better preoperative identification of these lesions and improvements in microsurgical techniques and skull base approaches resulted in more acceptable mortality and morbidity rates. However, the narrow surgical corridors to the petroclival region still stand as a challenging factor.

The suboccipital retrosigmoid approach (RS) approach was first described by Dandy in 1925 and is now widely used in neurosurgery practice. With this approach, it is possible to reach centrolateral tumors, lesions of the mid-clivus and petrous apex, and the tentorium region from the petrosal line to the adhesion angle. The advantages of this approach are it provides a physiological pathway to reach large petroclival masses infiltrating the internal acoustic meatus (IAM) and with a minimal neural tissue injury due to retraction. Minimal cerebellar retraction and a wide surgical opening could be achieved with gentle subarachnoid dissection and maximum cerebrospinal fluid (CSF) drainage. In this approach, mild–to-moderate cerebellar retraction is well tolerated. This becomes important especially in cases of severe brain stem compression due to tumoral mass. However, the main disadvantage of this route is the difficulty to remove the tumor through a narrow corridor bounded by the cranial nerves and vascular structures as well as inadequate exposure of the brain stem. The RS approach can be extended to the petrosal approach for large lesions, and the subtemporal approach can be combined with the transcochlear–translabyrinthine approach.[1,8] The advantage of these combined approaches is that they provide better visualization of the brain stem and facial nerve with minimal brain retraction in large tumors.[9]

Anterior subtemporal approach provides access to the upper and middle clivus and cavernous sinus without excessive temporal lobe retraction.[10,11] The posterior subtemporal approach may be associated with a high morbidity because of potential injury to vein of Labbé and cerebral edema because of temporal lobe retraction. However, the anterior temporal approach is particularly advantageous when combined with the transsylvian approach, and when an extensive sylvian dissection is performed, the temporal lobe retraction is

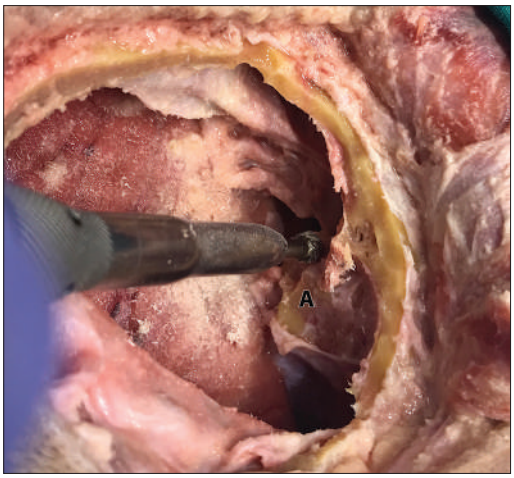

Figure 3: (A) Posterolateral subarcuate petrosectomy (drilling process)

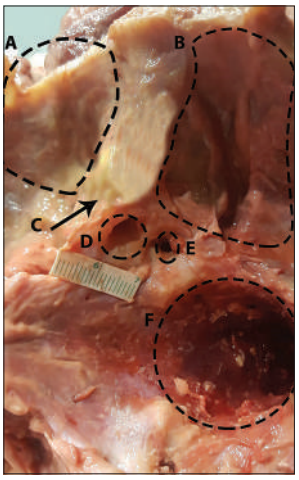

Figure 4: After posterolateral subarcuate petrosectomy. (A) Middle fossa. (B) Posterior fossa. (C) Posterolateral subarcuate petrosectomy area. (D) Internal acoustic canal. (E) Jugular foramen. (F) Foramen magnum

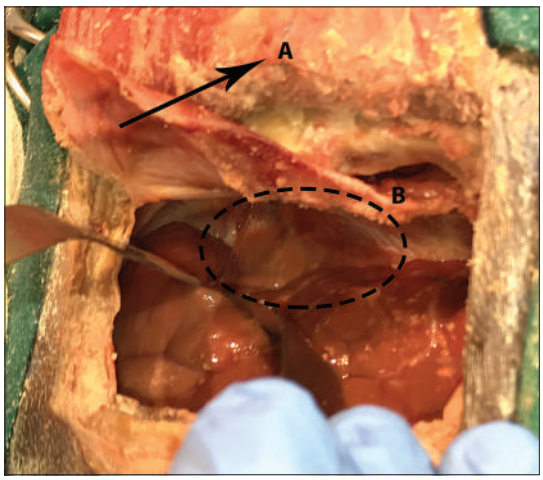

Figure 5: Intradural view after posterolateral subarcuate petrosectomy (A) Dura mater (B) Posterolateral subarcuate petrosectomy area

minimized compared to the subtemporal approach. With this combination, an excellent opening is provided for resection of the upper clivus and tentorial notch tumors. In selected cases, zygomatic osteotomy or orbitozygomatic ostetomy may be added to the cavernous sinus approach to provide a clival angle of view extending from the parasellar area to the basion. This approach is also suitable for opening the ipsilateral side of the upper clivus and the anterior temporal notch. Mid-clivus tentorium can be seen easily by cutting or suturing the tentorial edge toward the lateral side.[12,13]

Transpetrosal approaches offer direct access to the upper and middle clivus when combined with the other approaches as suggested by many authors. One major drawback of transpetrosal approaches is even if they provide direct access to the supratentorial and infratentorial compartment, they have a high morbidity rate. Anterior transpetrosal approach was first used by Kawase in the sphenopetroclival meningiomas adjacent to the CNVII and provided access to the middle clivus and cavernous sinus.[14] The resection of the petrosal bone in this approach increases the surgical exposure of the petroclival area by allowing the brain stem and the petroclival groove to be exposed laterally.[15] Anterior, posterior, or combined petrosal approaches can be used depending on the extension pattern of the involved tumor. While posterior petrosal approach seems more appropriate for tumors extending to the lateral side of the posterior fossa and to the posterior cavernous sinus in the Meckel's cave, the anterior petrosal approach is more suitable for the exposure of the area adjacent to the anterior cavernous sinus, and for the lesions located on the midline and contralateral area or for those localized in IAM.[16] Anterior extradural petrosal approach for Meckel cave, petroclival region, and brain stem lesions intended to be an excellent surgical way by some authors.[17,18] In patients with large tumors and hearing loss, complete petrosectomy provides the most extensive surgical exposure and it allows anterior, posterior, and lateral exposures in the petroclival area. The disadvantage of this approach is prolonged surgical time during drilling the petrous bone. Postoperative hearing loss is unavoidable in patients who undergo complete petrosectomy and this technique is only preferred in patients with complete hearing loss. There is also a risk of facial nerve injury. Petrosal approach is the most preferred approach for total mass resection, especially in large meningiomas with middle fossa and posterior fossa extension. Large petroclival meningiomas cannot be totally removed even after total petrosectomy and reoperations may be required for residual or recurrent lesions.

The most important common features of these two petrosal approaches are both are using a physiological pathway to access to the lesions, obtaining a wide surgical opening with minimal neurovascular injury, protecting the pertinent arterial and venous anatomy, and to combining with other approaches easily.

In this study, we tried to describe an alternative anatomical route to reach lesions of this region and posterior fossa. As a novel contribution, we tried an alternative route to reach to the intradural space with microdisection of the SS and the SPS extradurally. Mastoidectomy was not required in this approach. So, we could reduce the risk of CSF fistula (otorrhea) which may develop postoperatively. Also in this approach just petrous apicectomy is enough. In addition to these, hearing can be preserved. Obviously, the microdissection of the SPS and the SS from the skull base are difficult tasks and potentially fatal. However, we noticed that the dural thickness of the sinuses fixed to the skull base was thicker than those of the free dural faces. As a result, we offered a new alternative route to the Trautmann's triangle in this cadaveric study.

Advantages of this route are as follows:
1. Direct access to the CN. 7–8 complex
2. Short working distance
3. No need for mastoidectomy
4. No need for petrosal sinus ligation
5. Easy visualization of tumor portions extending to the brain stem
6. Larger surgical area
7. No hearing loss (no need for total petrosectomy) and
8. No potential risk of facial nerve injury (no need for extreme cerebellar retraction).

Disadvantage of this route are as follows:
1. Risk of damage to the sigmoid and SPS during extradural dissection
2. Risk of damage to the superior and posterior semicircular canals during drilling procedure
3. Duration of surgery may be longer (extradural dissection and drilling process may be more time consuming).

Conclusion

Petroclival region tumors are rare in neurosurgical practice and the surgical access to the petroclival area is quite challenging in terms of microneurosurgical technique. Because of the relationship between tumor spread and skull base structures, one or more of the existing skull base approaches may be required. Petroclival region tumor surgery is still a pathology with high morbidity and mortality.

In this cadaveric study, we tried to describe a new and an alternative route for petroclival tumors with posterior fossa portion without mastoidectomy and SPS ligation. Of course, this approach has some advantages and disadvantages. We ponder to find an ideal approach for this region tumors and the main aim is to preserve more vascular and neural structure. For this new idea to become the ideal procedure, much more cadaver work is required and the advantages and disadvantages of its suitability for clinical use need to be determined. We hope this study can be a spark for a brain storming.

Acknowledgment

We gratefully acknowledge the cadaver donors.

Financial support and sponsorship

Nil.

Conflicts of interest

There are no conflicts of interest.

References

1. Al-Mefty O, Borba LA. Skull base chordomas: A management challenge. J Neurosurg 1997;86:182-9.
2. Harsh GR 4th, Sekhar LN. The subtemporal, transcavernous, anterior transpetrosal approach to the upper brain stem and clivus. J Neurosurg 1992;77:709-17.
3. Vinchon M, Pertuzon B, Lejeune JP, Assaker R, Pruvo JP, Christiaens JL. Intradural epidermoid cysts of the cerebellopontine angle: Diagnosis and surgery. Neurosurgery 1995;36:52-6.
4. Schmidek HH, Roberts DW. Schmidek & Sweet Operative Neurosurgical Techniques: Indications, Methods, and Results. Saunders Elsevier: 2006.
5. Sekhar L, Janecka I, Munro I. Surgery of cranial base tumors. Ann Plast Surg 1993;30:572.
6. Bambakidis NC, Kakarla UK, Kim LJ, Nakaji P, Porter RW, Daspit CP, *et al*. Evolution of surgical approaches in the treatment of petroclival meningiomas: A retrospective review. Neurosurgery 2008;62:1182-91.
7. Bambakidis NC, Kakarla UK, Kim LJ, Nakaji P, Porter RW, Daspit CP, *et al*. Evolution of surgical approaches in the treatment of petroclival meningiomas: A retrospective review. Neurosurgery 2007;61:202-9.
8. Gay E, Sekhar LN, Rubinstein E, Wright DC, Sen C, Janecka IP, *et al*. Chordomas and chondrosarcomas of the cranial base: Results and follow-up of 60 patients. Neurosurgery 1995;36:887-96.
9. Drake CG. Bleeding aneurysms of the basilar artery. Direct surgical management in four cases. J Neurosurg 1961;18:230-8.
10. Shiokawa Y, Saito I, Aoki N, Mizutani H. Zygomatic temporopolar approach for basilar artery aneurysms. Neurosurgery 1989;25:793-6.
11. Sen CN, Sekhar LN. The subtemporal and preauricular infratemporal approach to intradural structures ventral to the brain stem. J Neurosurg 1990;73:345-54.
12. Al-Mefty O, Ayoubi S, Smith RR. The petrosal approach: Indications, technique, and results. Acta Neurochir Suppl (Wien) 1991;53:166-70.
13. Samii M, Tatagiba M. Experience with 36 surgical cases of petroclival meningiomas. Acta Neurochir (Wien) 1992;118:27-32.
14. Kawase T, Shiobara R, Toya S. Anterior transpetrosal-transtentorial approach for sphenopetroclival meningiomas: Surgical method and results in 10 patients. Neurosurgery 1991;28:869-75.
15. Jung HW, Yoo H, Paek SH, Choi KS. Long-term outcome and growth rate of subtotally resected petroclival meningiomas: Experience with 38 cases. Neurosurgery 2000;46:567-74.
16. Erkmen K, Pravdenkova S, Al-Mefty O. Surgical management of petroclival meningiomas: Factors determining the choice of approach. Neurosurg Focus 2005;19:E7.
17. Roche PH, Troude L, Peyriere H, Noudel R. The epidural approach to the Meckel's cave: A how I do it. Acta Neurochir (Wien) 2014;156:217-20.
18. Roche PH, Lubrano VF, Noudel R. How I do it: Epidural anterior petrosectomy. Acta Neurochir (Wien) 2011;153:1161-7.

Original Article

Demonstration of the Decrease in Locomotor Activity and Central Nervous System in the Demyelination Model, in Which the Toxic Agent is Realized by Gavage

Serra Ozturk, Gunes Aytac[1], Asiye Kubra Karadas[2], Betul Danisman[3], Gamze Tanriover[2], Narin Derin[4], Gokhan Akkoyunlu[2], Ferah Kizilay[5], Muzaffer Sindel

Departments of Anatomy, [2]Histology and Embryology, and [4]Biophysics, Faculty of Medicine, Akdeniz University, [3]Department of Biophysics, Faculty of Medicine, Ataturk University, [1]Department of Anatomy, Faculty of Medicine, TOBB University of Economics and Technology, [5]Department of Neurology, Faculty of Medicine, Akdeniz University, Antalya, Turkey

Abstract

Introduction: The cuprizone model is a well-established instance to study demyelination and remyelination in rodents. The primary aim of this study was to demonstrate the loss of function in motor activity. Second, it was evaluated together with the changes in the amount of myelin in the ongoing process. **Materials and Methods:** This study is based on the administration of the cuprizone model in male C57BL/6 mice by oral gavage. The advantage of the oral gavage model is that mice were subjected to the equal dose of cuprizone. For this reason, the nonequal in demyelination was minimized. We have designed four groups, including demyelination/control and remyelination/control. **Results:** The results of the walking test and open field test showed that locomotor activity in the demyelination group deteriorated. Increased glial fibrillary acidic protein and decreased myelin basic protein expressions were shown in the corpus callosum of the demyelination group compared to the control and remyelination groups. The g-ratio of the demyelination group was calculated 0.86 ± 0.07, the g-ratio of the demyelination control group was calculated 0.66 ± 0.1, the g-ratio of the remyelination group was calculated 0.83 ± 0.06, and the g-ratio of the remyelination control group was calculated 0.76 ± 0.09. **Discussion and Conclusion:** In conclusion, in this demyelination model, which was applied differently from the literature, in our study, the behavioral effect on motor activity and to what extent it appeared histologically was evaluated. Thus, investigating the loss of function in motor activity as well as histological examination increased the reliability of the model we created in our study.

Keywords: *Animal model, cuprizone, demyelination, oral gavage, ultrastructural*

Introduction

Multiple sclerosis (MS) is a chronic, autoimmune, inflammatory, demyelinating disease that affects the central nervous system (CNS).[1]

Demyelination refers to a pathological process that causes the loss of myelin sheaths without damaging the axons.[2] An animal model is a valuable tool to investigate the mechanisms underlying demyelination and remyelination and to study the cellular responses and interplay during these processes. It provides a enable to clarify assumed therapeutic targets.[3] The most commonly studied animal models of MS are the experimental autoimmune/allergic encephalomyelitis (EAE); viral-induced models, mainly Theiler's murine encephalomyelitis virus (TMEV) infection and consequential chronic demyelination and toxin-induced models of demyelination, such as the cuprizone and the lysophosphatidylcholine (lysolecithin) models.[4]

Basically, EAE is mentioned in autoimmune models.[5] EAE is an excellent model for demonstrating postvaccination encephalitis and general inflammation in the brain and is often used to model the inflammatory properties of MS.[6]

To date, no specific virus has been found to cause the primary cause of MS. Although there is no current virus infection specific to MS, experimental models of virus-induced inflammatory demyelination can provide insight into the basic mechanisms, why such a pathological condition is induced or spreads in the brain and spinal cord.[7] Since the virus-induced pathology has similarities with human MS, the TMEV model is

How to cite this article: Ozturk S, Aytac G, Karadas AK, Danisman B, Tanriover G, Derin N, *et al*. Demonstration of the decrease in locomotor activity and central nervous system in the demyelination model, in which the toxic agent is realized by gavage. J Anat Soc India 2023;72:48-57.

Article Info

Received: 19 August 2021
Revised: 02 December 2022
Accepted: 05 December 2022
Available online: 24 March 2023

Address for correspondence:
Prof. Muzaffer Sindel, Departments of Anatomy, Akdeniz University Faculty of Medicine, Antalya, Turkey.
E-mail: sindelm@akdeniz.edu.tr

Access this article online

Website: www.jasi.org.in
DOI: 10.4103/jasi.jasi_144_21
Quick Response Code:

considered to be a good model. Unlike EAE, the disease in susceptible mice is always chronically progressive. However, there is no consensus on the exact mechanism of demyelination in the TMEV model.[8,9]

In toxic-based models, demyelination is created by chemical agents that are given to animals by various methods. The cuprizone model is one of the most widely used demyelination models due to the ease of application with a diet.[10] The cuprizone is a copper chelator that is used as a toxic agent.[11,12] In the cuprizone model, young adult mice are fed with cuprizone, which leads to significant demyelination of the white matter within weeks.[13] In current cuprizone models, animals fed with either powder diet mixed with cuprizone or cuprizone-containing pellets.[14] It is not known whether cuprizone in the powdered diet was mixed homogeneously, and the amounts of cuprizone intake were the same in different animals.[3] It is also known that cuprizone can easily degrade under room conditions.[15] As a result, in each study, the cuprizone intake of each animal may vary, resulting in a discrepancy in the demyelination of each animal. In our study, oral administration was performed to control the amount of cuprizone administration to solve this problem. The primary objective of this demyelination model, which is applied differently from the existing literature, is to show the behavioral effect of demyelination on motor activity and to evaluate the extent of myelin loss from a histological point of view as a secondary objective. Thus, in addition to histological examination, the investigation of loss of function in motor activity increased the reliability of the model we created in our study.

Materials and Methods

Animals

Male *C57BL/6* mice (8 weeks old) with body weight ranging between 19 and 25 g were obtained from …… Animal Experiment Unit (……, Turkey) and kept at room temperature between 22°C and 24°C, under a 12 hlight–dark cycle and an *ad libitum* diet. All protocols were approved by …… Faculty of Medicine Institutional Animal Care and Use Committee and carried out under the supervision of them (Date-Number of the ethical approval: November 09, 2015-70904504).

Cuprizone treatment

Cuprizone (*Bis[cyclohexanone] oxaldihydrazone*; Sigma-Aldrich Inc.) powder was mixed with corn oil and vortexed to obtain a homogeneous cuprizone–corn oil suspension.[16] Mice were given the suspension by gastric gavage with 10 ml/kg volume.[3] Cuprizone and corn oil suspension were freshly prepared and daily given at 08.00 am. The control groups received 1% corn oil without cuprizone by gavage. A total of 40 mice were randomly divided into four groups, and the researchers performing the gavage and analyzing the data were blind to the treatment.

Experimental design

(i) Demyelination control group (DC) was fed 6 weeks with normal chow and received 1% corn oil without cuprizone by gavage
(ii) Demyelination group (D) was administered 0.2% cuprizone for 6 weeks through gavage daily
(iii) Remyelination control (RC) group which was fed with normal chow for 12 weeks and received 1% corn oil without cuprizone by gavage
(iv) Remyelination group (R) was administered 0.2% cuprizone for 6 weeks via gavage and then fed with normal chow for 6 weeks [Figure 1].

Behavioral experiments

Walking test

All groups underwent a walking test to evaluate the effect of cuprizone on motor impairment at the end of the 2nd, 6th, and 10th weeks of the experiment. The experimental protocol was performed as described before by Inserra *et al*.[17] The tracks were evaluated for four different parameters: toe spread, the distance between the first and fifth toes; intermediate toe spread, the distance between the second and fourth toes; print length, the distance between the third toe and the hind pad; toe to other foot (TOF), the orthogonal distance from the third toe of one paw to the hind pad of the contralateral paw, overlap [Figure 2].[17]

Open-field test

All groups underwent open field test to evaluate the effect of cuprizone on motor impairment of the experiment [Figure 1]. Each animal was placed in an open-field box, and movements were tracked over a 5-min period. Exploratory activity was assessed in an open field, a 50 cm × 50 cm square surrounded by 40-cm high walls. The action track of each animal was recorded by a video camera placed above the area. A video-tracking program (The Noldus EthoVision) was used to evaluate motor function by measuring the total distance moved (cm) and velocity (cm/s).[18]

Tail-flick test

The tail-flick test apparatus (catalog no. TF211-01 TAIL FLICK SYSTEM for Rart's) with a radiant heat source connected to an automatic timer was used to calculate acute nociception response. The heat stimulus was applied 3 cm proximal to the distal end of the tail. The time between the beginning of the heat stimulus to the retraction of the tail from the heat point was measured.[19] A cutoff time of 20 s was used to minimize tissue damage.[20]

Tissue preparation

Brains were carefully removed from the skull. Three brains from each group were randomly selected for electron microscopy. Corpus callosums (CCs) of these brains were dissected for transmission electron microscopy (TEM)

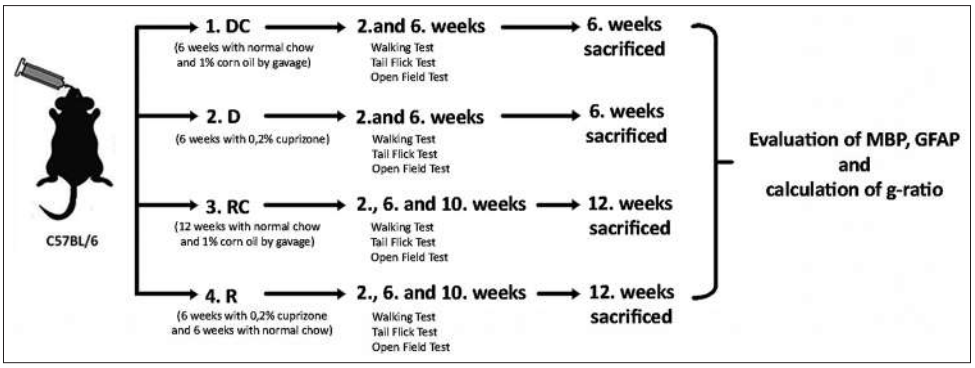

Figure 1: Experimental design. DC: Demyelination control, D: Demyelination, RC: Remyelination control, R: Remyelination

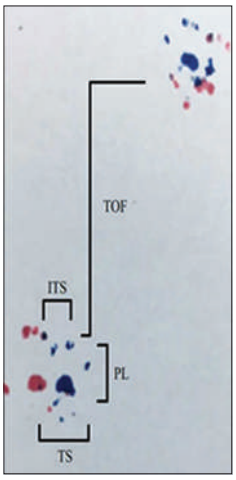

Figure 2: Paw trace pattern of control mouse. TS: Toe spread, PL: Print length, IT: Intermediate toe spread, TOF: Toe to other foot

imaging and were fixed for 2 h at 4°C by immersion in 4% glutaraldehyde in 0.1 m Sorensen's phosphate buffer (pH 7.3), rinsed three times with 6.5% saccharose for 10 min each time and then postfixed in 1% osmium tetroxide for 2 h at room temperature. After rinsing, specimens were dehydrated in ascending concentrations of ethanol, cleared in propylene oxide, and embedded in Araldite CY-212 (SPI-CHEM, Structure Probe, West Chester, PA, USA). Semithin sections (1 μm) were stained with 1% toluidine blue for light microscopy. Ultrathin sections (300 Å), obtained using an LKB ultratome (LKB2188; Ultratome Nova, Bromma, Sweden) and contrasted with saturated uranyl acetate and lead citrate, were examined with a LEO906E TEM (Zeiss, Oberkochen, Germany). The preparation and examination of all specimens were conducted in the TEMGA Unit, Akdeniz University, Antalya, Turkey. The g-ratio is defined as the ratio of the diameter of a given axon and the diameter of the axon plus myelin unit.[21] Images were analyzed in Image-Pro for g-ratio measurements by manually drawing lines across 2 perpendicular diameters each for axons and axons plus myelin. Lengths of the lines (in pixels) as generated by Image-Pro were averaged across the 2 perpendicular measurements and converted to micrometers (μm) using the image scale bars. Approximately 1000 axons and axon plus myelin units were measured for each treatment group.

Seven brains from each group were taken for immunohistochemical staining and fixed in 10% formalin solution overnight and embedded in paraffin. Five μm thick parafin sections were taken for immunohistochemical staining. Immunostaining was performed using standard protocols that described Lindner *et al*.[22] Anti-myelin basic protein (MBP) (#ab40390, Abcam) to evaluate the demyelination and anti-glial fibrillary acidic protein (GFAP) (#ab7260, Abcam) to evaluate the astrogliosis were used as primary antibodies. The CC regions of the brain tissue were analyzed separately and separated into anatomical subdivisions. Sections were examined by a Zeiss-Axioplan (Carl Zeiss GmbH, Jena, Germany) microscope.

Statistical analysis

Micrographs were taken using SPOT Advanced 4.6 at ×20 magnification. All these micrographs were analyzed with Image-J 1.46 (Image Processing and Analysis in Java; US National Institutes of Health, Bethesda, MD; https://imagej.nih.gov/ij/). IBM SPSS Statistics Software version 23 (IBM Corp, Armonk, NY, USA) was used for statistical analysis.

Shapiro–Wilk test was used for testing normality. The numerical data of more than two groups were compared using Kruskal–Wallis Test (for nonnormal distribution) or one-way ANOVA test (for normal distribution). Repeated measures of ANOVA were performed to evaluate the change in time-dependent weights. When a significant difference was found, paired comparisons were performed using Bonferroni–Dunn procedure.

Data obtained from gait analysis and open field tests were analyzed by One-way ANOVA. And then Tukey test was used as *post hoc* test. Data obtained from tail-flick test were tested by Kruskal–Wallis variance analysis and Mann–Whitney-*U* test was used for binary comparison.

G-ratio values are expressed as arithmetic mean ± standard deviation for statistical analysis, nonparametric tests were performed (Kruskal–Wallis test with Dunn multiple

comparisons test, Mann–Whitney *U*-test). Alpha significance level < 0.05 was considered statistically significant.

Results

Behavioral experiments

Gait analysis

A significant difference was observed distance between the groups in terms of TOF and overlap (vertical) values. The TOF values at the 6th week of the group D and the 10th week of the group R were higher than the control groups at the same week ($P < 0.001$). No significant difference was found in the measured overlap (vertical) values, at the 6th week of group D, at the 10th week of the group RC and at the 10th week of the group R. The vertical overlap distance measured at the 6th week of group D was higher than the other three groups ($P < 0.001$) [Figure 3].

Open-field test

Each group was evaluated according to their total distance and velocity parameters according to their baseline data.

No significant difference was found between the repetitive parameters of the control groups. The total distance covered by the mice at the 6th week of the group D was found lesser than at the 6th week of the group DC ($P < 0.01$) [Figure 4a]. The total distance covered by the mice at the 10th week of the group R was higher than in the 6th week of the group D [Figure 4a]. Total distance covered by the mice at the 6th week of the group D was found lesser than the 2nd week of group D ($P < 0.01$) [Figure 4b].

There was no significant difference in terms of velocity between the repetitive parameters of the control groups. However, the speed of the mice in group D at the 6th week was found lower than the 6th week of group DC ($P < 0.01$) [Figure 5a]. The velocity of the mice in the group R at the 10th week was found than 6th week of the group D [Figure 5a]. The speed of the animals in group D at the 6th week was found lower than the 2nd week of group D ($P < 0.01$) [Figures 4 and 5].

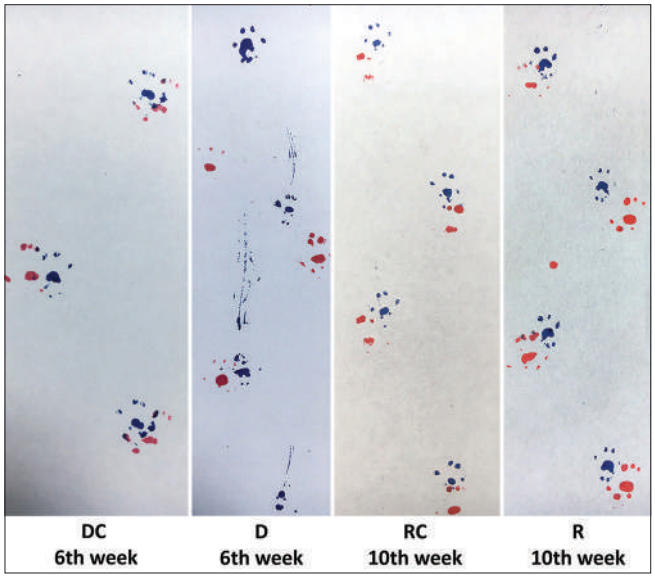

Figure 3: The picture represents walking patterns of the groups. The overlap distance of the foot prints of group D was increased when compared to the DC, RC and R groups and a trace of foot rub ($P < 0.001$). DC: Demyelination control, RC: Remyelination control, R: Remyelination

Tail-flick test

The tail-flick showed that the mean withdrawal time of the group D was significantly higher than the groups DC, RC, and R [Table 1] ($P < 0.001$).

Immunohistochemical findings

Evaluation of corpus callosum

Expression of GFAP in group D was higher than the group DC ($P = 0.017$) and group R ($P < 0.001$) in the total CC [Figure 6a]. The expression of MBP in group D was lower than the group DC ($P < 0,001$) [Figure 6].

Evaluation of splenium, truncus, and genu

In the splenium, GFAP expression was higher in the group D compared to the group R ($P < 0.001$). There was no significant difference between the groups in the truncus area ($P > 0.05$). In the genu, GFAP expression was higher in the group R compared to the group RC ($P = 0.006$). It was lower in the group R compared to the group D ($P = 0.003$) [Figures 7 and 8].

The decrease in the MBP expression due to demyelination in the splenium, truncus, and genu areas of CC was noteworthy. In the splenium, genu and truncus MBP expression was lower in the group D when compared to the group DC ($P < 0.001$). MBP expression in the genu was higher in the group R when compared to the group D ($P = 0.042$) [Figures 9 and 10].

Evaluation of electron microscopy

The g-ratio of the groups was calculated as follows: group D − 0.86 ± 0.07; group DC − 0.66 ± 0.1; group R − 0.83 ± 0.06; group RC − 0.76 ± 0.09. In the demyelination group, the intensity of MBP expression was lower when compared with the group DC [Figures 11 and 12].

Table 1: Tail-flick test

Groups	*n*	Weeks	Mean (s)	SE
Demyelination	10	6	2.53	0.42
Demyelination control	10	6	7.22	0.74
Remyelination	10	10	3.23	0.70
Remyelination control	10	10	3.40	0.76
Total	40	10	4.49	0.46

The time from onset of stimulation to the withdrawal of the tail from heat source. The tail-flick showed that the mean withdrawal time of group demyelination was significantly higher than other groups. SE: Standart error

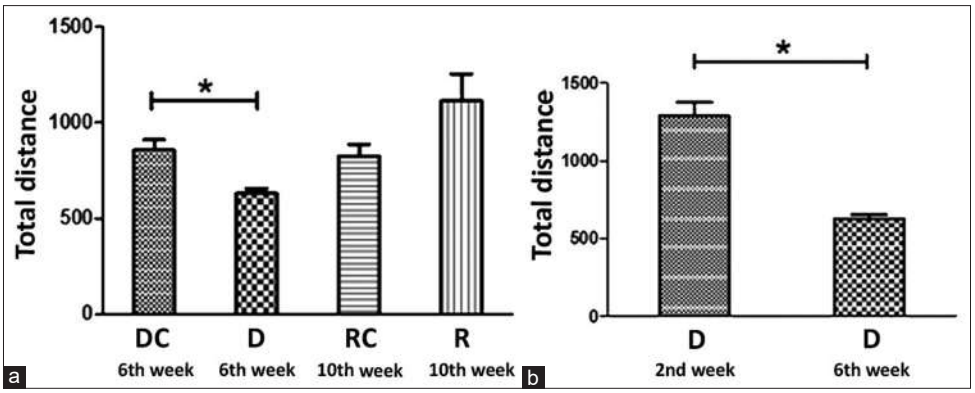

Figure 4: (a) Comparison the total distance at 6th week of the group D and to the group DC (*P < 0.01); (b) Comparison the total distance at the 2nd and 6th weeks of the group D. DC: Demyelination control, D: Demyelination

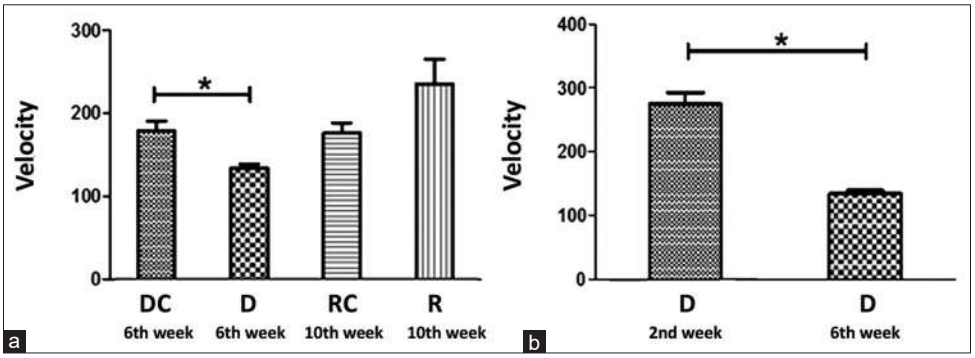

Figure 5: (a) The rates were lower in the 6th week of group D when compared to the group DC (*P < 0.01). (b) The rates were decreased in the 6th week of group D when compared to the 2nd week (*P < 0.01). D: Demyelination

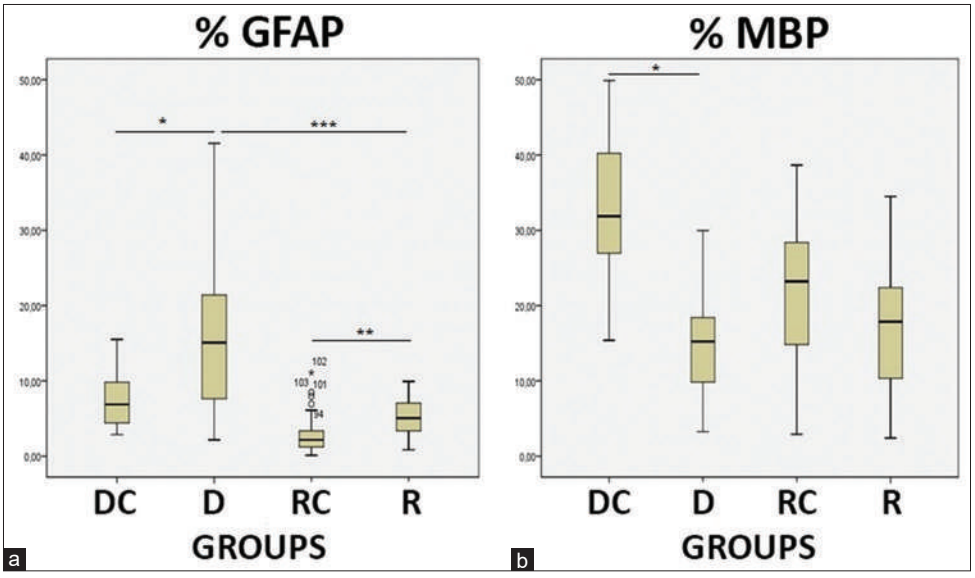

Figure 6: The box plots shows persentages of GFAP and MBP expression in total corpus callosum. (a) Persentages of GFAP (*P < 0.017, **P < 0.001, ***P < 0,001), (b) Persentages of MBP (*P < 0.001). GFAP: Glial fibrillary acidic protein, MBP: Myelin basic protein

Discussion

MS is a chronic neuroinflammatory disease that affects more than 2 million people worldwide.[23] To explain the pathogenesis of this disease, several different animal models have been described.[24] Although there are many current studies on the EAE model in the literature, some researchers have stated that limiting this mechanism in EAE cannot carry the research further.[25-27] This has led to the preference of alternative models. The major disadvantages of viral models are their direct viral effects, antiviral immunity, and the presence of complex mechanisms

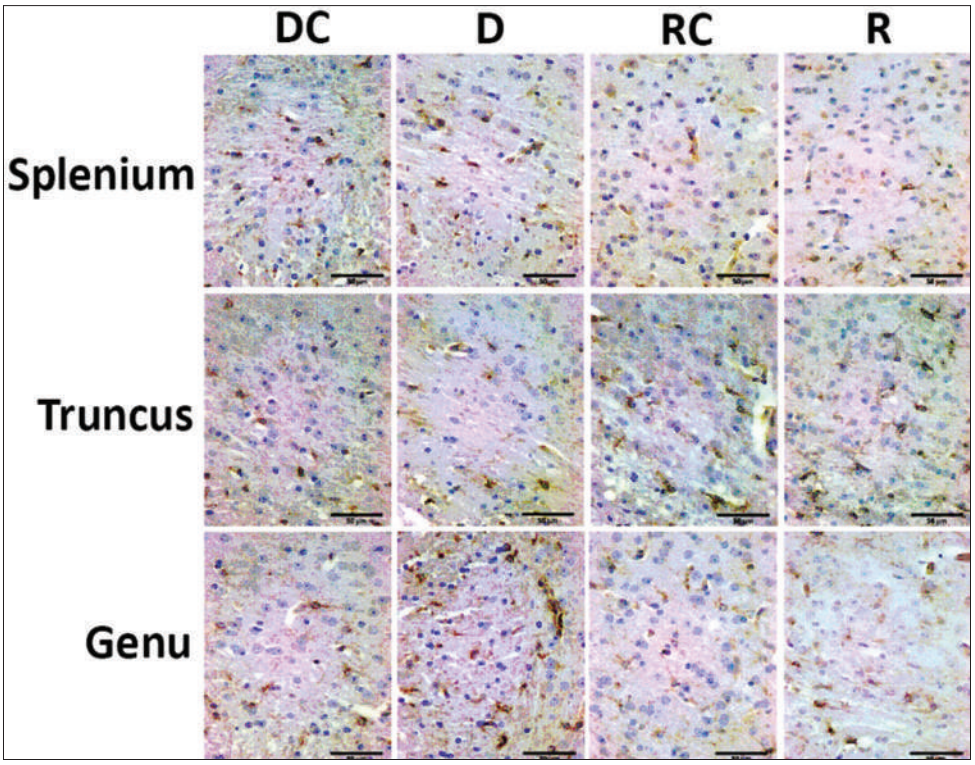

Figure 7: GFAP immunoreaction in the parts of the corpus callosum. Scale bars 50 μm. GFAP: Glial fibrillary acidic protein

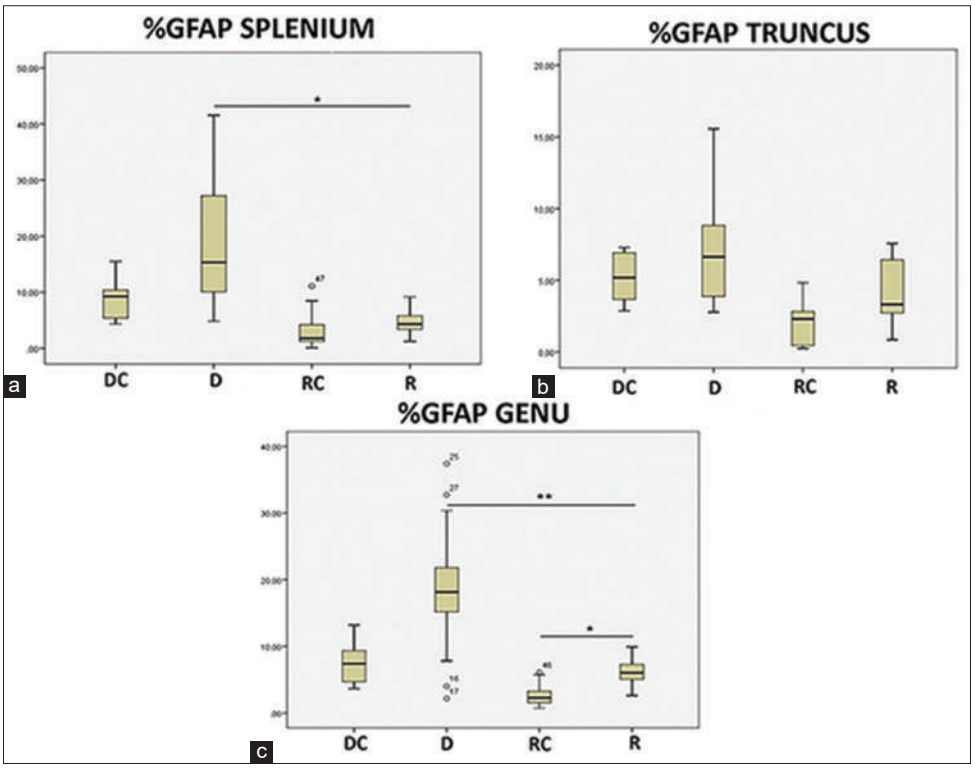

Figure 8: The box plots shows persentages of GFAP expression in splenium, truncus and genu parts of the corpus callosum. (a) In the splenium (P* < 0.001), (b) In the truncus, (c) In the genu (**P* = 0,006, ***P* = 0.003). GFAP: Glial fibrillary acidic protein**

involving additional autoimmune steps. Furthermore, the demonstration of the role of viruses in MS pathogenesis has been reported to be indirect and limited.[7] Among these models, the toxic models are useful to study both demyelination and remyelination mechanisms. One of the agents used to create toxic models, cuprizone, provides a

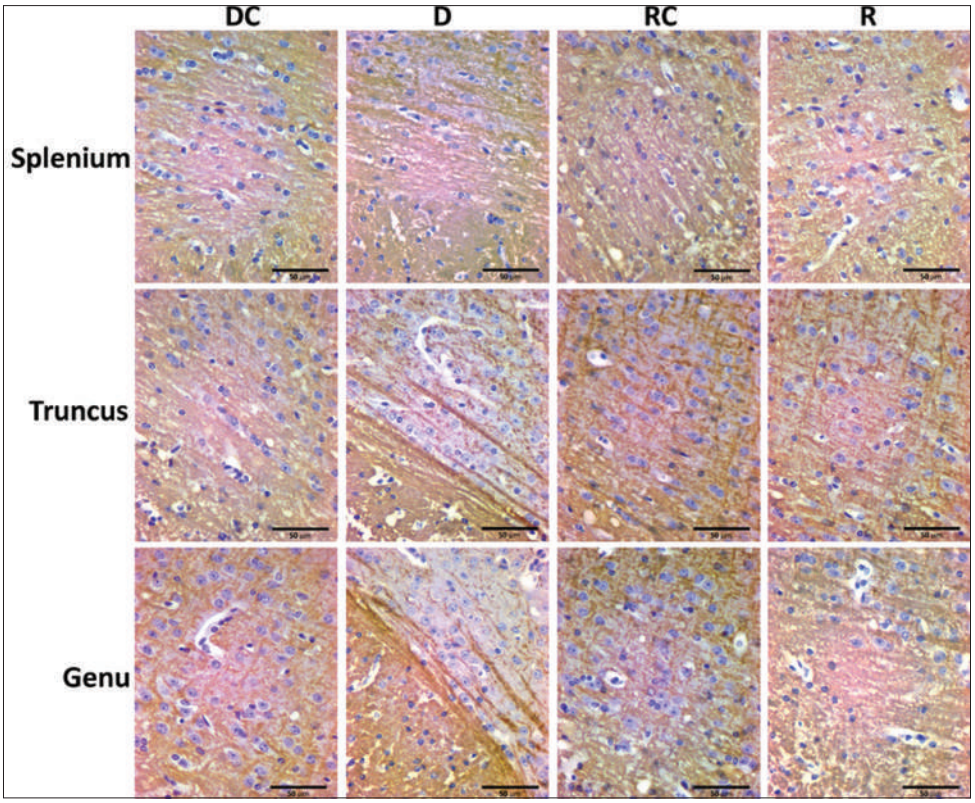

Figure 9: MBP immunoreaction in the parts of the corpus callosum. Scale bars 50 μm. MBP: Myelin basic protein

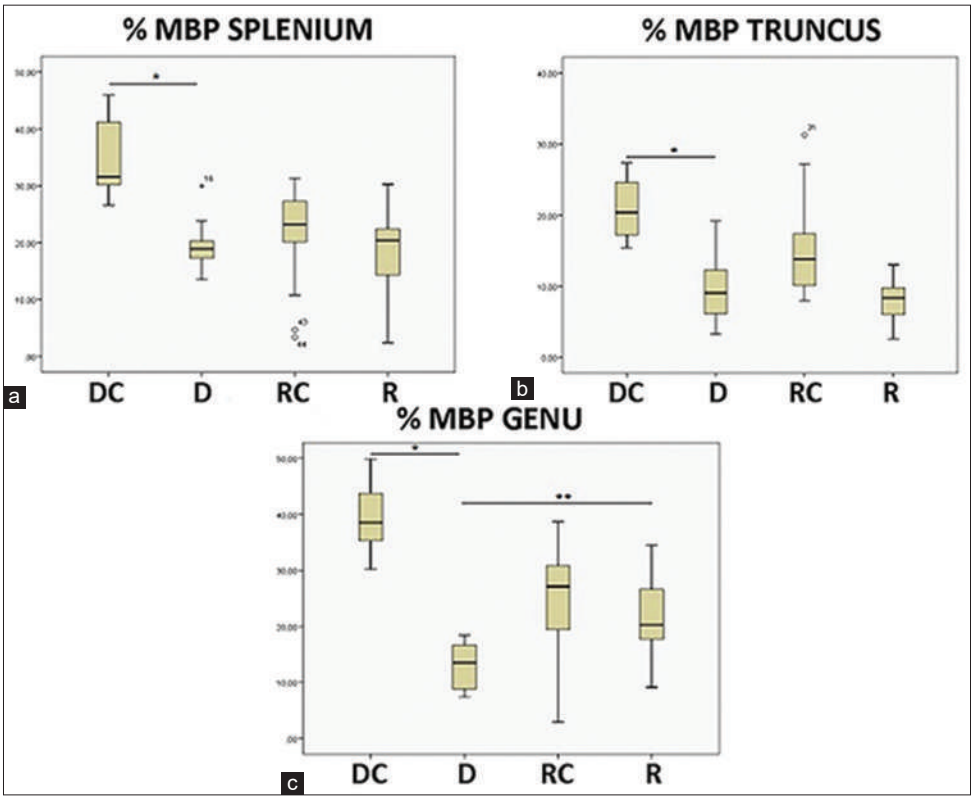

Figure 10: The box plots shows persentages of MBP expression in splenium, truncus and genu parts of the corpus callosum. (a) In the splenium (P* < 0.001), (b) In the truncus (**P* < 0,001), (c) in the genu (**P* < 0.001, ** *P* = 0.042). MBP: Myelin basic protein**

consistent, anatomically reproducible demyelination and spontaneous remyelination.[28-30] The available literature revealed that cuprizon can be administered to mice in a variety of different ways to induce demyelination.

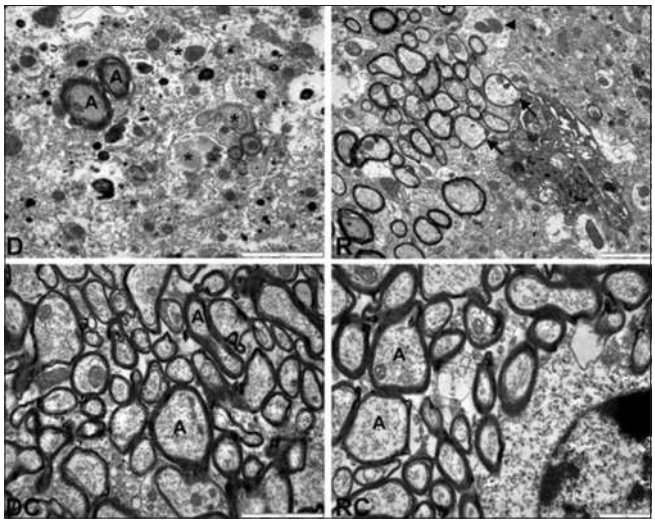

Figure 11: Electron microscopy was performed on cross-sections of the corpus callosum. A significantly increased g-ratio was detectable in group D compared to DC group (*); decreasing myelin sheat, (A); points to healthy myelin sheat, (arrows); newly formed myelin fibers. Scale bars = 2μm

It is emphasized in the literature that among these application methods oral gavage has several advantages to the other methods. They said that the administration of cuprizone through oral gavage minimizes the difference in demyelination between animals and thus creates a consistent model for pharmacological assessments.[3] In our study, both the changes in the locomotor activity of the mouse and the histological reflection of demyelination were evaluated together in the MS model created by oral gavage. It was designed to be able to see responses in both the periphery and the CNS following the formation of the mouse model with cuprizone, which is preferred as a toxic agent.

Numerous studies have shown that abnormal behaviors and cognitive impairments, which are believed to be the direct results of demyelination, are also seen in the cuprizone model.[31-33] Vakilzadeh *et al*. in two different studies, it was shown that the total distance and speed of the cuprizone group decreased significantly compared to the control group. Our results are consistent with these two studies.[19,34]

Carter *et al.,* in their study in which a motor disorder was characterized, showed that the height of the overlap was increased as the animals old.[35] In our study, it was found that the length of the overlay distance of the demyelination group increased compared to the control group. This suggests that demyelination may also cause gait anomalies.

In a study that performed the tail-flick test, there was no significant difference in nociceptive responses of the cuprizone-treated group compared to the control group.[34] Unlike this study, a significant delay in the tail-pulling time in the demyelination group was shown in our study. The reason for this difference may be due to the difference in the mechanisms of the studies. As in our study, the effect of demyelination can be reflected in the peripheral system.

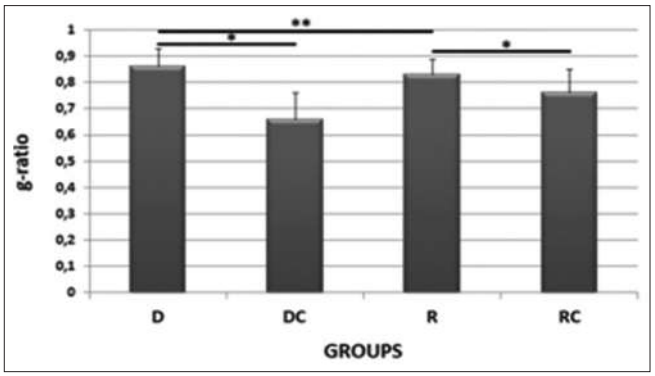

Figure 12: Representative figure shown the g-ratio of the groups (* *P* < 0.001, ** *P* = 0.004)

As shown in the literature, the loss of intense myelin in CC created by cuprizone can be proven by immunohistochemical methods.[36] In our study, significant demyelination was observed in CC, consistent with the literature, which was interpreted by immunohistochemical evaluation of MBP expression.

Demyelination and a spontaneous remyelination process occur as shown in the literature.[11,37] In our study, demyelination and subsequent remyelination in CC were reflected in both behavioral tests and expression analyses evaluated as immunohistochemically.

Severe microgliosis has been observed in the medial and lateral part of the CC, which is known to be affected by cuprizone intoxication, in the lateral part of the caudal part of the putamen, and in the deep layers of the cortex on the leukocortical border.[11] In our study, GFAP expression increased in the splenium and genu region of the CC in the group given cuprizone. When splenium parts were examined, a significant difference was observed between groups.

The g-ratio is the ratio obtained by dividing the axonal diameter by the diameter of the axon and myelin sheath. Most myelinated axons in any animal have the same g ratio, and this value is usually between 0.6 and 0.7.[38] This means that the thickness of the myelin sheath varies with the diameter of the axon: larger axons contain thicker myelin and vice versa. Accordingly, when we examined the myelin sheath of the nerve fiber with an electron microscope, we encountered results that support our other findings. While the g-ratio was consistent with the literature in the control group, it increased in the demyelination group.

Behavioral and histological evaluation of demyelination by creating a reliable and consistent model was the main goal of our study.

Conclusion

At the end of the study, the model created by applying 0.2% cuprizone freshly prepared daily with oral gavage causes damage to the nerve fibers both ultrastructurally and

immunohistochemically. In addition to demyelination, a decrease in locomotor activity also attracts attention. In this context, it is thought that the model in which the cuprizone is administered through gavage may serve as a basis for new projects on demyelinating diseases of the CNS.

Financial support and sponsorship

This study was supported by Akdeniz University Scientific Research Projects with project number TYL-2016-1552 and a Master of Science thesis of Serra OZTURK.

Conflicts of interest

There are no conflicts of interest.

References

1. Hafler DA, Slavik JM, Anderson DE, O'Connor KC, De Jager P, Baecher-Allan C. Multiple sclerosis. Immunol Rev 2005;204:208-31.
2. Lampert PW. Autoimmune and virus-induced demyelinating diseases. A review. Am J Pathol 1978;91:176-208.
3. Zhen W, Liu A, Lu J, Zhang W, Tattersall D, Wang J. An alternative cuprizone-ınduced demyelination and remyelination mouse model. ASN Neuro 2017;9:1-9.
4. Procaccini C, De Rosa V, Pucino V, Formisano L, Matarese G. Animal models of Multiple Sclerosis. Eur J Pharmacol 2015;759:182-91.
5. Robinson AP, Harp CT, Noronha A, Miller SD. The experimental autoimmune encephalomyelitis (EAE) model of MS: utility for understanding disease pathophysiology and treatment. Handb Clin Neurol 2014;122:173-89.
6. Denic A, Johnson AJ, Bieber AJ, Warrington AE, Rodriguez M, Pirko I. The relevance of animal models in multiple sclerosis research. Pathophysiology 2011;18:21-9.
7. Lassmann H, Bradl M. Multiple sclerosis: Experimental models and reality. Acta Neuropathol 2017;133:223-44.
8. Olson JK, Croxford JL, Calenoff MA, Dal Canto MC, Miller SD. A virus-induced molecular mimicry model of multiple sclerosis. J Clin Invest 2001;108:311-8.
9. Tsunoda I, Fujinami RS. Inside-out versus outside-ın models for virus induced demyelination: Axonal damage triggering demyelination. Springer Semin Immunopathol 2002;24:105-25.
10. Rawji KS, Yong VW. The benefits and detriments of macrophages/microglia in models of multiple sclerosis. Clin Dev Immunol 2013;2013:948976.
11. Matsushima GK, Morell P. The neurotoxicant, cuprizone, as a model to study demyelination and remyelination in the central nervous system. Brain Pathol 2001;11:107-16.
12. Varga E, Pandur E, Abrahám H, Horváth A, Ács P, Komoly S, *et al.* Cuprizone administration alters the ıron metabolism in the mouse model of multiple sclerosis. Cell Mol Neurobiol 2018;38:1081-97.
13. Skripuletz T, Bussmann JH, Gudi V, Koutsoudaki PN, Pul R, Moharregh-Khiabani D, *et al.* Cerebellar cortical demyelination in the murine cuprizone model. Brain Pathol 2010;20:301-12.
14. Liu L, Belkadi A, Darnall L, Hu T, Drescher C, Cotleur AC, *et al.* CXCR2-positive neutrophils are essential for cuprizone-induced demyelination: relevance to multiple sclerosis. Nat Neurosci 2010;13:319-26.
15. Gudi V, Gingele S, Skripuletz T, Stangel M. Glial response during cuprizone-induced de and remyelination in the CNS: lessons learned. Front Cell Neurosci 2014;8:73.
16. Xing YL, Röth PT, Stratton JA, Chuang BH, Danne J, Ellis SL, *et al.* Adult neural precursor cells from the subventricular zone contribute significantly to oligodendrocyte regeneration and remyelination. J Neurosci 2014;34:14128-46.
17. Inserra MM, Bloch DA, Terris DJ. Functional indices for sciatic, peroneal, and posterior tibial nerve lesions in the mouse. Microsurgery 1998;18:119-24.
18. Li Z, He Y, Fan S, Sun B. Clemastine rescues behavioral changes and enhances remyelination in the cuprizone mouse model of demyelination. Neurosci Bull 2015;31:617-25.
19. Vakilzadeh G, Khodagholi F, Ghadiri T, Ghaemi A, Noorbakhsh F, Sharifzadeh M, *et al.* The effect of melatonin on behavioral, molecular, and histopathological changes in cuprizone model of demyelination. Mol Neurobiol 2016;53:4675-84.
20. Kariuki HN, Kanui TI, Yenesew A, Patel NB, Mbugua PM. Antinocieptive activity of *Toddalia asiatica (L) Lam*. İn models of central and peripheral pain. Phytopharmacology 2012;3:122-9.
21. Pfeifenbring S, Nessler S, Wegner C, Stadelmann C, Brück W. Remyelination after cuprizone-ınduced demyelination ıs accelerated in juvenile mice. J Neuropathol Exp Neurol 2015;74:756-66.
22. Lindner M, Heine S, Haastert K, Garde N, Fokuhl J, Linsmeier F, *et al.* Sequential myelin protein expression during remyelination reveals fast and efficient repair after central nervous system demyelination. Neuropathol Appl Neurobiol 2008;34:105-14.
23. Álvarez-Sánchez N, Cruz-Chamorro I, Díaz-Sánchez M, Sarmiento-Soto H, Medrano-Campillo P, Martínez-López A, *et al.* Melatonin reduces inflammatory response in peripheral T helper lymphocytes from relapsing-remitting multiple sclerosis patients. J Pineal Res 2017;63:12442.
24. Kipp M, Clarner T, Dang J, Copray S, Beyer C. The cuprizone animal model: new insights into an old story. Acta Neuropathol 2009;118:723-36.
25. Mashayekhi F, Salehi Z. Administration of vitamin D3 induces CNPase and myelin oligodendrocyte glycoprotein expression in the cerebral cortex of the murine model of cuprizone-induced demyelination. Folia Neuropathol 2016;54:259-64.
26. Ransohoff RM. Animal models of multiple sclerosis: The good, the bad and the bottom line. Nat Neurosci 2012;15:1074-7.
27. Tejedor LS, Wostradowski T, Gingele S, Skripuletz T, Gudi V, Stangel M. The effect of stereotactic ınjections on demyelination and remyelination: A study in the cuprizone model. J Mol Neurosci 2017;61:479-88.
28. Praet J, Guglielmetti C, Berneman Z, Van der Linden A, Ponsaerts P. Cellular and molecular neuropathology of the cuprizone mouse model: clinical relevance for multiple sclerosis. Neurosci Biobehav Rev 2014;47:485-505.
29. Skripuletz T, Gudi V, Hackstette D, Stangel M. De- and remyelination in the CNS white and grey matter induced by cuprizone: the old, the new, and the unexpected. Histol Histopathol 2011;26:1585-97.
30. Tagge I, O'Connor A, Chaudhary P, Pollaro J, Berlow Y, Chalupsky M, *et al.* Spatio-temporal patterns of demyelination and remyelination in the cuprizone Mouse Model. PLoS One 2016;11:e0152480.
31. Skripuletz T, Lindner M, Kotsiari A, Garde N, Fokuhl J, Linsmeier F, *et al.* Cortical demyelination is prominent in the murine cuprizone model and is strain-dependent. Am J Pathol 2008;172:1053-61.
32. Taylor LC, Gilmore W, Matsushima GK. SJL mice exposed to cuprizone intoxication reveal strain and gender pattern differences in demyelination. Brain Pathol 2009;19:467-79.
33. Wang H, Li C, Wang H, Mei F, Liu Z, Shen HY, *et al.*

Cuprizone-induced demyelination in mice: Age-related vulnerability and exploratory behavior deficit. Neurosci Bull 2013;29:251-9.

34. Vakilzadeh G, Khodagholi F, Ghadiri T, Darvishi M, Ghaemi A, Noorbakhsh F, *et al.* Protective effect of a cAMP analogue on behavioral deficits and neuropathological changes in cuprizone model of demyelination. Mol Neurobiol 2015;52:130-41.
35. Carter RJ, Lione LA, Humby T, Mangiarini L, Mahal A, Bates GP, *et al.* Characterization of progressive motor deficits in mice transgenic for the human Huntington's disease mutation. J Neurosci 1999;19:3248-57.
36. Partridge MA, Gopinath S, Myers SJ, Coorssen JR. An initial top-down proteomic analysis of the standard cuprizone mouse model of multiple sclerosis. J Chem Biol 2016;9:9-18.
37. Armstrong RC, Le TQ, Frost EE, Borke RC, Vana AC. Absence of fibroblast growth factor 2 promotes oligodendroglial repopulation of demyelinated white matter. J Neurosci 2002;22:8574-85.
38. Sherman DL, Brophy PJ. Mechanisms of axon ensheathment and myelin growth. Nat Rev Neurosci 2005;6:683-90.

Original Article

Histopathological Evaluation of Ethanolic Leaf Extract of *Lippia adoensis* on the Liver, Kidney, and Biochemical Parameters in Swiss Albino Mice

Abayneh Tunta, Peter Etim Ekanem, Tesfamichael Berhe Hailu

Department of Anatomy, College of Health Sciences, Mekelle University, Mekelle, Ethiopia

Abstract

Background: Eighty percent of Ethiopians use traditional medicine, one of which is the leaf of *Lippia adoensis*. **Objective:** The objective of this study was to investigate subacute toxicity of aqueous extract of *L. adoensis* leaves on the liver, kidney, and some biochemical parameters in Swiss albino mice. **Subjects and Methods:** LD50 was conducted with nine experimental and one control groups of adult female Swiss albino mice. In the subacute study, 40 mice of both sexes were randomly divided into four groups of ten mice per group. Group I served as control and received distilled water. Groups II–IV were used as treatment groups. They received aqueous leaf extract of *L. adoensis* orally at 500 mg/kg, 1000 mg/kg, and, 2000 mg/kg per body weight, respectively. SPSS version 20 statistical software was used to analyze the data. Differences at $P < 0.05$ were considered statistically significant. **Results:** In the subacute test, general signs of toxicity such as piloerection, lethargy, and convulsion were observed at 2000 mg/kg. From the 3rd week of administration, both male and female mice receiving 500 mg/kg and 2000 mg/kg and all treatment groups in the 4th week showed significant ($P < 0.05$) weight loss compared to control groups. Biochemical parameters under study were found to increase in all treatment groups. Several histopathological changes such as congestion, hemorrhage, severe necrosis, and infiltration of inflammatory cells in both liver and kidney in the *L. adoensis*-treated rats were observed at all doses of treatments. **Conclusion:** In the present study, the ethanolic leaf extract of *L. adoensis* produced dose-dependent changes such as weight loss and histopathological and biochemical changes in Swiss albino mice.

Keywords: *Ethanolic extract, histopathology, Lippia adoensis, subacute, toxicological*

Introduction

The World Health Organization (WHO) defines traditional medicine (TM) as health practices, approaches, knowledge, and beliefs incorporating plant, animal and mineral-based medicines, spiritual therapies, manual techniques, and exercises, applied singularly or in combination to treat, diagnose, and prevent illnesses and maintain well-being.[1]

The popularity of TM has continued in all regions of the developing world and its use is rapidly spreading in the industrialized countries also. Many countries in the world use TM to meet some of their primary health-care needs.[2] According to the estimate made by the WHO, the annual global market of TM is approximately US $83 billion.[3] In Africa, up to 80% of the population uses TM for primary health care.[2] The same holds for Ethiopia where there are reports of around 80% population dependent on TM for primary health needs.[4] The increasing popularity of herbal medicines is based on their perceived belief of effectiveness in the treatment and prevention of disease, the cultural acceptability of healers, the relatively low cost of TM when compared to modern medicine, and the difficult access to modern health-care facilities.[5]

Lippia adoensis is one of the medicinal plants commonly used in Ethiopia and is also distributed throughout Africa, South, and Central American countries.[6] *Lippia* species occurs as an erect woody shrub, which grows up to 1–3 m tall. It is an endemic medicinal plant and cultivated variety commonly found in home gardens in different regions of Ethiopia with an altitudinal range of 1600–2200 m. *L. adoensis var. Koseret sebsebe* is widely grown in the central and southern highlands of Ethiopia. Most of the *Lippia* species are traditionally utilized as gastrointestinal and respiratory disease remedies. Some *Lippia*

How to cite this article: Tunta A, Ekanem PE, Hailu TB. Histopathological evaluation of ethanolic leaf extract of *Lippia adoensis* on the liver, kidney, and biochemical parameters in Swiss albino mice. J Anat Soc India 2023;72:58-66.

Article Info

Received: 12 September 2021
Accepted: 13 January 2023
Available online: 24 March 2023

Address for correspondence:
Prof. Peter Etim Ekanem, College of Health Sciences, P.O. Box 1871, Mekelle, Ethiopia.
E-mail: etimakpan@gmail.com

Access this article online

Website: www.jasi.org.in
DOI: 10.4103/jasi.jasi_160_21
Quick Response Code:

species have shown antimalarial, antiviral, and cytostatic activities. Besides this, the leaves from the majority of these species are utilized as a seasoning for food preparation.[6] In Ethiopia, the fragrant leaves of the variety *Koseret* are used by the Gurage and Oromo tribes in the region as one of the condiments in the preparation of spiced butter. The special taste and flavor of the "Gurage Kitfo" (minced meat with spiced butter) is attributed to the oils imparted by the leaves.[7] *L. adoensis* extracts are used medicinally by a variety of Ethiopian communities for the treatment of skin infections including eczema and superficial fungal infections. Besides, the dried leaves of *Koseret sebsebe* powdered together with barley are also used in treating stomach problems.

Modern drugs generally undergo extensive formal testing for therapeutic and adverse effects before being licensed. No such controls in the risk of adverse effects exist for the majority of herbal remedies, which are being provided for their perceived use only.[8] Despite the use of *L. adoensis* for TM in different parts of Ethiopia, there is sparse literature regarding its safety and toxicity. Even if the pharmacological effect of *L. adoensis* and its essential oils is addressed by some scientific investigations, the toxicity profile of this plant is not known. The current study, which focuses on the subacute toxicity of ethanolic leaf extract of *L. adoensis* on the liver and kidney, as well as some biochemical parameters of Swiss albino mice aims to provide the needed information on the toxicity of this plant.

Subjects and Methods

Study design and setting

A laboratory-based experiment was employed on mice of both sexes to investigate the toxic effects of leaf extracts of *L. adoensis* on the histopathology of the liver and kidney as well as biochemical markers in Swiss albino mice. The study was conducted at Mekelle University, College of Health Sciences, Department of Anatomy (Histology Laboratory).

Plant collection and authentication

The leaves of *L. adoensis var. Koseret* were collected from the Wolaita zone, which is located at 343 km south of Addis Ababa, the capital city of Ethiopia. A Botanist at Addis Ababa University, Department of Biology, authenticated the plant.

Preparation of plant extract

All parts of the plant were dried in open air protected from direct exposure to sunlight to prevent loss of volatile components. The leaves were ground into a fine powder and suspensions prepared in ethanol 80%. Three hundred grams of the fine powder was suspended in 450 ml of ethanol 80% separately in sterilized screw-capped 500 ml glass beakers. The suspension was macerated with ethanol 80% for 2 h with intermittent agitation by an orbital shaker at room temperature for 3 consecutive days. The supernatant was then decanted and filtered using a 0.1 mm^2 mesh gauze from the undissolved portion of the plant. The suspension was then filtered three times using Whatman No. 1 filter paper and evaporated using a vacuum evaporator to remove the solvent. The final stock solution was stored in a deep freezer at a temperature of −20°C until further use.[6] Following maceration, sedimentation, filtration, and concentration of 600 g powder of *L. adoensis* leaves using ethanol as solvent, 111.7 g crude extract was obtained with a percentage yield of 18.6%.

Selection and preparation of experimental animals

A total of 90 healthy adult Swiss albino mice were used in this study. To conduct the LD50, 50 adult female mice were used, and for the subacute test, 40 mice of both sexes (20 male and 20 female) weighing 25–30 g were used. Mice in this experiment were between 8 and 12 weeks old and females were kept nulliparous and nonpregnant. The animals were kept in well-ventilated plastic cages under standard laboratory conditions (temperature of 22°C [±3°C]), and were exposed to photoperiods of 12-h light/12-h dark cycles. A conventional rodent laboratory diet was used for feeding with an unlimited supply of drinking water throughout the experiment. The animals were acclimatized to laboratory conditions for 1 week before the experiment.

Method of extract administration

LD_{50} determination

A total of ten groups of mice were used (9 – treatment and 1 – control) each consisting of five adult female Swiss albino mice. To increase the rate of absorption of the extract, all groups of mice were fasted overnight prior to administration. The doses were calculated and administered to the mice in the treatment groups based on their body weight. Each treatment group (Group I to Group IX) received designated doses of 2000 mg/kg to 10,000 mg/kg of the extract of *L. adoensis* per body weight spaced by 1000 mg/kg to produce test groups with a range of toxic effects and mortality rates in 48-h observation. The extract was administered orally by gavage.

Subacute test

Forty mice of both sexes were randomly assigned into four groups of ten mice (five male and five female) per group. Group I served as control and was administered distilled water and feeds only. Groups II, III, and IV were used as treatment groups and calculated doses based on LD50, that is, 500 mg/kg, 1000 mg/kg, and 2000 mg/kg body weight of aqueous leaf extract of *L. adoensis* daily for 28 days. The extract was given once a day after the animals fasted for 3–4 h with free access to water. The plant extract was administered orally using gavages and animals fasted for 1–2 h after the administration before

routine feeding. The animals were treated daily throughout the experiment (28 days). All equipment used were cleaned and placed in an oven after each administration to prevent any contamination.

Data collection techniques

Data were collected from the experimental animals before and after they were sacrificed.

Body weight measurement and cage-side observations

Body weights of the experimental and control groups of animals were recorded using a digital electronic balance (PA4102C, China) before the beginning of the 1st day of administration and then weekly till the last day of administration of the extract. In each cage, mice were carefully observed individually before and after dosing the plant extract periodically for any changes in skin and fur, eyes, and respiration. Besides, the occurrences of autonomic effects such as salivation, diarrhea, urination, and central nervous system effects such as tremors were also followed.

Blood collection and testing

At the end of the experimental period (on the 29th day), animals belonging to each group were weighed on a digital electronic balance (PA4102C, China) and were anesthetized under diethyl ether. Blood samples were collected by cardiac puncture after letting all animals fast overnight on the last day of the experiment. Blood samples of approximately 1.3–1.5 ml were drawn quickly using 5 ml syringes and collected in vacutainers. For biochemical analysis, the blood samples in the plain vacutainers were allowed to stand for 3 h for complete clotting and then centrifuged at 5000 rpm for 15 min using a benchtop centrifuge (HUMAX-K, HUMAN GmbH, Germany). The concentrations of alanine aminotransferase (ALT), aspartate aminotransferase (AST), alkaline phosphatase (ALP), urea, and creatinine were automatically determined using AUTO LAB 18, Clinical Chemistry Analyzer, Italy.

Dissection and tissue collection

Each animal was sacrificed by cervical dislocation. The abdominal cavity was opened and the liver and kidney were removed carefully. Organ samples were cleared from any surrounding tissues by washing in normal saline. They were put on clean paper and weighed immediately on a digital balance. Samples from the left and right kidneys as well as the liver were preserved in 10% neutral buffered formalin fixative for 24 h and thoroughly rinsed over running tap water overnight.[9]

Tissue processing

Isolated liver and kidneys were observed for gross pathological changes in the color and texture of the organs. Randomly, the longitudinal and transverse sections of the organs were taken and fixed for histological processing. The samples were then processed according to the standard technique of dehydration, clearing, infiltration, and embedding.[9] Tissue blocks were then sectioned with a thickness of 5 μm using Leica Rotary (Leica RM 2125RT Nussloch GmbH, Germany). Ribbons of the tissue sections were gently collected using a piece of brush and placed on the surface of a warm water bath of temperature at 40°C. After the sections were appropriately spread on the water bath, they were mounted on tissue slides and stained regressively with routine Harris hematoxylin for 6 min and eosin for 17–20 s (H and E) and mounted with DPX (Dibutylphthalate Polystyrene Xylene).[12]

Light microscopy and photomicrography

Stained tissue sections of the liver and kidney were carefully examined under a compound light microscope in the histology laboratory of the Anatomy Department, Mekelle University. Tissue sections from the treated groups were examined for any evidence of histopathological changes compared with those of the controls. Photomicrographs of selected slides from both the treated and control groups were taken under magnifications of ×10 and ×40 objectives by using (EVOS XI, China) automated built-in digital photo camera to examine the liver and kidney tissues for any histopathological changes.

Data processing and analysis

SPSS (Statistical Package for the Social Sciences) statistical software was used to analyze the data, which were represented in numbers. Values of parameters were expressed in mean ± standard error of mean. One-way analysis of variance was used to compare treatment over time between control and treated groups. Differences at $P < 0.05$ were considered statistically significant.

Ethical considerations

An ethical clearance letter was obtained from the Health Research and Ethics Review Committee of the College of Veterinary Medicine, Mekelle University. Animals used for this study were kept from any unnecessary painful and terrifying situations. To keep the animals from pain and suffering during any surgical interventions, appropriate anesthesia was given. Animals were protected from pathogens and placed in an appropriate environment.

Results

Acute toxicity and LD_{50} of ethanolic extract of *Lippia adoensis*

The administration of the ethanolic leaf extract of *L. adoensis* to the mice did not show any death up to a dose of 6000 mg/kg body weight. Observed general signs of toxicity were seen from 5000 mg/kg body weight. These include loss of appetite, hypoactivity, piloerection, lethargy, and a single episode of convulsion observed at 5000 mg/kg. Eighty percent of death occurred at 10,000 mg/kg body weight dose; therefore, the LD50 value was considered to be 10,000 mg/kg body weight.

Subacute toxicity

Effect of Lippia adoensis ethanolic leaf extract on general body weight of mice

In the first 2 weeks of the experiment following administration of the extract, the mean body weight of both male and female mice at dose 500 mg/kg, 1000 mg/kg, and 2000 mg/kg body weight did not show any significant changes as compared with controls. However, starting from the 3rd week of administration, both male and female mice in the 500 mg/kg and 2000 kg/kg and all treatment groups in the 4th week showed significant ($P < 0.05$) weight loss as compared with control groups. Although both sexes showed weight loss with increasing dose, these weight changes were more prominent in female groups ($P < 0.01$), except at 1000 mg/kg dose groups, as shown in Table 1.

Effect of ethanolic leaf extract of Lippia adoensis on organ weight of mice

The mean weight of the liver increased in female mice at a dose of 1000 mg/kg and 2000 mg/kg compared with the controls ($P > 0.05$). However, an increase in mean liver weight among male mice in the treatment groups was not evident. The mean kidney weight increased in male mice at a dose of 1000 mg/kg and female mice at both 1000 mg/kg and 2000 mg/kg body weight [Table 2].

Effects of subacute administration of Lippia adoensis on biochemical parameters of mice

The biochemical parameters under study were found to increase in the groups treated with ethanolic leaf extract of *L. adoensis*. There were significant ($P < 0.05$) increases in the values of ALT, AST, and ALP in both male and female mice groups that received *L. adoensis* doses at 1000 mg/kg and 2000 mg/kg per body weight compared with that of the controls, as shown in Table 3. Furthermore, there were significant ($P < 0.05$) increases in values of creatinine in the mice of both sexes treated with 1000 mg/kg and 2000 mg/kg per body weight doses of *L. adoensis*. Urea was found to increase in male groups at the dose of 2000 mg/kg and all doses in female groups treated with *L. adoensis*.

Effects of subacute administration of Lippia adoensis on the histology of the liver of mice

Histopathological analysis of liver sections from the control group showed normal histology of the liver with normal hepatic cells, visible central veins (CVs), and thin sinusoids. The CV and the portal area containing branches of the hepatic artery, biliary duct, and portal vein (PV) revealed a normal appearance [Figure 1].

In comparison to the control, the general microscopic architecture of the liver tissue sections of both male and female mice that received 500 mg/kg body weight dose of the extract of *L. adoensis* showed congestion of the PV [Figure 2a], mild focal necrosis and degeneration of hepatocytes [Figure 2b], and congestion and hemorrhage of CV [Figure 2c]. Liver sections of mice from 1000 mg/kg body weight dosed groups exhibited hemorrhage [Figure 2d], infiltration [Figure 2e], severe necrosis, and infiltration of inflammatory cells [Figure 3a and b]. Similarly, sections of liver from

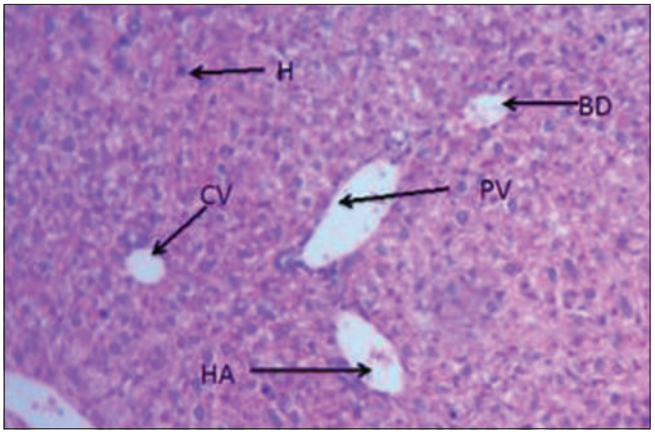

Figure 1: Photomicrograph of H and E (×100) stained liver sections of control mice showing CV, hepatocytes (H), HA, PV, and BD. CV: Central vein, HA: Hepatic artery, PV: Portal vein, BD: Bile duct

Table 1: Comparison of the mean body weights of male and female mice treated with the leaves *Lippia adoensis* for 4 weeks

Duration of administration	Sex	Control groups	Treatment groups (mg/kg body weight/day)		
			500	1000	2000
Initial weight	Male	27.22±0.85	29.72±1.28 (0.209)	32.38±0.55 (0.003)	28.76±0.51 (0.595)
	Female	23.70±0.83	24.60±0.68 (0.830)	25.80±0.83 (0.243)	25.90±0.65 (0.207)
Week 1	Male	28.52±1.16	29.06±1.56 (0.981)	31.18±1.05 (0.384)	27.64±0.60 (0.947)
	Female	24.56±0.74	23.18±0.50 (0.431)	24.04±0.48 (0.936)	24.16±0.74 (0.969)
Week 2	Male	28.82±1.06	28.04±0.82 (0.931)	30.30±1.07 (0.672)	26.54±0.62 (0.330)
	Female	25.22±0.87	22.48±0.48 (0.203)	23.54±0.49 (0.281)	23.08±0.32 (0.081)
Week 3	Male	29.98±1.09	25.98±0.53 (0.006)	27.72±0.37 (0.155)	26.18±0.64 (0.008)
	Female	26.73±0.74	21.44±0.61 (0.06)	22.12±0.33 (0.254)	21.48±0.60 (0.006)
Final weight	Male	30.46±1.05	25.44±0.62 (0.001)	27.34±0.50 (0.045)	25.64±0.74 (0.002)
	Female	26.73±0.74	21.22±0.56 (0.000)	22.04±0.37 (0.000)	21.22±0.65 (0.000)

Values are expressed as mean±SEM, n=5 per sex for each group, numbers in the bracket indicate P value. SEM: Standard error of mean

Table 2: Comparison of the mean organ weights of male and female mice treated with 500 mg/kg, 1000 mg/kg, and 2000 mg/kg body weights of the *Lippia adoensis*

Dose (mg/kg/body weight)	Sex	Mean weight (g; mean±SDE; *n*=40)	
		Liver	Kidney (single)
Control	Male	1.8820±0.0569	0.2620±0.0066
	Female	1.3400±0.0994	0.1540±0.0060
500	Male	1.6440±0.15955 (0.353)	0.2400±0.00663 (0.546)
	Female	1.1920±0.04067 (0.577)	0.1380±0.00200 (0.669)
1000	Male	1.8120±0.05453 (0.958)	0.2760±0.00663 (0.825)
	Female	3.8840±2.50404 (0.982)	0.1640±0.01568 (0.890)
2000	Male	1.8100±0.08550 (0.954)	0.2600±0.00663 (0.999)
	Female	1.3760±0.11952 (0.989)	0.1640±0.01030 (0.890)

Values are expressed as mean±SEM, *n*=5 per sex for each group, numbers in the bracket indicate *P* value. SEM: Standard error of mean, SDE: Standard deviation of errors

Table 3: Comparison of biochemical parameters between female and male mice treated with 500, 1000, and 2000 mg/kg body weight doses of leave *Lippia adoensis* with the control group

Biochemical parameters	Sex	Control	500 mg/kg	1000 mg/kg	2000 mg/kg
ALT	Male	36.57±1.31	37.99±0.40 (0.773)	64.44±1.14 (0.000)	81.09±1.09 (0.000)
	Female	42.05±0.92	58.70±2.70 (0.010)	63.91±2.29 (0.000)	82.6420±2.75 (0.000)
AST	Male	82.46±1.12	87.5020±1.74 (0.509)	99.88±4.09 (0.001)	126.0940±2.06 (0.000)
	Female	86.87±1.22	88.25±1.046 (0.981)	111.12±3.30 (0.000)	124.8140±3.62 (0.000)
ALP	Male	52.06±1.99	55.63±1.37 (0.781)	64.92±2.76 (0.017)	76.8080±3.88 (0.000)
	Female	48.59±1.30	58.46±2.54 (0.310)	67.37±2.82 (0.000)	84.83±2.03 (0.000)
Creatinine	Male	0.67±0.02	0.81±0.03 (0.169)	0.96±0.04 (0.001)	1.23±0.06 (0.000)
	Female	0.70±0.02	0.73±0.02 (0.997)	1.08±0.08 (0.007)	1.2960±0.11 (0.000)
Urea	Male	40.30±0.61	41.83±0.44 (0.880)	45.22±2.24 (0.119)	53.94±1.69 (0.000)
	Female	40.27±0.54	48.27±0.79 (0.010)	50.56±2.79 (0.001)	58.99±0.83 (0.000)

Values are expressed as mean±SEM, *n*=5 per sex for each group, numbers in the bracket indicate *P* value. ALT: Alanine aminotransferase, AST: Aspartate aminotransferase, ALP: Alanine amino phosphate, SEM: Standard error of mean

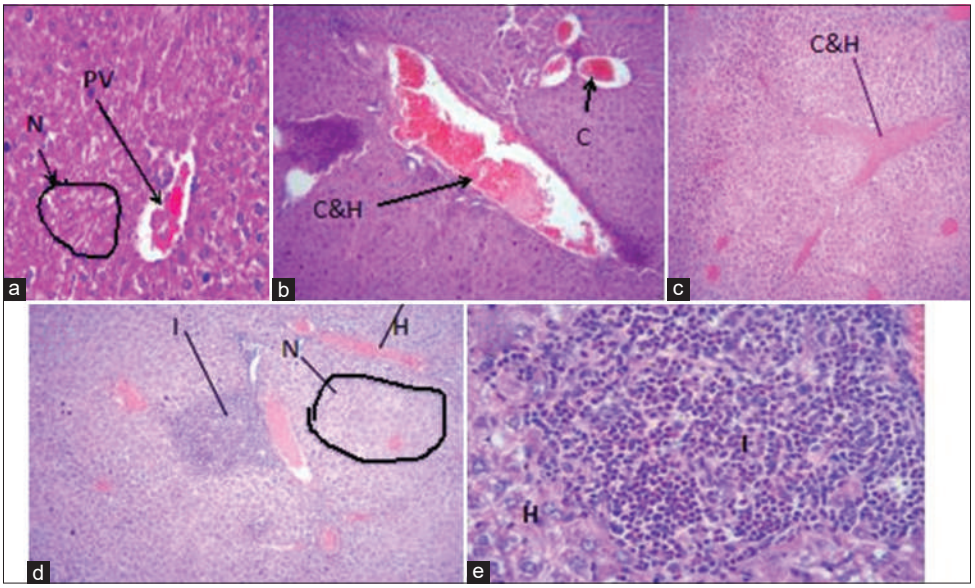

Figure 2: (a) Photomicrographs of H and E (×100), stained liver sections of female mice treated with the ethanolic leaf extract of *Lippia adoensis* at 1000 mg/kg showing congestion of PV and mild necrosis (N), (b) H and E (×400), showing congestion and hemorrhage (C and H) in the PV, (c) H and E (×100), stained liver sections of female mice treated with the ethanolic leaf extract of *Lippia adoensis* at 1000 mg/kg showing IC and hemorrhage (C and H), (d) H and E (×100) stained liver sections of female mice treated with the ethanolic leaf extract of *Lippia adoensis* at 1000 mg/kg showing hemorrhage (H), pale areas showing necrosis of hepatocytes (N), and infiltration of inflammatory cells (I) in centrilobular area, (e) H and E (×400) stained liver sections of female mice treated with the ethanolic leaf extract of *Lippia adoensis* at 1000 mg/kg showing infiltration of inflammatory cells (I), normal hepatic cells (H). PV: Portal vein

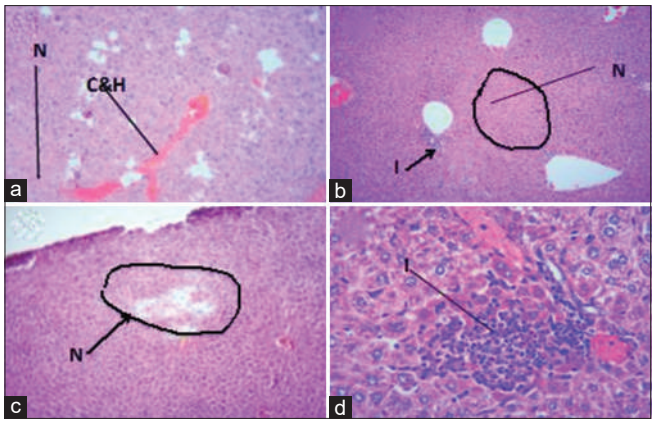

Figure 3: (a) Photomicrographs of H and E (×100) stained liver sections of female mice treated with the ethanolic leaf extract of *Lippia adoensis* at 2000 mg/kg showing congestion and hemorrhage (C and H), areas of necrosis or cell death (N), (b) H and E (×100) stained liver sections of female mice treated with the ethanolic leaf extract of *Lippia adoensis* at 2000 mg/kg shows areas of necrosis (N) and accumulation of inflammatory infiltrates (I) around the CV, (c) H and E (×100) stained liver sections of male mice treated with the ethanolic leaf extract of *Lippia adoensis* at 2000 mg/kg shows areas of severe necrosis (N) scattered circle in the parenchyma of the liver, (d) H and E (×400) stained liver sections of female mice treated with the ethanolic leaf extract of *Lippia adoensis* at 2000 mg/kg shows areas of inflammatory infiltration (I). CV: Central vein

2000 mg/kg body weight dose groups showed multi-focal congestion and hemorrhage [Figure 3c], severe necrosis, and infiltration of inflammatory cells [Figure 3d] besides pale necrotized areas indicating severe cell death.

Effects of subacute administration of Lippia adoensis on histology of the kidney of mice

Examinations of sections of kidney of mice from both sexes in the control group indicated normal kidney histology; renal corpuscles show normal size of urinary space and tubular structures, proximal and distal convoluted tubules, and glomerulus [Figure 4a]. However, sections of kidney from both male and female mice in 500 mg/kg dose group revealed focal congestion and hemorrhage [Figure 4b], interstitial congestion [Figure 4c], necrosis, and interstitial inflammatory cells [Figure 4d]. At 1000 mg/kg body weight administration, necrosis of the tubules and hemorrhage within the stromal tissue were observed [Figure 4e], multifocal congestion and necrosis [Figure 4f], and edema and hemorrhage [Figure 4g]. Both male and female mice in 2000 mg/kg sections indicated congestion and hemorrhage, necrosis with focal tubular destruction [Figure 4h], hemorrhage, and infiltration of inflammatory cells [Figure 4i].

Discussion

Despite being natural and biologic, the phytoconstituents in this plant exert unanticipated toxicities that target visceral organs that are loaded with metabolic activities such as the liver and the kidney.[15] *L. adoensis* has phytochemicals such as alkaloids, tannins, terpenoids, saponins, and flavonoids, which have been reported to be toxic.[10,11]

According to the findings from this study, acute administration of *L. adoensis* to the mice did not show any mortality in the experimental mice with single oral doses up to 8000 mg/kg body weight. However, following single oral dose of extract at dose level of 8000 mg/kg body weight and above, the animals showed more severe symptoms of toxicity and exhibited weakness, hypoactivity, poor appetite, piloerection, lethargy, and convulsions. The LD_{50} value was considered to be 10,000 mg/kg body weight as 80% death occurred at this dose. This dose is within the range of rodent oral LD_{50} values for linalool, which is one of the major constituents of *L. adoensis* reported by Bickers *et al*.[13]

Cage-side observations from the subacute study revealed that mice in 1000 mg/kg and 2000 mg/kg groups had mild-to-severe signs of toxicity. Mice in the 1000 mg/kg group showed piloerection, hypoactivity, and loss of appetite. Observation of mice in 2000 mg/kg revealed the above signs plus some severe ones such as lethargy and intermittent episodes of convulsions. This is in line with a study reported by Masran *et al*.[14] in which essential oils from *Litsea elliptica* leaves in rats showed hypoactivity, lacrimation, and piloerection. Hypoactivity and loss of appetite might be associated with the compounds in extract, which could have interfered with the intake and metabolism of dietary nutrients and their anorexic effects. Lethargy and convulsions are probably due to the reported central depressive effects of monoterpens specifically linalool from the extract.[18]

Changes in the body and internal organ weights (in a significant magnitude) are considered good indices of toxicity.[16] The findings from this study indicated a significant ($P < 0.05$) decrease in body weight of mice treated with 500 mg/kg and 2000 mg/kg body weight of *L. adoensis* in the 3rd week and all dose groups in the 4th week. This is in line with findings from Arika *et al*.,[10] which reported dose-dependent decreases in body weight following the oral and intraperitoneal administration of *Lippia javanica* for 28 days in mice. Weight loss is a sensitive index of toxicity after an exposure to a toxic substance.[17] A decrease in body weight might be due to phytochemicals in the plant that could suppress food intake or interfere with its metabolism. Phytochemicals are known to affect body weight through manipulating the energy expenditure, appetite suppression, satiety enhancement, and fat-glucose absorption blocking.[18]

Organ weight data can also provide sensitive indices of toxicological change.[19] In our study, the subacute administration of *L. adoensis* ethanolic leaf extract induced an increase in organ weights of liver and kidney in mice of both sexes, which is congruent with the findings of Arika *et al*.[10] This may be due to increased metabolic activity and facilitated protein synthesis in these organs induced by extracts.[10] Another possibility of increased weight in

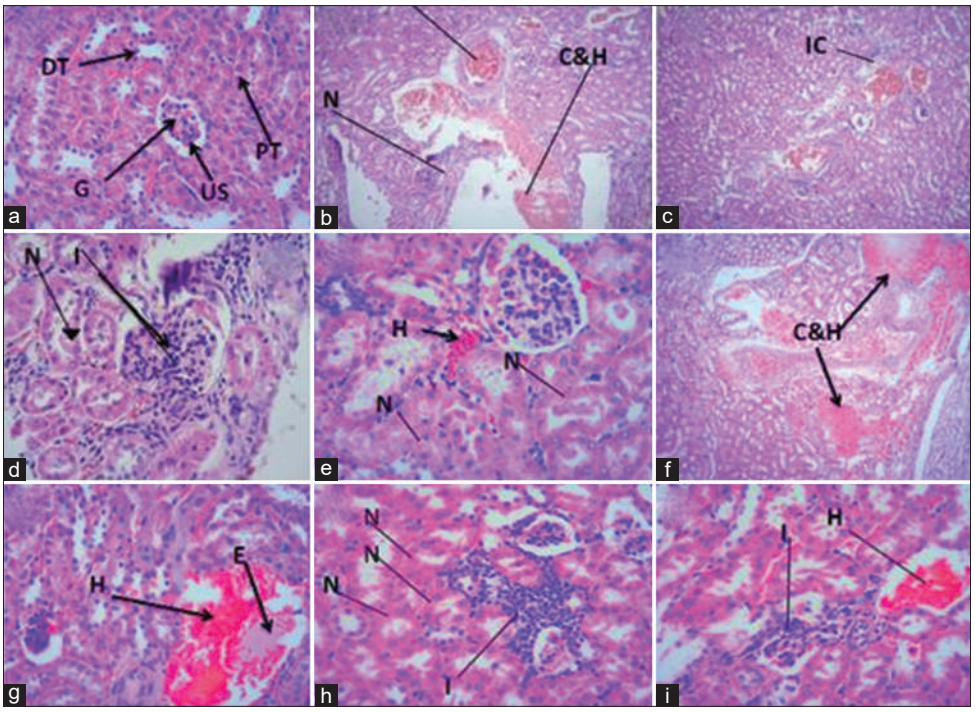

Figure 4: Photomicrographs of H and E, (a) ×100 stained kidney sections of female control mice showing glomerulus (G), distal convoluted tubules (DCT), PT, US, (b) ×100 stained kidney sections of male mice treated with ethanolic extract of *Lippia adoensis* at 500 mg/kg body weight/day showing IC and hemorrhage (C and H) and tubular necrosis (N), (c) ×100 stained kidney sections of male mice treated with ethanolic extract of *Lippia adoensis* at 500 mg/kg body weight/day showing IC, (d) ×400 stained kidney sections of male mice treated with ethanolic extract of *Lippia adoensis* at 500 mg/kg body weight/day showing tubular necrosis (N) of proximal tubules and inflammatory infiltration (I), (e) ×400 stained kidney sections of male mice treated with ethanolic extract of *Lippia adoensis* at 1000 mg/kg body weight/day showing tubular necrosis (N) of both proximal and distal tubules and interstitial hemorrhage (H), (f) ×100 stained kidney sections of female mice treated with ethanolic extract of *Lippia adoensis* at 1000 mg/kg body weight/day showing multifocal congestion and hemorrhage (C and H) indicated by black arrows, (g) ×400 stained kidney sections of male mice treated with ethanolic extract of *Lippia adoensis* at 1000 mg/kg body weight/day showing severe edema (E), (h) ×400 stained kidney sections of male mice treated with ethanolic extract of *Lippia adoensis* at 2000 mg/kg body weight/day showing PT cell necrosis (N) and infiltration of inflammatory cells (I), (i) ×400 stained kidney sections of male mice treated with ethanolic extract of *Lippia adoensis* at 2000 mg/kg body weight/day showing PT cell necrosis, inflammatory infiltration (I) and hemorhage (H). PT: Proximal tube, US: Urinary space, IC: Interstitial congestion

kidneys and liver could indicate hypertrophy, related to underlying pathology such as edema and congestion as supported by the histopathological findings of this study. Hypertrophy of the organs is a first-hand indication of toxicity of chemical or biological substance.[20] Linalool is also reported to cause epithelial hyperplasia in kidney.[15]

Liver and renal function tests are of great importance to evaluate changes produced by a toxicant. Raised blood levels of hepatic biomarkers and nitrogenous wastes to be excreted by the kidney are usually considered in the toxicity due to their spillage into the bloodstream as a result of necrosis of the tissues.[21] In the present study, there were significant ($P < 0.05$) increases in measured mean values of ALT, AST, and ALP in 1000 mg/kg and 2000 mg/kg treatment groups as compared with controls. This is supported by findings from histological examinations of liver whereby increasing doses of ethanolic extract of *L. adoensis* caused mild-to-severe alterations in histomorphology of liver. Such findings are in line with reports from other authors,[10,16] which showed dose-dependent increase in ALT, AST, and ALP. An increase in serum levels of these enzymes might have resulted from damage to the liver cells. Another possibility of these elevations could be due to enterohepatic circulation of linalool that has the effect of prolonging the metabolic load on the liver, consequently leading to hepatocellular damage.[22]

Both urea and creatinine serum levels were found to increase in a significant manner in mice treated with 1000 mg/kg and 2000 mg/kg body weight oral doses of *L. adoensis* except the values of urea in male groups which did not show significant changes. The rise in the serum levels of these biomarkers might have resulted from dose-related damage to renal parenchyma. This is also supported by histopathological findings of the same mice groups, which showed severe structural damage after receiving the extract at corresponding doses, which caused elevated levels of renal biomarkers.

Histopathological examinations provide synergistic information in addition to biochemical and hematological parameters in assessment of toxicity. The main morphological changes, which may suggest mechanism of liver injury, include zonal necrosis, hepatitis, cholestasis, steatosis, granuloma, and vascular lesions.[23] The findings of this study are in agreement with other authors,[13,16]

who reported vascular congestion, vacuolated nuclei, congested sinusoids, and moderate scar of necrosis besides edema in the livers of mice treated with 60-day subchronic administration of *Zingiber officinale*. This finding is also supported by Fandohan *et al*.,[24] who that observed hepatocyte hydrophic changes at 1500 mg/kg and 2000 mg/kg body weight involving several liver cells, and the interstitium around hepatocyte layers significantly diminished. These changes could be due to the presence of monoterpens such as linalool in *L. adoensis* whose repeated dosing induces oxidative metabolic pathways, which are potentially toxic.[15] Furthermore, the hepatocellular injury due to cytotoxic effects of other phytochemicals in the extract may have caused these kinds of alterations in the histoarchitecture of the liver in mice.

Microscopic examinations of tissue slides of kidney from treatment groups revealed findings that are in agreement with the results of biochemical parameters. Mice in 500 mg/kg body weight developed mild congestion, hemorrhage, and tubular cell necrosis. Furthermore, sections of kidney from both male and female mice in 1000 mg/kg and 2000 mg/kg dose groups have shown multifocal congestion and hemorrhage. These observations are in accordance with findings from Ebeye *et al*.[25] in which the kidney of *Ocimum gratissimum*-treated rats revealed vascular congestion, unremarkable appearance of the interstitial spaces, and glomeruli with varying degrees of interstitial infiltration by inflammatory cells. Our study findings also included occluded lumen (PT), infiltration of inflammatory cells, edema, and tubular necrosis (PT), especially in mice from 2000 mg/kg dose groups in consonance with the results of Ali Noori *et al*.,[26] in which *Agave deserti* extract showed significant histopathological alterations such as degeneration in the wall of proximal and distal tubules, atrophied glomeruli, and inflammatory cells with the increasing doses. It is also supported by Ahmad *et al*.[17] that serious signs of toxicity were observed in the kidney of the rats treated with 2000 mg/kg Cinnamon bark aqueous extract. This could be caused by the presence of compounds like terpenoids in the extract, which have been reported to increase membrane permeability, thereby causing congestion and edema.[16]

Conclusion

In the present study, the ethanolic leaf extract of *L. adoensis* at doses of 500 mg/kg, 1000 mg/kg, and 2000 mg/kg body weight produced dose-dependent changes in body weight and biochemical parameters when compared with the control groups. Moreover, the ethanolic leaf extract of *L. adoensis* also resulted in pathological changes in the histological structure of liver and kidney in Swiss albino mice. In the acute toxicity study, the plant produced 80% mortality of experimental animals at dose of 10,000 mg/kg; the LD50 may be <10,000 mg/kg.

Recommendations

In addition, to the above conclusions, the observed results also raised the following concerns. First, although the subacute study produced a significant level of adverse effect on the study animals, further toxicity studies are needed to extend the time of study to subchronic and chronic levels. Second, studies focusing on the specific isolate compounds, which are responsible for the above-noticed adverse effects, are needed in order to establish the toxicity profile of the plant. Third, further investigations of toxicity on other parts of the plant should also be considered.

Financial support and sponsorship

This study was financially supported by Mekelle University.

Conflicts of interest

There are no conflicts of interest.

References

1. WHO. Traditional Medicine. Geneva: WHO; 2008.
2. Kassaye KD, Amberbir A, Getachew B, Mussema Y. A historical overview of traditional medicine practices and policy in Ethiopia. Ethiop J Health Dev 2006;20:127-34.
3. Wassie SM, Aragie LL, Taye BW, Mekonnen LB. Knowledge, attitude, and utilization of traditional medicine among the communities of Merawi Town, Northwest Ethiopia: A cross-sectional study. Evid Based Complement Alternat Med 2015;2015:138073.
4. Lambert J. Ethiopia; Traditional Medicine and the bridge to better health, World Bank Ethiop. J Health Dev 2006;20:5.
5. Debjit B, Pawan D, Margret C, Kumar K. Herbal drug toxicity and safety evaluation of traditional medicines. Arch Appl Sci Res 2009;1:32-56.
6. Pascual ME, Slowing K, Carretero E, Sánchez Mata D, Villar A. Lippia: Traditional uses, chemistry and pharmacology: A review. J Ethnopharmacol 2001;76:201-14.
7. Demissew S. A confusion in *Lippia (Verbenaceae)* in tropical Africa. Kew bulletin 1993:375-9.
8. Stickel F, Patsenker E, Schuppan D. Herbal hepatotoxicity. J Hepatol 2005;43:901-10.
9. Ayele M. Evaluation of Acute and Sub-Chronic Toxicity of Aqueous Leaves Extracts of Maytenus Gracilipes *Celastraceae* (Kombolcha) on Some Blood Parameters and Histopathology of Liver and kidney in Swiss Albino Mice: Addis Abeba University; 2015.
10. Arika W, Ogola P, Abdirahman Y, Mawia A, Wambua F. *In vivo* Safety of aqueous leaf extract of *Lippia javanica* in mice models. Biochem Physiol 2015;5:2.
11. Liebelt AG. Unique Features of Anatomy, Histology, and Ultrastructure Kidney, Mouse. Urinary system 1998:37-57.
12. Rozman KK, Klaassen CD. Casarett and Doull‘s Toxicology: The Basic Science of Poisons. New York: McGraw-Hill; 2007.
13. Bickers D, Calow P, Greim H, Hanifin J, Rogers A, Saurat J, *et al.* A toxicologic and dermatologic assessment of linalool and related esters when used as fragrance ingredients. Food Chem Toxicol 2003;41:919-42.
14. Masran S, Salji MR, Othman H, Budin SB, Taib IS, editors. Acute Toxicity (oral) Information of *Litsea elliptica* Blume essential oil. Int Conf Biosci Biochem Bioinf 2011;5:399-403.
15. Powers KA, Beasley VR. Toxicological aspects of linalool:

A review. Vet Hum Toxicol 1985;27:484-6.
16. Idang EO, Yemitan OK, Mbagwu HO, Udom GJ, Ogbuagu EO, Udobang JA. Toxicological assessment of Zingiber officinale Roscoe (Ginger) root oil extracts in Albino rats. Toxicology Digest 2019;4:108-19.
17. Ahmad RA, Serati-Nouri H, Abdul Majid F, Sarmidi MR, Abdul Aziz R. Assessment of potential toxicological effects of Cinnamon bark aqueous extract in rats. Int J Biosci Biochem Bioinform 2015;5:36-44.
18. Pasman WJ, Heimerikx J, Rubingh CM, van den Berg R, O'Shea M, Gambelli L, *et al.* The effect of Korean pine nut oil on *in vitro* CCK release, on appetite sensations and on gut hormones in post-menopausal overweight women. Lipids Health Dis 2008;7:10.
19. Yang X, Schnackenberg LK, Shi Q, Salminen WF. Hepatic toxicity biomarkers. In: Biomarkers in Toxicology. Academic Press; 2014. p. 241-59.
20. Yuet Ping K, Darah I, Chen Y, Sreeramanan S, Sasidharan S. Acute and subchronic toxicity study of *Euphorbia hirta* L. methanol extract in rats. Biomed Res Int 2013;2013:182064.
21. Rahman M, Siddiqui MK, Jamil K. Effects of Vepacide (*Azadirachta indica*) on asp artate and al anine aminotransferase profiles in a subchronic study with rats. Hum Exp Toxicol 2001;20:243-9.
22. Parke DV, Rahman KM, Walker R. Effect of linalool on hepatic drug-metabolizing enzymes in the rat. Portland Press Ltd 1974.
23. Zárybnický T, Boušová I, Ambrož M, Skálová L. Hepatotoxicity of monoterpenes and sesquiterpenes. Arch Toxicol 2018;92:1-13.
24. Fandohan P, Gnonlonfin B, Laleye A, Gbenou JD, Darboux R, Moudachirou M. Toxicity and gastric tolerance of essential oils from *Cymbopogon citratus*, *Ocimum gratissimum* and *Ocimum basilicum* in Wistar rats. Food Chem Toxicol 2008;46:2493-7.
25. Ebeye O, Ekundina O, Wilkie I. Histological and biochemical effects of aqueous extract of *Ocimum gratissimum* on the liver and kidney of adult Wistar rats. Afr J Cell Pathol 2014;2:59-64.
26. Noori A, Amjad L, Yazdani F. The effects of *Artemisia* deserti ethanolic extract on pathology and function of rat kidney. Avicenna J Phytomed 2014;4:371-6.

Case Report

A Rare Aortic Arch Anomaly: Combination of Vertebral Arteria Lusoria with Kommerell's Diverticulum, Bovine Aortic Arch, and Left Vertebral Artery with Extreme Proximal Origin

Fatih Erdem, Erdoğan Bülbül, Bahar Yanık, Emrah Akay

Department of Radiology, Balikesir University Hospital, Balikesir, Turkey

Abstract

Vertebral arteria lusoria (VAL), defined as the right vertebral artery (VA) originating from the aortic arch distally to the left subclavian artery (SCA) and progressing retroesophageally, is a rare vascular anomaly. This anomaly is rarely associated with abnormalities such as aortic coarctation, Bovine aortic arch, and Kommerell's diverticulum. It is uncommon for VAs to originate from the SCA below the level of the 1st rib. To our knowledge, no instance of VAL has been described, in which the left VA originates from the SCA below the first rib. We aimed to present computed tomography findings in a patient with VAL, Kommerell's diverticulum, Bovine aortic arch, and a left VA with the extreme proximal origin, which could be also defined as "vertebrosubclavian trunk," in this case report.

Keywords: *Bovine aortic arch, Kommerell's diverticulum, vertebral arteria lusoria, vertebral artery with extreme proximal origin*

Introduction

The "typical" three-branch aortic arch pattern includes: the brachiocephalic trunk that gives off the right subclavian artery (SCA) and the right common carotid artery (CCA), the left CCA, and the left SCA.[1]

Vertebral artery (VA) typically originates (50.6%–99.9%) from the posterosuperior aspect of the 1st part of the SCA, 0.5–2 cm medial to the thyrocervical trunk origin.[1] Aberrant origin of the VAs is not very usual, with a reported incidence of 4.7% in a recent systematic literature review based on 32 original studies encompassing 14738 subjects.[1] Variations of the VA origin usually occur on the left side, and rarely occur on the right side with a reported incidence of only 0.69%.[1,2] The most common reported atypical VA origin is from the aortic arch with an incidence of 5.5%. A left VA with an aortic arch origin is the commonest reported variation (range 0.79%–8%) most frequently located in between left CCA and left SCA, while most rarely originates distal to left SCA.[1] The aortic origin of the right VA and especially its origin as the last branch is very rare.[1,2]

In rare cases, the right VA originates from the aorta, and even more rarely from the descending part. Like the classic arteria lusoria, it usually takes a retroesophageal course, probably the main reason why this VA variant is also named lusoria. Like the classic arteria lusoria, the vertebral arteria lusoria (VAL) has been shown to originate from Kommerell's diverticulum.[2] Bilateral aortic origin of the VA has been reported, too.[1] The VA origin below the level of the first rib has been reported in the literature as a rare entity with an incidence of 2.94%, without definition of right or left direction (3 out of 102 cases). Such condition, which is the extreme proximal origin of left VA, has been also reported as "vertebrosubclavian trunk" in the literature with an incidence of 0.3%–0.73%.[3-5]

In cross-sectional radiological imaging, vascular anatomical variations of the aortic arch are often encountered incidentally.[6] These variations of great vessels are generally asymptomatic and can be noticed later in life. However, it may rarely be closely related to tracheoesophageal structures and cause symptoms due to variation of the course.[2,6] We aimed to present computed tomography (CT) findings of a rarely seen VAL abnormality accompanied by

How to cite this article: Erdem F, Bülbül E, Yanık B, Akay E. A rare aortic arch anomaly: Combination of vertebral arteria lusoria with Kommerell's diverticulum, bovine aortic arch, and left vertebral artery with extreme proximal origin. J Anat Soc India 2023;72:67-9.

Article Info

Received: 11 June 2021
Accepted: 03 June 2022
Available online: 24 March 2023

Address for correspondence:
Dr. Fatih Erdem, Department of Radiology, Balikesir University Hospital, 10145 Altieylül, Balikesir, Turkey.
E-mail: mdfatiherdem@gmail.com

Access this article online

Website: www.jasi.org.in
DOI: 10.4103/jasi.jasi_106_21
Quick Response Code:

Kommerell's diverticulum, bovine aortic arch, and a left VA with the extreme proximal origin, which could be also defined as "vertebrosubclavian trunk," in this case report.

Case Report

An 82-year-old male patient, who had no complaints and was followed up for a history of lymphoma, underwent thorax CT for follow-up. Incidentally, it was observed that the right VA originated from the aortic arch distal to the left SCA and had a retroesophageal course. Focal dilatation consistent with Kommerell's diverticulum was observed in the origin of the right VA [Figure 1a and b]. The innominate artery (IA) and left CCA emerged as a single trunk from the aortic arch, which is consistent with the Bovine aortic arch. Furthermore, the left VA, as the first branch of the left SCA, originated from the more proximal and posteromedial part of the left SCA [Figure 2a and b]. The patient did not have any symptoms related to these variations.

Discussion

The most common variation in the aortic arch branching pattern is the so-called "Bovine arch" in which the IA and left CCA fuse as a single root.[6] This variation was also observed in our case. Normally, VAs arise as the first branch from the posterosuperior parts of the ipsilateral SCAs and above the level of the 1st rib (97.1%).[6,7] Many papers have been published about the types of anomalies of origin of the vertebral arteries in the literature. The most common VA variation is the type, in which the left VA arises directly from the aortic arch in the region between the left CCA and the left SCA and accounts for 2.4%–5.8% of instances.[7] In our case, the left VA emerged as the first branch of the left SCA as expected, but its origin was caudal to the 1st rib level. The VA origin below the level of the first rib may be encountered rarely, and its incidence has been reported as 2.94%, without definition of right or left direction (3 out of 102 cases).[7] The proximal origin of left VA from the left SCA could be also referred as "vertebrosubclavian trunk" and its incidence in a radiological study was found to be 0.3% (8 out of 2287 cases), and 0.73% in another study in the literature.[3-5]

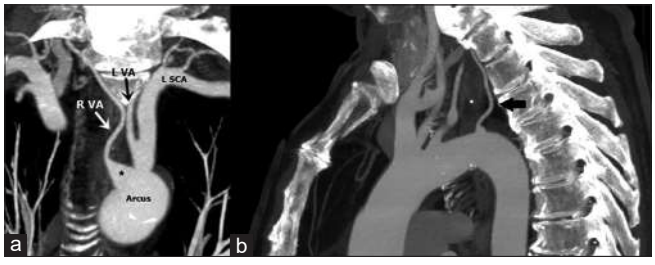

Figure 1: (a) The coronal CT maximum intensity projection image showed Kommerell's diverticulum (*) in the origin of the RVA and the extreme proximal origin of the LVA from the LSCA (arrow). (b) vThe sagittal maximum intensity projection CT image showed the retroesophageal course of the aberrant RVA. RVA: Right vertebral artery, LVA: Left vertebral artery, LSCA: Left subclavian artery, CT: Computed tomography

Variations in the right VA are seen less frequently, and the most common type is that the right VA emerges from the root of the right SCA (76.6%).[7] In our case, the right VA originated as the last branch of the aorta and had a retroesophageal course. Therefore, this anomaly is called VAL.[2,8] The incidence of VAL has been reported very low in the literature.[2,7,9,10] Its association with anomalies such as coarctation of the aorta, Bovine arch, and bilateral VAs originating from the aortic arch have been published in a limited number of articles.[6,9-11] As in our case, its association with focal enlargement at the level of origin called Kommerell's diverticulum is also rare.[2,8,9,12] To our knowledge, extreme proximal left VA origin from the left SCA, caudal to the 1st rib, has not been defined before together with these anomalies.

In 1948, Edwards first proposed the double aortic arch system hypothesis to explain the embryological process of branching.[13] According to this hypothesis, most congenital aortic arch anomalies are caused by the persistence of a segment that should normally regress or regression of a segment that should persist. VAs are formed by the vertical connection of the first seven cervical intersegmental arteries. The horizontal segments of the cervical intersegmental arteries are connected to the dorsal aorta. During the development of the horizontally positioned cervical intersegmental arteries, all but the proximal part of the SCA and the 7th cervical intersegmental artery, which forms the origin of the VA, disappear.[8] However, it is suggested that the connection of the right VA with the right SCA is lost due to obliteration of the distal right dorsal aorta segment between the 6th and 7th cervical intersegmental arteries during the formation of VAL anomaly. The right SCA normally develops from the 7th cervical intersegmental artery, but the right VA is thought to originate from the persistent proximal right dorsal aorta distal to the left SCA [Figure 3]. There are publications claiming that the Kommerell's diverticulum seen in the right VA origin, which we detected in our case, is the remnant of this right dorsal aortic origin.[8,9]

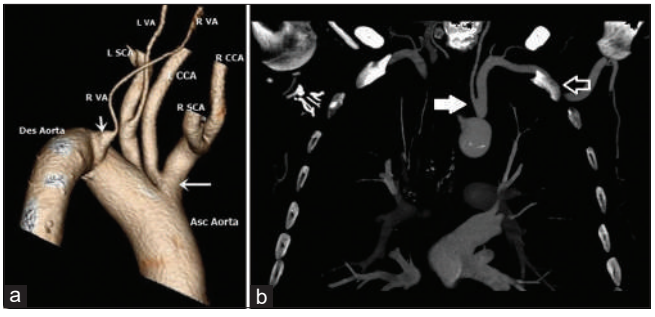

Figure 2: (a) a-The dorsal oblique 3D CT image showed the RVA with Kommerell's diverticulum in its origin, arising from the dorsal aspect of the aortic arch and distal to the LSCA (small arrow). Also, bovine arch was seen (large arrow). (b) The coronal maximum intensity projection CT image showed that the origin of the LVA (white arrow) was below the first rib (open arrow). Des Aorta: Descending aorta, LVA: Left vertebral artery, LCCA: Left common carotid artery, RCCA: Right common carotid artery, RSCA: Right subclavian artery, Asc Aorta: Ascending Aorta, RVA: Right vertebral artery, LSCA: Left subclavian artery, CT: Computed tomography

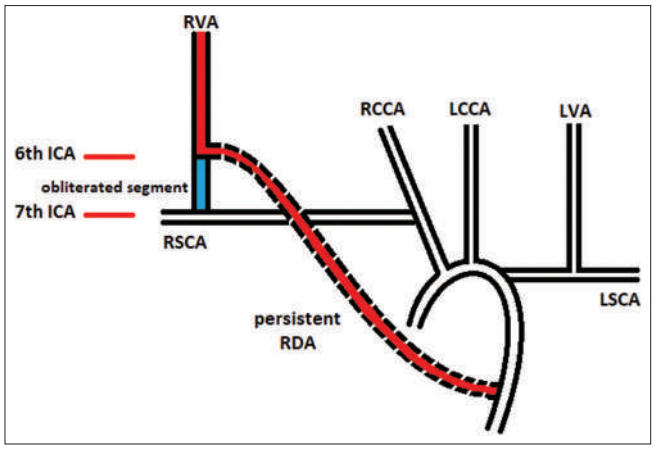

Figure 3: A simple scheme of the embryological development of vertebral arteria lusoria. Due to the obliteration of the vertical segment between the 6th and 7th intersegmental arteries, the connection between the RVA and the RSCA get lost. Instead, the RDA does not regress and provides the continuity of the RVA with aortic arch. ICA: Cervical Intersegmental Artery, RCCA: Right Common Carotid Artery, LCCA: Left Common Carotid Artery, LVA: Left Vertebral Artery, LSCA: Left Subclavian Artery, RDA: Right dorsal aorta, RSCA: Right subclavian artery, RVA: Right vertebral artery

Few cases in the literature have been reported as symptomatic. VAL may compress the esophagus or trachea as in dysphagia lusoria due to aberrant SCA. Apart from dysphagia, since the VA is thinner than the SCA, headache and dizziness may be rarely seen due to the influence of the VA that feeds the cerebral system.[9] We think these symptoms are less common thanks to the compensation mechanisms (posterior communicating arteries) between the posterior and anterior vascular circulations of the brain and the support of the opposite VA in the posterior circulation. However, it has been reported that variations in the great vessels of the aortic arch may adversely affect hemodynamics and predispose to vascular pathologies such as dissection, aneurysm, and arteriovenous fistula.[7,9] Our case did not have any symptoms related to these anomalies or a vascular pathology detected by imaging methods.

VAL may be detected incidentally by catheter angiography examination or encountered in multislice CT examinations, which are more frequently used in daily practice. In contrast to the right aberrant SCA, the VAL is thinner and may be overlooked by the radiologist. Failure to draw attention to this anomaly by the radiologist may lead to life-threatening neurological complications such as large hemomediastinum or stroke due to unstoppable hemorrhages due to arterial damage during esophageal surgeries, minimally invasive endoscopic procedures, or interventional endovascular procedures that are increasing nowadays.[8]

Conclusion

As a result, we may encounter vascular anomalies of the aortic arch incidentally during cross-sectional radiological imaging. Furthermore, other rare variations may accompany rare anomalies such as VAL. It is important to keep these in mind and draw attention to them, as it will reduce the wrong evaluation and complications that may occur during surgical, endoscopic, or interventional endovascular procedures.

Declaration of patient consent

The authors certify that they have obtained all appropriate patient consent forms. In the form the patient(s) has/have given his/her/their consent for his/her/their images and other clinical information to be reported in the journal. The patients understand that their names and initials will not be published and due efforts will be made to conceal their identity, but anonymity cannot be guaranteed.

Financial support and sponsorship

Nil.

Conflicts of interest

There are no conflicts of interest.

References

1. Lazaridis N, Piagkou M, Loukas M, Piperaki ET, Totlis T, Noussios G, *et al.* A systematic classification of the vertebral artery variable origin: Clinical and surgical implications. Surg Radiol Anat 2018;40:779-97.
2. Ventosa A, Bilreiro C, Brito J. Vertebral arteria lusoria: A rare anatomical variant to recognize before cervical and thoracic procedures. Case 17319. Eurorad 2021 [Doi: 10.35100/eurorad/case. 17319].
3. Rameshbabu CS, Sharma V, Kumar A, Qasim M, Gupta OP. Vertebro-subclavian trunk. A rare aortic arch anomaly. J Clin Diagn Res 2018;12:AC01-4.
4. Babu CS, Sharma V. Two common trunks arising from arch of aorta: Case report and literature review of a very rare variation. J Clin Diagn Res 2015;9:AD05-7.
5. Uchino A, Saito N, Takahashi M, Okada Y, Kozawa E, Nishi N, *et al.* Variations in the origin of the vertebral artery and its level of entry into the transverse foramen diagnosed by CT angiography. Neuroradiology 2013;55:585-94.
6. Saeed UA, Gorgos AB, Semionov A, Sayegh K. Anomalous right vertebral artery arising from the arch of aorta: Report of three cases. Radiol Case Rep 2017;12:13-8.
7. Yuan SM. Aberrant origin of vertebral artery and its clinical implications. Braz J Cardiovasc Surg 2016;31:52-9.
8. Lacout A, Khalil A, Figl A, Liloku R, Marcy PY. Vertebral arteria lusoria: A life-threatening condition for oesophageal surgery. Surg Radiol Anat 2012;34:381-3.
9. Goldbach A, Dass C, Surapaneni K. Aberrant right vertebral artery with a diverticulum of Kommerell's: Review of a rare aortic arch anomaly. J Radiol Case Rep 2018;12:19-26.
10. Case D, Seinfeld J, Folzenlogen Z, Kumpe D. Anomalous right vertebral artery originating from the aortic arch distal to the left subclavian artery: A case report and review of the literature. J Vasc Interv Neurol 2015;8:21-4.
11. Goray VB, Joshi AR, Garg A, Merchant S, Yadav B, Maheshwari P. Aortic arch variation: A unique case with anomalous origin of both vertebral arteries as additional branches of the aortic arch distal to left subclavian artery. AJNR Am J Neuroradiol 2005;26:93-5.
12. Balani A, Marda SS, Kumar AD, Alwala S. Kommerell's diverticulum: Unusual case expanding the horizon. Can Assoc Radiol J 2015;66:298-9.
13. Edwards JE. Anomalies of the derivatives of the aortic arch system. Med Clin North Am 1948;32:925-49.

Case Report

Horseshoe Appendix with Double Insertion of Base: A Previously Unreported Anomaly

Sourav Roy, Partha Chakraborty, Manoranjan Shaw[1], Pankaj Kumar Halder

Department of Pediatric Surgery, R. G. Kar Medical College and Hospital, [1]Department of Plastic Surgery, IPGMER and SSKM (H), Kolkata, West Bengal, India

Abstract

Duplication of appendix including horseshoe appendix (HA) is well reported. We present the case of acute appendicitis in a 19-year-old male where we found the appendicular base was doubly inserted into the cecum, and the tip was attached to the cecum at sagittal disposal. Ligation and transection of both bases and tip individually were carried out. This is a previously undescribed variety of appendiceal anomalies in the form of HA with double insertion of the base. This report will be a step toward broadening the horizon of knowledge regarding appendiceal anomalies and better delineation of such anomalies.

Keywords: *Anomalies, appendectomy, appendix, double insertion, horseshoe appendix*

Introduction

Appendiceal anomalies are challenging entities for the operating surgeon. A duplication of the vermiform appendix is among the most frequently found congenital anomalies of the appendix, with 100 cases already reported worldwide. However, no literature yet reports double insertion of the appendiceal base in a horseshoe appendix (HA). We present a case of acute appendicitis where two bases and one tip were found to be communicating with the cecum by a central mesoappendix, and the body of the appendix adhered to the cecum. As per our knowledge, this is an undocumented anatomical identity to date.

Case Report

A 19-year-old male patient presented with acute onset of abdominal pain, nausea, and a few episodes of vomiting for the past 48 h. He was a known case of cerebral palsy (CP) with level II disability (Gross Motor Function Classification System Expanded and Revised) and gross developmental lag in all four domains. He could not localize pain due to cognitive dysfunction. There was no history of similar episodes in the past. The relevant medical, family, or allergy history along with other pertinent comorbidities (except CP) was not significant. The vital signs of the patient were blood pressure of 124/82 mmHg, pulse rate of 114 beats/min, respiration rate of 15 breaths/min, and body temperature of 37.5°C. Tenderness, guarding, and rebound tenderness in the right lower quadrant of the abdomen were appreciable with positive McBurney's sign and Iliopsoas signs. The blood hemogram showed leukocytosis (10,500/μL) with a shift to the left and raised C-reactive protein (56 mg/L). An abdominal ultrasound revealed an aperistaltic, blind-ended, noncompressible gut loop (2.5 cm × 1.0 cm) adjacent to the cecum, suggestive of acute appendicitis. The patient was resuscitated accordingly and taken for an emergency appendectomy. The abdomen was opened by standard McBurney's incision. The appendix was found to have grossly adhered to the cecum. Initially, what was thought to be the base of the appendix was found to be the so-called tip later. Careful dissection revealed a double insertion of the base of the appendix, the bases were ligated separately [Figures 1 and 2]. All the bases and the so-called tip were found along with the tenia coli. The appendicular artery in the mesoappendix was found to be thrombosed, and vascular disposition of the appendix could not be elicited. The mesoappendix was ligated and transected. The abdominal wound was closed in layers. The postoperative (PO) period was uneventful. The patient was discharged on the 2nd PO day. He recovered well with normal wound healing.

How to cite this article: Roy S, Chakraborty P, Shaw M, Halder PK. Horseshoe appendix with double insertion of base: A previously unreported anomaly. J Anat Soc India 2023;72:70-3.

Article Info

Received: 24 June 2021
Revised: 16 August 2022
Accepted: 13 September 2022
Available online: 24 March 2023

Address for correspondence:
Dr. Pankaj Kumar Halder, Saroda Palli, Sitko Road, Baruipur, Kolkata - 700 144, India.
E-mail: pankaj.cnmc@gmail.com

Access this article online

Website: www.jasi.org.in
DOI: 10.4103/jasi.jasi_112_21
Quick Response Code:

Discussion

The incidence of the duplex appendix is 0.004%–0.009%, comprising the highest among the appendiceal anomalies.[1] The incidence of HA is even rarer, with only 15 reports of this case [Table 1].

The embryological cause, leading to horseshoe or duplex appendix is still unclear. A "transient appendix" develops in the 5th week of intrauterine life from the terminus of the cecum, and atrophies by the 7th week. Singh *et al*. put forward HA may develop from the fusion of the tip of the normal appendix with that of the variant appendix which is at the abnormal site, thereby giving rise to the so-called horseshoe anomaly. The other possible explanation could be that the HA develops from the fusion of the tip of the normal appendix with another part of the cecum which later on, becomes the second base.[2] However, these theories fail to explain why the HA is supplied by a single blood vessel in the mesoappendix as opposed to an arcade artery. An older theory by Gupta *et al*. stated the HA could result from a peculiar cascade where the base of the appendix somehow split in two, and during development and cecal growth gets separated further, leading to a double-based, yet single structure.[3] However, cases of the triplicate appendix and our case cannot be explained by these theories.

Precise classification of appendiceal anomaly is an ever-changing system spanning over the past century. It was first developed by Cave in 1936, modified by Wallbridge in 1963, and further modified by Biermann in 1993. These classification systems did not include the HA,

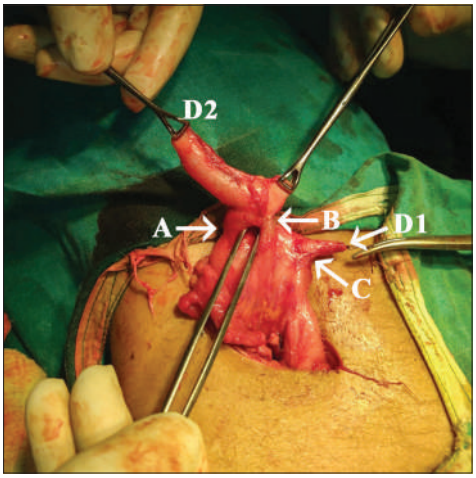

Figure 1: Intraoperative photograph of the case (after ligation and transection of the tip). A, B: Two bases of the appendix, C: The tip of the appendix, D1, D2: Transected ends

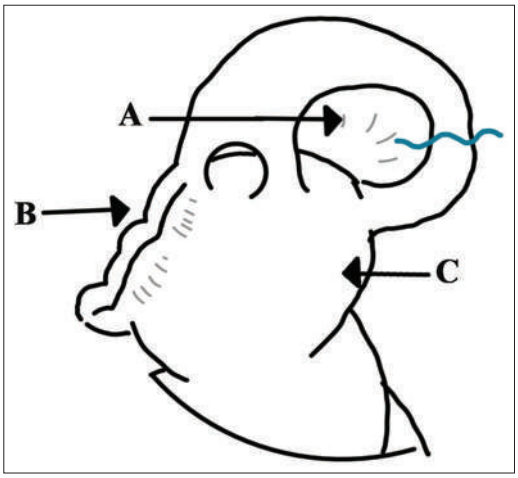

Figure 2: Schematic diagram of intraoperative findings. A: Mesoappendix (thrombosed), B: Tenia coli, C: Cecum, the blue line denotes the plane of transaction

Table 1: Classification of appendiceal anomalies (Takabatake *et al*., 2016)

Number anomalies
1. Agenesis: Absence of appendix
2. Duplex appendix
A: Partial duplication with both appendices sharing a common base like "Y-shaped" on a single cecum
B: Complete duplication of the appendix on a single cecum
B1 avian type: Two appendices symmetrically placed on either side of the ileocecal valve
B2 tenia coli cecum type: One appendix arising from the usual site of the cecum and the other arising from the cecum along the tenia
B3 tenia coli hepatic flexure type: One appendix arising from the usual site of the cecum and the other arising from the hepatic flexure of the colon along the tenia
B4 tenia coli splenic flexure type: One appendix arising from the usual site of the cecum and the other arising from the splenic flexure of the colon along the tenia
C: Duplication of the cecum, each has its own appendix
3. Triplex appendix: Complete triplication of the appendix on the cecum
Shape anomalies: Horseshoe appendix
According to disposal of the mesentery
Sagittal disposal: Both bases of the appendix are along the tenia in a sagittal direction
Frontal disposal: The bases of the appendix are not on the tenia.
According to the location of the orifice
Cecum-cecum
Cecum-ascending colon

which was first incorporated by Calota *et al*.[4] in 2010 under a different entity named "Shape Anomaly," which was modified by Takabatake *et al*.[5] to encompass different types of HA [Table 2].

Analysis of the 16 reported cases of HA (including our case) shows the incidence among 11 males and 5 females, who ranged in age from 4 to 78 years with a mean age of 38 years. Preoperative diagnosis was possible in only two cases using ultrasound and 3D reconstructed imaging. Irrespective of the anomalies, the choice of treatment for acute appendicitis is appendectomy. Intraoperatively, a single fan-shaped vessel supplied the appendix in all of the described cases. The location of the mesentery was found to be almost equally divided into two subgroups: frontal types (7/16), with the bases of the appendix not on the tenia, and sagittal types (6/16), with the bases of the appendix along the tenia.[14] Interestingly, duplication of the appendix is commonly reported with other gastrointestinal, genitourinary anomalies, anorectal malformation, and situs inversus totalis, but reports of HA lacked any association with any other anomalies. However, an internal hernia induced by HA, complicating the PO period by partial gangrene of the cecum, followed by fistula formation, possibly explained by the presence of anomalous vascularization in the area had been reported.[17,18] The anomalies of the appendix stand with serious medicolegal significance, as multiple reports of litigation are present in appendicitis in the second appendix, which was not identified and transected during the appendectomy.[6,11] As clearly evident, none of the classification systems could include the anomaly in our case (double insertion of the appendiceal base in HA). Hereby, we propose to extend Takabatake's classification system to include another major subtype, namely, "Complex anomalies," to include a combination of multiple number anomalies and shape

Table 2: Documented cases of horseshoe appendix

Author	Age (years)/ sex	Diagnosis	Length (cm)	Type	Internal hernias	Association appendiceal anomalies	Other congenital anomalies	Orifice	Procedure
Mesko *et al*., 1989[6]	33/male	Appendicitis	NA	NA	NA	No	NA	NA	Appendectomy
Dong *et al*., 1994[7]	46/male	Bowel occlusion	20	Frontal	Yes/ ileum	No	NA	Cecum-cecum	Appendectomy + enterotomy
Dasgupta *et al*., 1999[8]	48/male	Appendicular mass	NA	Frontal	No	No	NA	Cecum-cecum	Appendectomy
Li and Yu *et al*., 2000[9]	30/female	Appendicitis	NA	Frontal	No	No	NA	Cecum-cecum	Appendectomy
Cai and Lin., 2006[10]	56/male	Appendicitis	8	Sagittal	No	No	NA	Cecum-cecum	Appendectomy
Calotă *et al*., 2010[4]	43/female	Bowel occlusion	13.5	Sagittal	No	No	NA	Cecum-cecum	Appendectomy
Ninos *et al*., 2010[11]	20/female	B-cell nonHodgkin's lymphoma	4	Sagittal	No	No	NA	Cecum-cecum	Appendectomy + chemotherapy
Dube *et al*., 2011[12]	32/male	Appendicitis	7	Sagittal	No	No	NA	Cecum-hepatic flexure of the colon	Appendectomy
Li and Liu *et al*., 2012[13]	46/male	Appendicitis + bowel occlusion	7	NA	Yes/ ileum	No	NA	Cecum-cecum	Appendectomy + enterotomy
Oruç *et al*., 2013[14]	64/female	Appendicitis	NA	NA	No	No	NA	Cecum-cecum	Appendectomy
Bulut *et al*., 2016[13]	52/female	Appendicitis	8	Frontal	No	No	NA	Cecum-cecum	Appendectomy
Singh *et al*., 2016[2]	5/male	Appendicitis	NA	Frontal	No	No	None	Cecum-Cecum	Appendectomy
Takabatake *et al*., 2016[5]	78/male	Tubulovillous adenoma in ascending colon	NA	Sagittal	No	No	NA	Cecum-ascending colon	Ileocecal resection
Jin Liu *et al*., 2018[15]	22/male	Appendicular mass	15	Frontal	No	No	NA	Cecum-cecum	Appendectomy
Sang-Ji Choi *et al*., 2019[16]	33/male	Appendicitis	NA	Sagittal	No	No	None	Cecum-ascending colon	Appendectomy
Our case 2021	19y/male	Appendicitis		Frontal	No	Double insertion of base	None	Cecum-cecum	Appendectomy

NA: Data not available or undocumented

Table 3: Proposed modification of appendiceal anomalies classification

I. Number anomalies
1. Agenesis: Absence of appendix
2. Duplex appendix
A: Partial duplication with both appendices sharing a common base like "Y-shaped" on a single cecum
B: Complete duplication of the appendix on a single cecum
B1 avian type or "bird-like appendix": Two appendices symmetrically placed on either side of the ileocecal valve. In humans, it is found associated with intestinal and/or genitourinary anomalies
B2 tenia coli cecum type: One appendix arising from the usual site of the cecum and the other arising from the cecum along the tenia
B3 tenia coli hepatic flexure type: One appendix arising from the usual site of the cecum and the other arising from the hepatic flexure of the colon along the tenia
B4 tenia coli splenic flexure type: One appendix arising from the usual site of the cecum and the other arising from the splenic flexure of the colon along the tenia
C: Duplication of the cecum, each has its own appendix
3. Triplex appendix: Complete triplication of the appendix on the cecum
II. Shape anomalies: Horseshoe appendix
1. Sagittal disposal: Both bases of the appendix are along the tenia in a sagittal direction
Cecum-cecum
Cecum-ascending colon
Cecum-hepatic flexure of the colon
2. Frontal disposal: The bases of the appendix are not on the tenia
Cecum-cecum
III. Complex anomalies: Combination of multiple number anomalies and shape anomalies

anomalies [Table 3]. We want to emphasize equally that identification, classification, and reporting of appendiceal anomalies are important for developing knowledge about the etiology of the conditions and association with anomalies, gastrointestinal, or otherwise.

Declaration of patient consent

The authors certify that they have obtained all appropriate patient consent forms. In the form the patient (s) has/have given his/her/their consent for his/her/their images and other clinical information to be reported in the journal. The patients understand that their names and initials will not be published and due efforts will be made to conceal their identity, but anonymity cannot be guaranteed.

Financial support and sponsorship

Nil.

Conflicts of interest

There are no conflicts of interest.

References

1. Chen W, Guo Z, Qian L, Wang L. Comorbidities in situs inversus totalis: A hospital-based study. Birth Defects Res 2020;112:418-26.
2. Singh CG, Nyuwi KT, Rangaswamy R, Ezung YS, Singh HM. Horseshoe appendix: An extremely rare appendiceal anomaly. J Clin Diagn Res 2016;10:PD25-6.
3. Liu J, Dong C, Wang H, Sun D, Liang R, Gao Z, *et al*. One type of duplex appendix: Horseshoe appendix. Ther Clin Risk Manag 2018;14:1987-92.
4. Calotă F, Vasile I, Mogoantă S, Zavoi R, Paşalega M, Moraru E, *et al*. Horseshoe appendix: A extremely rare anomaly. Chirurgia (Bucur) 2010;105:271-4.
5. Takabatake K, Ikeda J, Furuke H, Kato C, Kishimoto T, Kumano T, *et al*. A case of a horseshoe appendix. Surg Case Rep 2016;2:140.
6. Mesko TW, Lugo R, Breitholtz T. Horseshoe anomaly of the appendix: A previously undescribed entity. Surgery 1989;106:563-6.
7. Dong Z, Fu X, Luo H. Horseshoe appendix induced intestinal obstruction. Chin J Clin Anat 1994;12:309-10.
8. DasGupta R, Reber PU, Patel AG. Horseshoe appendicitis. Eur J Surg 1999;165:1095-6.
9. Li C, Yu J. A horseshoe appendix. Guangdong Med J 2000;21:982-3.
10. Cai S, Lin M. A case of annular appendix with acute appendicitis. J Med Imaging 2017;17:27-8.
11. Ninos A, Douridas G, Papakonstantinou E. A horseshoe double appendix positioned on a non-Hodgkin lymphoma. Hellenic J Surg 2010;82:73-7.
12. Dube B, Manoharan GR, Daya M. Anomalous origin of the vermiform appendix. S Afr J Surg 2011;49:100.
13. Liu J, Dong C, Wang H. One type of duplex appendix: horseshoe appendix. Therapeut Clin Risk Manag 2018;14:1987-92.
14. Oruç C, Işık O, Ureyen O, Kahyaoğlu OS, Köseoğlu A. An extremely rare appendiceal anomaly: Horseshoe appendicitis. Ulus Travma Acil Cerrahi Derg 2013;19:385-6.
15. Bulut SP, Cabıoğlu N, Akıncı M. Perforated double appendicitis: Horseshoe type. Ulus Cerrahi Derg 2016;32:134-6.
16. Choi SJ, Chae G, Park SB, Hong SK, Kim YH, Moon SB, *et al*. Horseshoe appendix identified during laparoscopic appendectomy: A case report and literature review. Medicine (Baltimore) 2019;98:e14104.
17. Ngulube A, Ntoto CO, Matsika D, Ndebele W, Dube NS, Gapu P. A case report of complete appendiceal duplication on the normal site of a single caecum: A new variant? Int J Surg Case Rep 2020;74:168-72.
18. Alves JR, Maranhão IG, de Oliveira PV. Appendicitis in double caecal appendix: Case report. World J Clin Cases 2014;2:391-4.

Case Report

Patient with Two Left Cuneiform Bones Only: A First Documented Case Report

Abstract

The cuneiforms are three wedge-shaped bones, forming the tarsus of the foot along with the talus, calcaneus, navicular, and cuboid. We present the case of a 70-year-old Caucasian woman with a left unique lateral cuneiform instead of second and third cuneiform bones. Additional cuneiform bones are rare anatomical variants which have been well described in the literature. Conversely, a lesser number of cuneiform bones have never been previously reported. To our knowledge, our article represents the first documented case of this anatomical variation.

Keywords: *Anatomical variation, cuneiform bones, first case, foot, radiology*

Nicola Monteleone, Antonino Marcello Pilia[1], Cristiana Veltro[1], Jacopo Junio Valerio Branca[1], Federico Polidoro, Alberto Belluati, Ferdinando Paternostro[1]

Department of Orthopedics and Traumatology, Santa Maria Delle Croci Hospital, Ravenna, [1]Department of Experimental and Clinical Medicine, Anatomy and Histology Section, University of Florence, Florence, Italy

Introduction

The lateral, intermediate, and medial cuneiform are three wedge-shaped tarsal bones. They form with navicular and cuboid the midfoot, a section of the foot between the Chopart joint line proximally and the Lisfranc joint distally. The lateral cuneiform is smaller than the medial cuneiform and larger than the intermediate one. The lateral and medial cuneiforms are longer than the intermediate one, so that the base of the second metatarsal bone recesses between them, giving great stability in the frontal plane. These three bones articulate between each other, with the navicular bone proximally and each of them with their respective metatarsal base distally. The lateral one articulates with the cuboid. The tibialis posterior muscle attaches to all of the cuneiforms. Other musculotendinous attachments are flexor hallucis brevis for the lateral cuneiform and third plantar interosseous muscle, peroneus longus, and tibialis anterior for the medial one. Strong but small interosseous ligaments connect the nonarticular surfaces to adjacent cuneiforms. The vascular supply to medial and intermediate cuneiform originates from the branches of the dorsal arterial network, whereas lateral cuneiform receives blood from the lateral tarsal artery. The draining veins correspond to the arterial supply. The deep peroneal and medial plantar nerves provide innervation. Endochondral ossification in the extremities begins by the end of the embryonic period, and ossification centers arise from the first to the third year of life. Abnormalities with an excessive number of bones are mostly bilateral, whereas a lesser number is usually unilateral. In some cases, the bones actually fuse.[1-5]

Case Report

We present the case of a 70-year-old Caucasian woman with nocturnal diffuse lower limb and left foot pain. At the remote anamnesis, she was affected by hypercholesterolemia, treated with statins and left shoulder prosthesis was implanted. Inspectively, there is no remarkable difference of the anatomical profile between the right and left foot, and a hallux valgus tendency is present in both of them. The patient does not refer to pain during the deambulation, but tenderness is positive in the left tarsal region.

The left frontal radiograph [Figure 1] demonstrates a unique cuneiform bone instead of the second and third cuneiform bones, and synostosis of this one with the second and the third metatarsal bones. Figure 2 shows lateral foot projection.

Discussion

Additional cuneiform bones are rare anatomical variants which have been well-described in literature, such as the

How to cite this article: Monteleone N, Pilia AM, Veltro C, Branca JJ, Polidoro F, Belluati A, *et al*. Patient with two left cuneiform bones only: A first documented case report. J Anat Soc India 2023;72:74-5.

Article Info

Received: 12 January 2021
Revised: 30 September 2022
Accepted: 15 October 2022
Available online: 24 March 2023

Address for correspondence:
Prof. Ferdinando Paternostro, L.go Brambilla 3, 50134, Firenze, Italy.
E-mail: ferdinando.paternostro@unifi.it

Access this article online

Website: www.jasi.org.in
DOI: 10.4103/jasi.jasi_4_21
Quick Response Code:

Figure 1: Left foot – Weight bearing

Figure 2: Left foot – Non-weight bearing

bipartite medial cuneiform or small accessory ossicles. On the contrary, a lesser number of cuneiform bones have never been previously reported. It is important to be aware of these variations as they can alter the already complex biomechanics of the foot and cause symptoms, such as midfoot pain, which may be overlooked or misdiagnosed due to the vague disorder or chronic condition.

Recognizing such anatomical anomalies is essential also for preoperative planning of arthrodesis or open reduction and internal fixation procedures in this anatomical location.[6-9]

Although the presence of this couple of cuneiform seems congenital radiographically – And not an acquired synostosis – The nature of such variation needs further investigations.

Conclusion

To our knowledge, this is the first documented case of a human foot with only two cuneiform bones, which could be considered an additional contribution to the description of its other anatomical variations, with potential implications for foot pathology, radiology, diagnosis, and surgery.

Declaration of patient consent

The authors certify that they have obtained all appropriate patient consent forms. In the form, the patient(s) has/have given his/her/their consent for his/her/their images and other clinical information to be reported in the journal. The patients understand that their names and initials will not be published and due efforts will be made to conceal their identity, but anonymity cannot be guaranteed.

Financial support and sponsorship

Nil.

Conflicts of interest

There are no conflicts of interest.

References

1. Available from: https://radiopaedia.org/articles/lateral-cuneiform. [Last accessed on 2020 Nov 13].
2. Available from: https://radiopaedia.org/articles/intermediate-cuneiform. [Last accessed on 2020 Nov 13].
3. Available from: https://radiopaedia.org/articles/medial-cuneiform. [Last accessed on 2020 Nov 13].
4. MacGregor R, Byerly DW. Anatomy, bony pelvis and lower limb, foot bones. In: StatPearls. Treasure Island (FL): StatPearls Publishing; 2020.
5. Sadler TW, Langman J. Part two: Special embryology. In: Langman's Medical Embryology. Ch. 8. Philadelphia, Pa: Lippincott Williams & Wilkins; 2004. p. 183-91.
6. Serfaty A, Pessoa A, Antunes E, Malheiro E, Canella C, Marchiori E. Bipartite medial cuneiform: Magnetic resonance imaging findings and prevalence of this rare anatomical variant. Skeletal Radiol 2020;49:691-8.
7. Brookes-Fazakerley SD, Jackson GE, Platt SR. An additional middle cuneiform? J Surg Case Rep 2015;2015:rjv076.
8. Chang GH, Chang EY, Chung CB, Resnick DL. Bipartite medial cuneiform: Case report and retrospective review of 1000 magnetic resonance (MR) imaging studies. Case Rep Med 2014;2014:130979.
9. Steen EF, Brancheau SP, Nguyen T, Jones MD, Schade VL. Symptomatic bipartite medial cuneiform: Report of five cases and review of the literature. Foot Ankle Spec 2016;9:69-78.

Case Report

Amelanotic Mucosal Melanoma of the Nasal Cavity

Padmapriya Jaiprakash[1], Mary Mathew[1], Varun Kumar Singh[2], Dipak Ranjan Nayak[3]

Departments of [1]Pathology and [3]Otorhinolaryngology, Kasturba Medical College, Manipal Academy of Higher Education, [2]Department of Pathology, Melaka Manipal Medical College, Manipal Campus, Manipal Academy of Higher Education, Manipal, Karnataka, India

Abstract

Mucosal melanomas are rare head-and-neck tumors and have a distinct etiology and genetic profile different from cutaneous counterparts. They are most commonly seen in sixth–seventh decade of life and have aggressive behavior. The patients usually present with nodal metastasis, which is the most important poor prognostic indicator for mucosal melanomas. We present a case of mucosal melanomas in a young male (30 years), who presented with nonpigmented, polypoidal mass in the right nasal cavity simulating an inverted papilloma. Histological examination showed small to large pleomorphic cells and no melanin pigment. Based on the immunopositivity of the tumour cells were positive for HMB45 and S100 confirming a diagnosis of amelanotic mucosal melanoma. The partied had a localized disease to the right nasal cavity with no nodal involvement and no recurrences in the available follow-up of 24 months.

Keywords: *Amelanotic melanoma, HMB45, inverted papilloma, nasal cavity, S100*

Introduction

Mucosal melanoma is a malignant neoplasm arising from the melanocytes derived from the neural crest cells. Melanomas are common in the skin; other sites include the upper aerodigestive tract, eye, and meninges. Mucosal melanomas are rare and comprise approximately 1.3% of all melanomas.[1,2] Mucosal melanomas comprise about 4% of sinonasal tumors and around 13% of these melanomas do not show melanin pigment. Seen most commonly in the sixth–seventh decade of life, the most common site of sinonasal mucosal melanoma is the nasal cavity followed closely by maxillary and ethmoidal sinuses.[2] Mucosal melanoma differs considerably in risk factors, etiology, and biological behavior from cutaneous melanomas. They are not associated with solar exposure and are more aggressive with around 10%–30% presenting with lymphadenopathy at diagnosis. Due to their morphology, they have a wide range of differential diagnoses and their rarity has not enabled the development of standard therapeutic regimens.[1-3]

We present a case of amelanotic mucosal melanoma in a male at an unusual age of 35 years, the morphological diagnostic dilemmas, and postoperative follow-up information.

Case Report

A 35-year-old male presented with complaints of gradually worsening right-sided nasal blockage for 20 days, which aggravated on lying down and was associated with blood-tinged nasal discharge and headache. The patient underwent left eye evisceration following trauma 15 years back. Local examination revealed the fullness of the right nasolabial angle, a polypoidal, congested, and firm mass was seen arising from the right middle meatus, extending into the inferior meatus and bleeds on touch.

A high-resolution computerized tomography of the region showed a well-defined, nonenhancing soft-tissue density lesion seen in the right nasal cavity occupying the middle and inferior meatus, measuring 3.5 cm × 2.2 cm × 1.5 cm. The lesion caused the widening of the nasal cavity with a mild displacement of the nasal septum to the left with erosions. The inferior aspect of the right middle turbinate could not be visualized separately from the lesion. The lesion is causing occlusion of the right maxillary ostium and the infundibulum [Figure 1]. There was no evidence of adjacent bony destruction or extension of the lesion to the right maxillary sinus/choana. The patient

How to cite this article: Jaiprakash P, Mathew M, Singh VK, Nayak DR. Amelanotic mucosal melanoma of the nasal cavity. J Anat Soc India 2023;72:76-8.

Article Info

Received: 12 October 2020
Revised: 16 August 2022
Accepted: 16 August 2022
Available online: 24 March 2023

Address for correspondence:
Dr. Varun Kumar Singh, 305, Melaka Manipal Medical College, Manipal Academy of Higher Education, Madhav Nagar, Manipal, Udupi - 576 104, Karnataka, India.
E-mail: varunksingh2k5@gmail.com

Access this article online

Website: www.jasi.org.in
DOI: 10.4103/jasi.jasi_219_20
Quick Response Code:

Figure 1: Coronal sections of the nasal cavity and paranasal sinuses showing a soft-tissue density lesion in the right nasal cavity covering the middle and inferior turbinate

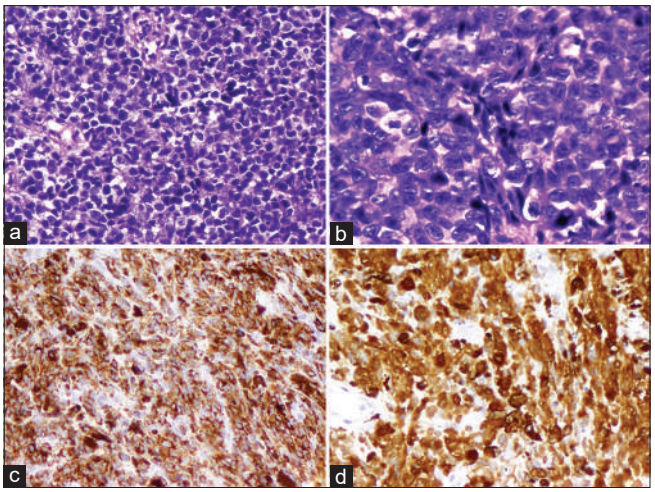

Figure 2: (a) Tumor cells with hyperchromatic nuclei and scant cytoplasm arranged in sheets (H and E, ×100). (b) Individual tumor cells pleomorphic nuclei, prominent nucleoli and no cytoplasmic melanin (H and E, ×400). (c) Tumor cells show cytoplasmic staining with HMB45 (×100). (d) Tumor cell show nuclear and cytoplasmic staining for S100 (×400)

underwent excision of the lesion with endoscopic right medial maxillectomy. Pathological examination of the lesion showed malignant cells arising from the epithelium and infiltrating into the stroma in the form of sheets and fascicles of malignant cells with large pleomorphic vesicular nuclei, prominent eosinophilic nucleoli, with brisk mitosis. Based on the immunopositivity of the cells with HMB45 and S100, a diagnosis of amelanotic malignant mucosal melanoma was given [Figure 2]. The margins of the maxillectomy were free of tumor. The patient did not show any recurrences for an available follow-up period of 24 months.

Discussion

The World Health Organization Classification of Tumors of the Head-and-Neck has established sinonasal and oral mucosal melanomas as distinct entities.[4] Seen most commonly in the seventh decade of life, they show a slight preponderance for the male population. They present with indistinct clinical features like nasal obstruction and epistaxis. These presenting symptoms overlap with benign, borderline, and malignant as well as metastatic entities described in the sinonasal region.[1,4-6] The most common site is the lateral wall and turbinates, followed by the nasal septum. They present as polyps and the presence of pigment is a clue to diagnosis; however, in cases of amelanotic lesions, the differential diagnosis is wide.[2,4] Amelanotic mucosal melanoma has been reported as case reports and forms a small part of large reported series.[2,3,7-9] The present case was unusual with a much younger age of presentation of 35 years. The lesion was polypoidal and nonpigmented, which suggested a clinical diagnosis of inverted papilloma.

Histologically, amelanotic mucosal melanoma shows varied morphological features. The major morphological types include the presence of epithelioid cells, spindle cells, also pleomorphic, small cell, and plasmacytoid cell variants. The absence of cytoplasmic melanin pigment makes the diagnosis even more uncertain. The major differential diagnosis of amelanotic mucosal melanomas include small blue cell tumors such as Ewings/primitive neuroectodermal tumor, and olfactory neuroblastoma, neuroendocrine carcinomas, sinonasal undifferentiated carcinomas, poorly differentiated squamous cell carcinoma, large B cell lymphoma, and spindle cell morphology may simulate a sarcoma.[4,10] Such a diagnostic conundrum can be addressed by the use of immunohistochemistry. Sinonasal mucosal melanomas show expression of melanocytic markers HMB45, Melan A, and tyrosinase in up to 65% of cases, S100 has the highest sensitivity of around 90%; however, the immunostaining also has a shortcoming in the form of aberrant expression of neuroendocrine markers such as synaptophysin, cytokeratins, and CD99 have been reported in approximately 10% of the cases. This warrants a careful examination and use of at least two positive markers to concur with a diagnosis of amelanotic mucosal melanoma.[1,2,4,10] The present case had a mixture of epithelioid and small cells and was positive for S100 and HMB45.

The management of mucosal melanoma has been a conventional surgery with wide marginal resection. The role of other modalities such as chemotherapy, radiotherapy, and immunotherapy has not been fully established. Genetic studies have revealed a higher prevalence of KIT mutation/amplification in mucosal melanomas (10%–25%), whereas BRAF V600E mutations are consistent with cutaneous melanomas. This has been the basis of clinical trials of BRAF inhibitors and imatinib in the treatment of mucosal melanomas.[1,4] Factors such as Breslow's depth and ulceration that are important for the prognosis of cutaneous melanoma do not hold for mucosal melanomas.

Metastasis is the most important poor prognostic factor for mucosal melanomas, other widely studied poor prognostic factors include age >67.6 years, middle turbinate lesion, and recurrence. Elderly male patients presenting with amelanotic mucosal melanomas are at a higher risk of recurrence.[2,4]

Conclusion

Sinonasal amelanotic mucosal melanoma is a rare aggressive malignancy with considerable morphological overlap with other malignancies of the region. A careful histological examination and judicious use of immunohistochemistry are needed to make an accurate diagnosis. Prognostic factors of mucosal melanomas are different from the cutaneous counterpart and more large-scale studies are warranted to understand the biology of the entity.

Declaration of patient consent

The authors certify that they have obtained all appropriate patient consent forms. In the form, the patient(s) has/have given his/her/their consent for his/her/their images and other clinical information to be reported in the journal. The patients understand that their names and initials will not be published and due efforts will be made to conceal their identity, but anonymity cannot be guaranteed.

Financial support and sponsorship

Nil.

Conflicts of interest

There are no conflicts of interest.

References

1. Williams MD, Speight P, Wenig BM. Mucosal melanoma. In: El-Naggar A, Chan JK, Grandis JR, Takata T, Slootweg PJ, editors. WHO Classification of Head and Neck Tumours. 4th ed. Lyon: IARC; 2017. p. 60-1.
2. Pontes FS, de Souza LL, de Abreu MC, Fernandes LA, Rodrigues AL, do Nascimento DM, *et al.* Sinonasal melanoma: A systematic review of the prognostic factors. Int J Oral Maxillofac Surg 2020;49:549-57.
3. Vučinić D, Zahirović D, Manestar D, Belac-Lovasić I, Braut T, Kovač L, *et al.* Recurrent amelanotic melanoma of nasal cavity: Biological variability and unpredictable behavior of mucosal melanoma. A case report. Clin Pract 2019;9:1157.
4. Williams MD. Update from the 4th edition of the World Health Organization Classification of Head and Neck Tumours: Mucosal Melanomas. Head Neck Pathol 2017;11:110-7.
5. Singh VK, Mathew M, Kudva R, Pai K, Vijay A. Sinonasal solitary fibrous tumour : A borderline entity with diagnostic challenges. Int J Clin Diagnostic Pathol 2019;2:316-20.
6. Singh VK, Mathew M, Kudva R, Pai K, Bishnu A. Sinonasal metastasis: A clinicopathological series of seven cases. Online J Heal Allied Sci 2020;19:12.
7. Singhvi A, Joshi A. A case of amelanotic malignant melanoma of the maxillary sinus presented with intraoral extension. Malays J Med Sci 2015;22:89-92.
8. Verma R, Lokesh KP, Gupta K, Panda NK. Sinonasal amelanotic malignant melanoma – A diagnostic dilemma. Egypt J Ear Nose Throat Allied Sci 2015;16:275-8.
9. Kaur K, Kakkar A, Rastogi S, Sharma MC. Sinonasal amelanotic melanoma with neuroendocrine differentiation: A diagnostic conundrum. Ultrastruct Pathol 2020;44:249-54.
10. Agaimy A. Poorly differentiated sinonasal tract malignancies: A review focusing on recently described entities. Cesk Patol 2016;52:146-53.

Case Report

Intracapsular Ossicle of the Knee Joint

Kumari Chiman, Anjali Aggarwal, Gupta Tulika, Sahni Daisy

Department of Anatomy, PGIMER, Chandigarh, India

Abstract

An accessory skeletal element in relation to a joint may alter the dynamics of the joint besides altering the diagnosis and treatment plan. Presence of any such variation has to be kept in mind so that unnecessary delay in intervention for any pathological conditions can be avoided. The occurrence of an accessory bone in the body has been reported by some authors. Its presence can be of medicolegal importance. Such bones may be mistaken for fracture. During routine dissection of the knee joint in the graduate teaching course, a bony element was found in the posterior aspect of the joint. The dimension of the bone-like structure was measured using digital vernier callipers. The structure was then processed for histological interpretations. It was hard in with a dimension of 15 mm. On histological examination, the sections showed characteristics of a matured bone.

Keywords: *Accessory bone, intracapsular ossicle, knee joint, tibia*

Introduction

An accessory bone in relation to the articulating elements of a joint, has the ability to change the dynamics of the joint. This may be misdiagnosed as a fracture or osteophyte. A prior knowledge of variant bones can have additional diagnostic importance in dealing with patients having joint problems. There are reports of the presence of sesamoid bones as well as supernumerary bones in different parts of the body.[1-3] Some authors have also reported about ossifications in rare areas such as the menisci and cruciate ligaments of the knee joint.[4-6] Such ossifications may occur following trauma.[7]

Case Report

Routine dissection was performed on a 59-year-old cadaver during the teaching of graduate students in the Department of Anatomy, PGIMER, Chandigarh. The knee joint was exposed both anteriorly and posteriorly by giving a circumscribed incision. As the capsule of the joint was reflected to expose the articular surfaces of the joint, a pea-shaped bone-like structure was observed in the posterior aspect of the joint, in relation to the medial condyle of the tibia. Its position was observed *in situ* and then detached from the surrounding structures. Adjacent structures such as the tendons, muscles, articular surfaces, menisci, and cruciate ligaments were also observed for any specific finding. The shape and size of the bony element were determined, and then, it was processed for histological preparation. Digital Vernier calipers were used for measuring the size. Six random measurements were taken, and the average of the measurements was considered the final size of the bone. The condition of the adjacent articulating surfaces of the joint was also looked for. Nikon D7000 camera (Nikon Co., Tokyo, Japan) was used for taking the required photos. Ground tissue section was prepared to see for the presence of the Haversian system. Furthermore, hematoxylin and eosin (H and E) and Masson's Trichome stains were done to look for other histological features. The sections were examined under the light microscope (Olympus-BX 53) and photographed with the help of C7 + ProgRes software.

Discussion

On gross examination, the bone-like structure was observed to be smooth and round in shaped with an average dimension of 15 mm. It was intracapsular and hard in consistency. It had a round, smooth articular area on one surface. A corresponding articular area was found in the posterior aspect of the medial condyle of the tibia, which indicated that the structure was articulating with the medial condyle of

How to cite this article: Chiman K, Aggarwal A, Tulika G, Daisy S. Intracapsular ossicle of the knee joint. J Anat Soc India 2023;72:79-80.

Article Info

Received: 16 November 2021
Accepted: 11 October 2022
Available online: 24 March 2023

Address for correspondence:
Dr. Anjali Aggarwal, Department of Anatomy, Research Block B, PGIMER, Chandigarh - 160 012, India.
E-mail: anjli_doc@yahoo.com

Access this article online

Website: www.jasi.org.in
DOI: 10.4103/jasi.jasi_187_21
Quick Response Code:

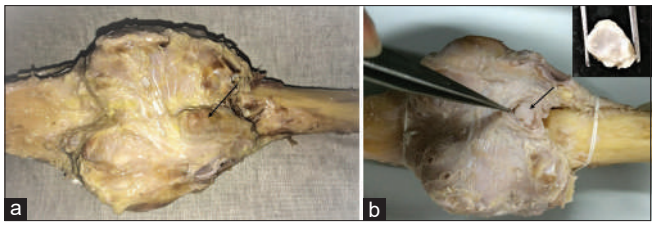

Figure 1: (a) Pea-shaped smooth bone (inset, b), dimension of 1.5 cm found articulating with the medial condyle of tibia (black arrow: a and b)

the tibia [Figure 1]. There were no osteophytic changes adjacent to the bones. There was also no gross evidence of fracture or trauma in either of the bones. The structure was not related to any tendons which were present around the knee joint, indicating that it is not sesamoid in nature. The adjacent tendons were normal in appearance. Further, ground tissue preparation of the bone showed Haversian systems having lamella with lacuna within them [Figure 2a]. In H and E, as well as Masson's trichome-stained sections, cell layers resembling that of epiphyseal growth plate were observed [Figure 2b and c]. Osteons were identified by the presence of the Haversian canal [Figure 2a]. The lamellar pattern was not observed on the surface where there was the presence of the periosteum. The thick collagen fibers were uniformly aligned [Figure 2c and d].

Conclusion

Both phylogeny and function contribute toward the formation of an accessory or a sesamoid bone. The formation depends on the phylogeny, while size depends on the function.[1,8] In the present case, the small bony element might be formed due to the friction caused by the overlying muscles. Another possibility is that, there might have been a separate ossification center which failed to join later, giving rise to an intracapsular ossicle. It may even be a case of posttraumatic ossification following meniscal tear. However, in our case, there is no reported history of trauma. The occurrence of an accessory bone in the body can be of medico-legal importance. Such bones may be mistaken as fractures. Some authors have mentioned articular sesamoid bone, which increases the joint surface and renders a comfortable movement. On the other hand, the clinical symptoms due to the presence of these types of bones may go unnoticed by clinicians. However, any accidental pathological findings have to be excluded.

Financial support and sponsorship

Nil.

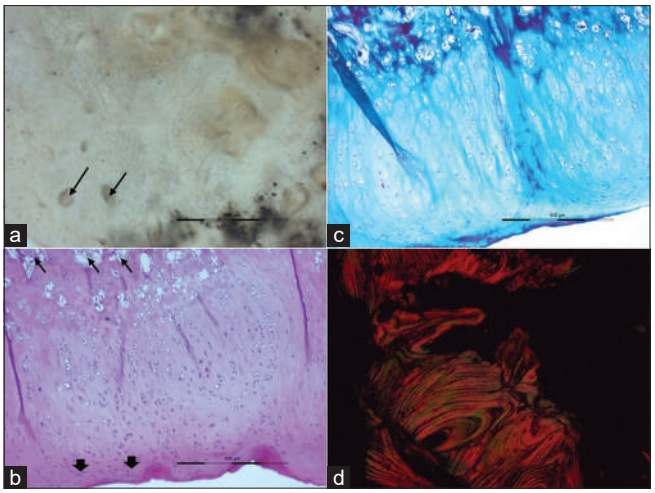

Figure 2: (a) Ground preparation of the bone, in which Haversian canal (black arrows), the lamellated pattern of bone along with lacuna are observed. (b) H and E, showing area resembling the epiphyseal growth plate (×10). The periosteum is observed in the periphery (black arrow head). Marrow cavity is also seen (black arrow) c and d. Masson-trichome stain and safranin O Stain showing the parallel orientation of the collagen fibers (×10)

Conflicts of interest

There are no conflicts of interest.

References

1. Bizarro AH. On sesamoid and supernumerary bones of the limbs. J Anat 1921;55:256-68.
2. Chen W, Cheng J, Sun R, Zhang Z, Zhu Y, Ipaktchi K, *et al*. Prevalence and variation of sesamoid bones in the hand: A multi-center radiographic study. Int J Clin Exp Med 2015;8:11721-6.
3. Gujar V, Bokariya P, Hiware S, Shende MR. Supernumerary bones in superior and inferior extremity. Forensic Med Toxicol 2015;9:1202.
4. Kumar P, Dey AK, Mittal K, Sharma R, Hira P. Double meniscal ossicle, the first description: CT and MRI findings-different etiologies. Case Rep Radiol 2015;2015:737506.
5. Conforty B, Lotem M. Ossicles in human menisci: Report of two cases. Clin Orthop Relat Res 1979;1:272-5.
6. Li C, Huang Z, Anil KC, Lao C, Wu Q, Jiang H. Heterotopic ossification in the post cruciate ligament of the knee: A case report and literature review. BMC Musculoskelet Disord 2021;22:304.
7. Mohankumar R, Palisch A, Khan W, White LM, Morrison WB. Meniscal ossicle: Posttraumatic origin and association with posterior meniscal root tears. AJR Am J Roentgenol 2014;203:1040-6.
8. Sarin VK, Erickson GM, Giori NJ, Bergman AG, Carter DR. Coincident development of sesamoid bones and clues to their evolution. Anat Rec 1999;257:174-80.

Case Report

Aneurysmal Dilatation of Vein of Galen Associated with Thalamic Arteriovenous Malformation and Straight Sinus Agenesis

Abstract

Straight sinus agenesis is a rare congenital anatomical variation that is usually accompanied by persistent falcine sinus. Concomitance of straight sinus agenesis and absence of falcine sinus are associated with thalamic arteriovenous malformation by the disturbance of the venous flow. In this report, a very rare case of aneurysmal dilatation of the vein of Galen associated with thalamic arteriovenous malformation and straight sinus agenesis is presented.

Keywords: *Aneurysm, falcine sinus, straight sinus agenesis, thalamic arteriovenous malformation, vein of Galen*

Sercan Özkaçmaz

Department of Radiology, Yüzüncü Yıl University Faculty of Medicine, Bardakçı, Van 65100, Turkey

Introduction

Intracranial arteriovenous malformations (AVMs) are usually developmental or congenital vascular malformations which are formed by abnormal arteriovenous shunts. The most common presentations of AVMs are life-threatening hemorrhage and seizures. They are usually diagnosed before 4th decade of life.[1,2]

Thalamic AVM secondary to straight sinus agenesis is extremely rare with only a few cases in literature. In this report, we aimed to present magnetic resonance imaging findings of an adult patient with a thalamic AVM and Galen Vein Aneurysmal dilatation associated with straight and falcine sinus agenesis.

Case Report

56-year-old female was admitted to the neurology clinic with a complaint of bilateral moderate headache for 2 years. Her neurological examination was normal and previous medical history was unremarkable with no surgery or trauma anamnesis. A nonenhanced brain magnetic resonance imaging demonstrated an arteriovenous malformation in the right thalamus associated with markedly dilated right basal veins. Furthermore, dilation of Galen and left basal vein was seen. Intracranial enlarged various venous collaterals which drained venous blood from the vein of Galen to the Superior Sagittal and bilateral Transverse sinuses were detected. The bilateral vein of the Trolard and Superior Sagittal Sinus were markedly dilated. Dilatations of cortical veins in bilateral temporal lobes were seen. Straight sinus was absent and also a persistent falcine sinus was not demonstrated. Atrophy and focal gliosis were detected in the right thalamus [Figures 1 and 2]. The patient was diagnosed as having a right thalamic arteriovenous malformation fed by lenticulostriate arteries and drained to cortical veins and superior sagittal sinus through basal veins. A digital subtraction angiography was recommended but the patient denied further examinations and treatment.

Discussion

The venous system of the brain is very complex which is composed of various superficial and deep venous structures including sinuses, veins, and plexuses. The straight sinus is one of the most important unpaired sinuses of the dural venous system as it drains high volume of venous blood and the congenital or acquired pathologies of this vein lead to major complications.

The inferior sagittal sinus joins to the vein of Galen (great cerebral vein) and forms the straight sinus which drains to the transverse sinus at the level of confluence of sinuses. It is usually average 5 cm in length. Besides

How to cite this article: Özkaçmaz S. Aneurysmal dilatation of vein of Galen associated with thalamic arteriovenous malformation and straight sinus agenesis. J Anat Soc India 2023;72:81-3.

Article Info

Received: 23 August 2021
Revised: 10 February 2022
Accepted: 11 October 2022
Available online: 24 March 2023

Address for correspondence:
Prof. Sercan Özkaçmaz, Department of Radiology, Yüzüncü Yıl University Faculty of Medicine, Bardakçı, Van 65100, Turkey.
E-mail: sercanozkacmaz@hotmail.com

Access this article online

Website: www.jasi.org.in
DOI: 10.4103/jasi.jasi_145_21
Quick Response Code:

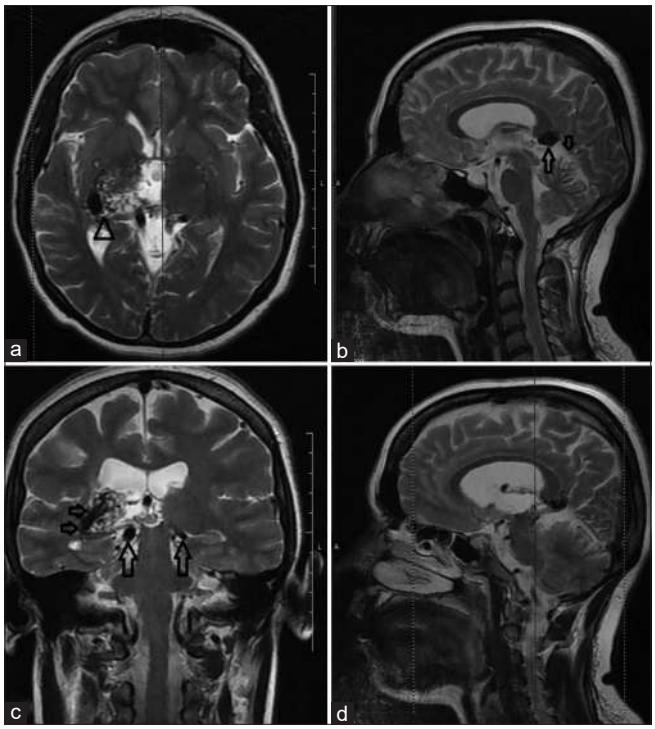

Figure 1: A right thalamic AVM (arrowhead) is seen (a). Dilated VOG (long arrow) and absent straight sinus (short arrow) (b). Thalamic AVM (short arrows) and dilated basal veins (long arrows) (c). Absent straight and falcine sinus (d). AVM: Arteriovenous malformations

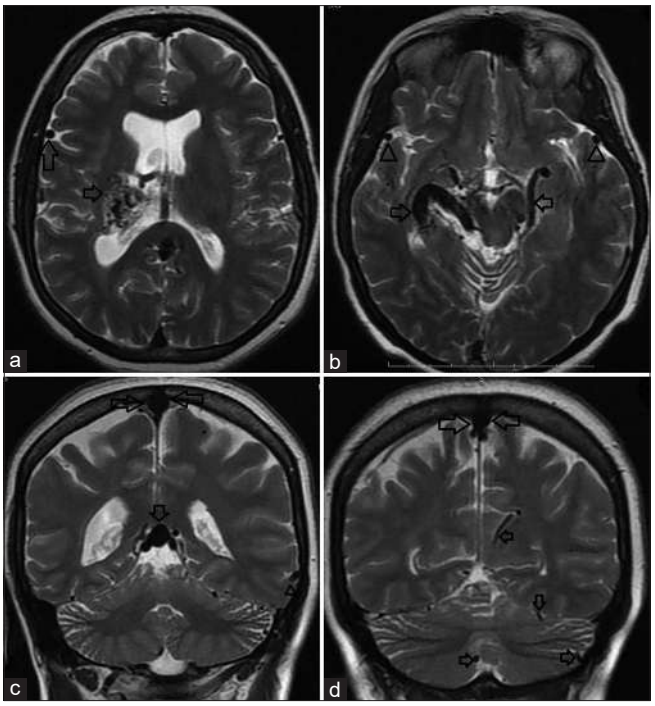

Figure 2: Right thalamic AVM (short arrows) and dilated right cortical (vein of trolard) vein (long arrow) (a). Bilateral dilated basal veins (arrows) and cortical veins (arrowheads) (b). Aneurysmal dilatation of vein of Galen (arrow) left cortical vein (arrowhead) and superior sagittal sinus (long arrows) (c). Prominent cortical veins (short arrows) and superior sagittal sinus (long arrows) also absent straight sinus (d). AVM: Arteriovenous malformations

this, it also drains the venous blood of superior aspects of cerebellum and occipital lobe.[3] The falcine sinus is an ascending midline vein which presents in during the fetal period. It is located between the dural leaves of falx cerebri which connects the superior sagittal sinus and vein of Galen. It usually closes before birth.[4] Persistence of this vein is usually associated with congenital straight sinus abnormalities including agenesis, stenosis, or duplication while recanalization is frequently due to obstructive events such as tumor compression or straight sinus thrombosis. It is likely to occur as a compensatory mechanism to maintain the venous blood flow through superior sagittal sinus which is blocked at straight sinus level by congenital or acquired conditions. Ryu detected persistent falcine sinus in 12 of (2.1%) 586 patients. Among these 12 patients, 8 were associated with rudimentary or absent straight sinus.[5]

Thalamic arteriovenous malformations and Galen Vein aneurysm are associated with straight sinus agenesis or thrombosis. Quisling and Mickle examined their 15 patients with Galen Vein aneurysm and they found straight sinus stenosis in 4 of them and concluded that straight sinus agenesis is associated with Galen vein aneurysm.[6] Minakawa *et al*. suggested an association between abnormal straight sinus flow with arteriovenous malformations in their 9 patients.[7]

Vein of Galen aneurysmatic dilatation (VGAD) must be differentiated from Vein of Galen malformations (VGM), as VGAD occurs secondary to an outflow obstruction[8] but VGM results from arteriovenous shunts which have arterial supply largely derived from choroidal arteries.[9] Persistent falcine sinus which drains deep venous system by connecting Vein Of Galen and Superior sagittal sinus is the most frequent venous anomaly which associated with VGM in children especially if the straight sinus is thrombosed or absent.[10] Although it is very rare in adult population, VGM may be a challenge for the differential diagnosis of dilatation of Galen of Vein in elder patients. Similarly to our patient, in type IV (Yaşargil classification), VGM patients have shunting from an adjacent thalamic arteriovenous malformation results in aneurysmal dilation of the vein of Galen.[11] Furthermore, headache may be present as the only complaint of an adult patient with choroidal type VGM.[12] However, the sizes of the sac of VGM are bigger than VGAD and cardiac symptoms usually accompany VGM. In our patient, we think that the aneurysmal dilatation of Vein of Galen is secondary to high-flow thalamic AVM draining into this vein and dilatation of bilateral basal veins secondary to the absence of straight and falcine sinuses since venous drainage is maintained through basal veins and cortical veins.

Conclusion

Congenital anatomical variations of Straight and Falcine sinuses must be kept in mind in especially patients with thalamic arteriovenous malformations. Also enlarged

cortical-basal veins and also Superior Sagittal sinus must raise a suspicion of a congenital or acquired blockage in the level of the straight sinus.

Declaration of patient consent

The authors certify that they have obtained all appropriate patient consent forms. In the form the patient (s) has/have given his/her/their consent for his/her/their images and other clinical information to be reported in the journal. The patients understand that their names and initials will not be published and due efforts will be made to conceal their identity, but anonymity cannot be guaranteed.

Acknowledgments

There are no conflicts of interest and no funding in this study. An informed written consent was obtained from the patient.

Financial support and sponsorship

Nil.

Conflicts of interest

There are no conflicts of interest.

References

1. Laakso A, Hernesniemi J. Arteriovenous malformations: Epidemiology and clinical presentation. Neurosurg Clin N Am 2012;23:1-6.
2. Tranvinh E, Heit JJ, Hacein-Bey L, Provenzale J, Wintermark M. Contemporary ımaging of cerebral arteriovenous malformations. AJR Am J Roentgenol 2017;208:1320-30.
3. Moore KL, Dalley AF, Agur AM. Clinically Oriented Anatomy. 5th ed. Baltimore: Lippincott Williams & Wilkins; 2006. p. 914-5.
4. Carpenter JS, Rosen CL, Bailes JE, Gailloud P. Sinus pericranii: Clinical and imaging findings in two cases of spontaneous partial thrombosis. AJNR Am J Neuroradiol 2004;25:121-5.
5. Ryu CW. Persistent falcine sinus: İs it really rare? AJNR Am J Neuroradiol 2010;31:367-9.
6. Quisling RG, Mickle JP. Venous pressure measurements in vein of Galen aneurysm. AJNR Am J Neuroradiol 1989;10:411-7.
7. Minakawa T, Tanaka R, Koike T, Takeuchi S, Abe H. Cerebral arteriovenous malformations associated with a straight sinus anomaly. Neurosurgery 1992;31:19-25.
8. Gupta AK, Varma DR. Vein of Galen malformations: Review. Neurol India 2004;52:43-53.
9. Raybaud CA, Strother CM, Hald JK. Aneurysms of the vein of Galen: Embryonic considerations and anatomical features relating to the pathogenesis of the malformation. Neuroradiology 1989;31:109-28.
10. Brunelle F. Arteriovenous malformation of the vein of Galen in children. Pediatr Radiol 1997;27:501-13.
11. Puvabanditsin S, Mehta R, Palomares K, Gengel N, Da Silva CF, Roychowdhury S, *et al*. Vein of Galen malformation in a neonate: A case report and review of endovascular management. World J Clin Pediatr 2017;6:103-9.
12. Pareek K, Shrivastava T, Sinha VD. Choroidal type of vein of galen aneurysmal malformation in adult patient with unusual presentation of orthostatic headache. Asian J Neurosurg 2018;13:418-20.

The Editorial Process

A manuscript will be reviewed for possible publication with the understanding that it is being submitted to Journal of the Anatomical Society of India alone at that point in time and has not been published anywhere, simultaneously submitted, or already accepted for publication elsewhere. The journal expects that authors would authorize one of them to correspond with the Journal for all matters related to the manuscript. All manuscripts received are duly acknowledged. On submission, editors review all submitted manuscripts initially for suitability for formal review. Manuscripts with insufficient originality, serious scientific or technical flaws, or lack of a significant message are rejected before proceeding for formal peer-review. Manuscripts that are unlikely to be of interest to the Journal of the Anatomical Society of India readers are also liable to be rejected at this stage itself.

Manuscripts that are found suitable for publication in Journal of the Anatomical Society of India are sent to two or more expert reviewers. During submission, the contributor is requested to provide names of two or three qualified reviewers who have had experience in the subject of the submitted manuscript, but this is not mandatory. The reviewers should not be affiliated with the same institutes as the contributor/s. However, the selection of these reviewers is at the sole discretion of the editor. The journal follows a double-blind review process, wherein the reviewers and authors are unaware of each other's identity. Every manuscript is also assigned to a member of the editorial team, who based on the comments from the reviewers takes a final decision on the manuscript. The comments and suggestions (acceptance/ rejection/ amendments in manuscript) received from reviewers are conveyed to the corresponding author. If required, the author is requested to provide a point by point response to reviewers' comments and submit a revised version of the manuscript. This process is repeated till reviewers and editors are satisfied with the manuscript.

Manuscripts accepted for publication are copy edited for grammar, punctuation, print style, and format. Page proofs are sent to the corresponding author. The corresponding author is expected to return the corrected proofs within three days. It may not be possible to incorporate corrections received after that period. The whole process of submission of the manuscript to final decision and sending and receiving proofs is completed online. To achieve faster and greater dissemination of knowledge and information, the journal publishes articles online as 'Ahead of Print' immediately on acceptance.

Clinical trial registry

Journal of the Anatomical Society of India favors registration of clinical trials and is a signatory to the Statement on publishing clinical trials in Indian biomedical journals. Journal of the Anatomical Society of India would publish clinical trials that have been registered with a clinical trial registry that allows free online access to public. Registration in the following trial registers is acceptable: http://www.ctri.in/; http://www.actr.org.au/; http://www.clinicaltrials.gov/; http://isrctn.org/; http://www.trialregister.nl/trialreg/index.asp; and http://www.umin.ac.jp/ctr. This is applicable to clinical trials that have begun enrollment of subjects in or after June 2008. Clinical trials that have commenced enrollment of subjects prior to June 2008 would be considered for publication in Journal of the Anatomical Society of India only if they have been registered retrospectively with clinical trial registry that allows unhindered online access to public without charging any fees.

Authorship Criteria

Authorship credit should be based only on substantial contributions to each of the three components mentioned below:

1. Concept and design of study or acquisition of data or analysis and interpretation of data;
2. Drafting the article or revising it critically for important intellectual content; and
3. Final approval of the version to be published.

Participation solely in the acquisition of funding or the collection of data does not justify authorship. General supervision of the research group is not sufficient for authorship. Each contributor should have participated sufficiently in the work to take public responsibility for appropriate portions of the content of the manuscript. The order of naming the contributors should be based on the relative contribution of the contributor towards the study and writing the manuscript. Once submitted the order cannot be changed without written consent of all the contributors. The journal prescribes a maximum number of authors for manuscripts depending upon the type of manuscript, its scope and number of institutions involved (vide infra). The authors should provide a justification, if the number of authors exceeds these limits.

Contribution Details

Contributors should provide a description of contributions made by each of them towards the manuscript. Description should be divided in following categories, as applicable: concept, design, definition of intellectual content, literature search, clinical studies, experimental studies, data acquisition, data analysis, statistical analysis, manuscript preparation, manuscript editing and manuscript review. Authors' contributions will be printed along with the article. One or more author should take responsibility for the integrity of the work as a whole from inception to published article and should be designated as 'guarantor'.

Conflicts of Interest/ Competing Interests

All authors of must disclose any and all conflicts of interest they may have with publication of the manuscript or an institution or product that is mentioned in the manuscript and/or is important to the outcome of the study presented. Authors should also disclose conflict of interest with products that compete with those mentioned in their manuscript.

Submission of Manuscripts

All manuscripts must be submitted on-line through the website https://review.jow.medknow.com/jasi. First time users will have to register at this site. Registration is free but mandatory. Registered authors can keep track of their articles after logging into the site using their user name and password.

- If you experience any problems, please contact the editorial office by e-mail at editor@jasi.org.in

The submitted manuscripts that are not as per the "Instructions to Authors" would be returned to the authors for technical correction, before they undergo editorial/ peer-review. Generally, the manuscript should be submitted in the form of two separate files:

[1] Title Page/First Page File/covering letter:

This file should provide

1. The type of manuscript (original article, case report, review article, Letter to editor, Images, etc.) title of the manuscript, running title, names of all authors/ contributors (with their highest academic degrees, designation and affiliations) and name(s) of department(s) and/ or institution(s) to which the work should be credited, . All information which can reveal your identity should be here. Use text/rtf/doc files. Do not zip the files.
2. The total number of pages, total number of photographs and word counts separately for abstract and for the text (excluding the references, tables and abstract), word counts for introduction + discussion in case of an original article;
3. Source(s) of support in the form of grants, equipment, drugs, or all of these;
4. Acknowledgement, if any. One or more statements should specify 1) contributions that need acknowledging but do not justify authorship, such as general support by a departmental chair; 2) acknowledgments of technical help; and 3) acknowledgments of financial and material support, which should specify the nature of the support. This should be included in the title page of the manuscript and not in the main article file.
5. If the manuscript was presented as part at a meeting, the organization, place, and exact date on which it was read. A full statement to the editor about all submissions and previous reports that might be regarded as redundant publication of the same or very similar work. Any such work should be referred to specifically, and referenced in the new paper. Copies of such material should be included with the submitted paper, to help the editor decide how to handle the matter.
6. Registration number in case of a clinical trial and where it is registered (name of the registry and its URL)
7. Conflicts of Interest of each author/ contributor. A statement of financial or other relationships that might lead to a conflict of interest, if that information is not included in the manuscript itself or in an authors' form
8. Criteria for inclusion in the authors'/ contributors' list
9. A statement that the manuscript has been read and approved by all the authors, that the requirements for authorship as stated earlier in this document have been met, and that each author believes that the manuscript represents honest work, if that information is not provided in another form (see below); and
10. The name, address, e-mail, and telephone number of the corresponding author, who is responsible for communicating with the other authors about revisions and final approval of the proofs, if that information is not included on the manuscript itself.

[2] Blinded Article file: The main text of the article, beginning from Abstract till References (including tables) should be in this file. The file must not contain any mention of the authors' names or initials or the institution at which the study was done or acknowledgements. Page headers/ running title can include the title but not the authors' names. Manuscripts not in compliance with the Journal's blinding policy will be returned to the corresponding author. Use rtf/doc files. Do not zip the files. **Limit the file size to 1 MB.** Do not incorporate images in the file. If file size is large, graphs can be submitted as images separately without incorporating them in the article file to reduce the size of the file. The pages should be numbered consecutively, beginning with the first page of the blinded article file.

[3] Images: Submit good quality color images. **Each image should be less than 2 MB in size.** Size of the image can be reduced by decreasing the actual height and width of the images (keep up to 1600 x 1200 pixels or 5-6 inches). Images can be submitted as jpeg files. Do not zip the files. Legends for the figures/images should be included at the end of the article file.

[4] The contributors' / copyright transfer form (template provided below) has to be submitted in original with the signatures of all the contributors within two weeks of submission via courier, fax or email as a scanned image. Print ready hard copies of the images (one set) or digital images should be sent to the journal office at the time of submitting revised manuscript. High resolution images (up to 5 MB each) can be sent by email.

Contributors' form / copyright transfer form can be submitted online from the authors' area on https://review.jow.medknow.com/jasi.

Preparation of Manuscripts

Manuscripts must be prepared in accordance with "Uniform requirements for Manuscripts submitted to Biomedical Journals" developed by the International Committee of Medical Journal Editors (October 2008). The uniform requirements and specific requirement of Journal of the Anatomical Society of India are summarized below. Before submitting a manuscript, contributors are requested to check for the latest instructions available. Instructions are also available from the website of the journal (www.jasi.org.in) and from the manuscript submission site https://review.jow.medknow.com/jasi.

Journal of the Anatomical Society of India accepts manuscripts written in American English.

Copies of any permission(s)

It is the responsibility of authors/ contributors to obtain permissions for reproducing any copyrighted material. A copy of the permission obtained must accompany the manuscript. Copies of any and all published articles or other manuscripts in preparation or submitted elsewhere that are related to the manuscript must also accompany the manuscript.

Types of Manuscripts

Original articles:

These include randomized controlled trials, intervention studies, studies of screening and diagnostic test, outcome studies, cost effectiveness analyses, case-control series, and surveys with high response rate. The text of original articles amounting to up to 3000 words (excluding Abstract, references and Tables) should be divided into sections with the headings Abstract, Key-words, Introduction, Material and Methods, Results, Discussion and Conclusion, References, Tables and Figure legends.

An abstract should be in a structured format under following heads: **Introduction, Material and Methods, Results,** and **Discussion and Conclusion.**

Introduction: State the purpose and summarize the rationale for the study or observation.

Material and Methods: It should include and describe the following aspects:

Ethics: When reporting studies on human beings, indicate whether the procedures followed were in accordance with the ethical standards of the responsible committee on human experimentation (institutional or regional) and with the Helsinki Declaration of 1975, as revised in 2000 (available at http://www.wma.net/e/policy/17-c_e.html). For prospective studies involving human participants, authors are expected to mention about approval of (regional/ national/ institutional or independent Ethics Committee or Review Board, obtaining informed consent from adult research participants and obtaining assent for children aged over 7 years participating in the trial. The age beyond which assent would be required could vary as per regional and/ or national guidelines. Ensure confidentiality of subjects by desisting from mentioning participants' names, initials or hospital numbers, especially in illustrative material. When reporting experiments on animals, indicate whether the institution's or a national research council's guide for, or any national law on the care and use of laboratory animals was followed. Evidence for approval by a local Ethics Committee (for both human as well as animal studies) must be supplied by the authors on demand. Animal experimental procedures should be as humane as possible and the details of anesthetics and analgesics used should be clearly stated. The ethical standards of experiments must be in accordance with the guidelines provided by the CPCSEA and World Medical Association Declaration of Helsinki on Ethical Principles for Medical Research Involving Humans for studies involving experimental animals and human beings, respectively). The journal will not consider any paper which is ethically unacceptable. A statement on ethics committee permission and ethical practices must be included in all research articles under the 'Materials and Methods' section.

Study design:

Selection and Description of Participants: Describe your selection of the observational or experimental participants (patients or laboratory animals, including controls) clearly, including eligibility and exclusion criteria and a description of the source population. *Technical information*: Identify the methods, apparatus (give the manufacturer›s name and address in parentheses), and procedures in sufficient detail to allow other workers to reproduce the results. Give references to established methods, including statistical methods (see below); provide references and brief descriptions for methods that have been published but are not well known; describe new or substantially modified methods, give reasons for using them, and evaluate their limitations. Identify precisely all drugs and chemicals used, including generic name(s), dose(s), and route(s) of administration.

Reports of randomized clinical trials should present information on all major study elements, including the protocol, assignment of interventions (methods of randomization, concealment of allocation to treatment groups), and the method of masking (blinding), based on the CONSORT Statement (http://www.consort-statement.org).

Reporting Guidelines for Specific Study Designs

Initiative	Type of Study	Source
CONSORT	Randomized controlled trials	http://www.consort-statement.org
STARD	Studies of diagnostic accuracy	http://www.consort-statement.org/stardstatement.htm
QUOROM	Systematic reviews and meta-analyses	http://www.consort- statement.org/Initiatives/MOOSE/moose.pdf statement.org/Initiatives/MOOSE/moose.pdf
STROBE	Observational studies in epidemiology	http://www.strobe-statement.org
MOOSE	Meta-analyses of observational studies in epidemiology	http://www.consort- statement.org/Initiatives/MOOSE/moose.pdf

Statistics: Whenever possible quantify findings and present them with appropriate indicators of measurement error or uncertainty (such as confidence intervals). Authors should report losses to observation (such as, dropouts from a clinical trial). When data are summarized in the Results section, specify the statistical methods used to analyze them. Avoid non-technical uses of technical terms in statistics, such as 'random' (which implies a randomizing device), 'normal', 'significant', 'correlations', and 'sample'. Define statistical terms, abbreviations, and most symbols. Specify the computer software used. Use upper italics (*P* 0.048). For all *P* values include the exact value and not less than 0.05 or 0.001. Mean differences in continuous variables, proportions in categorical variables and relative risks including odds ratios and hazard ratios should be accompanied by their confidence intervals.

Results: Present your results in a logical sequence in the text, tables, and illustrations, giving the main or most important findings first. Do not repeat in the text all the data in the tables or illustrations; emphasize or summarize only important observations. Extra- or supplementary materials and technical detail can be placed in an appendix where it will be accessible but will not interrupt the flow of the text; alternatively, it can be published only in the electronic version of the journal.

When data are summarized in the Results section, give numeric results not only as derivatives (for example, percentages) but also as the absolute numbers from which the derivatives were calculated, and specify the statistical methods used to analyze them. Restrict tables and figures to those needed to explain the argument of the paper and to assess its support. Use graphs as an alternative to tables with many entries; do not duplicate data in graphs and tables. Where scientifically appropriate, analyses of the data by variables such as age and sex should be included.

Discussion: Include summary of *key findings* (primary outcome measures, secondary outcome measures, results as they relate to a prior hypothesis); *Strengths and limitations* of the study (study question, study design, data collection, analysis and interpretation); *Interpretation and implications* in the context of the totality of evidence (is there a systematic review to refer to, if not, could one be reasonably done here and now?, what this study adds to the available evidence, effects on patient care and health policy, possible mechanisms); *Controversies* raised by this study; and *Future research directions* (for this particular research collaboration, underlying mechanisms, clinical research).

Do not repeat in detail data or other material given in the Introduction or the Results section. In particular, contributors should avoid making statements on economic benefits and costs unless their manuscript includes economic data and analyses. Avoid claiming priority and alluding to work that has not been completed. New hypotheses may be stated if needed, however they should be clearly labeled as such. About 30 references can be included. These articles generally should not have more than six authors.

Review Articles:

These are comprehensive review articles on topics related to various fields of Anatomy. The entire manuscript should not exceed 7000 words with no more than 50 references and two authors. Following types of articles can be submitted under this category:

- Newer techniques of dissection and histology
- New methodology in Medical Education
- Review of a current concept

Please note that generally review articles are by invitation only. But unsolicited review articles will be considered for publication on merit basis.

Case reports:

New, interesting and rare cases can be reported. They should be unique, describing a great diagnostic or therapeutic challenge and providing a learning point for the readers. Cases with clinical significance or implications will be given priority. These communications could be of up to 1000 words (excluding Abstract and references) and should have the following headings: Abstract (unstructured), Key-words, Introduction, Case report, Discussion and Conclusion, Reference, Tables and Legends in that order.

The manuscript could be of up to 1000 words (excluding references and abstract) and could be supported with up to 10 references. Case Reports could be authored by up to four authors.

Letter to the Editor:

These should be short and decisive observations. They should preferably be related to articles previously published in the Journal or views expressed in the journal. They should not be preliminary observations that need a later

paper for validation. The letter could have up to 500 words and 5 references. It could be generally authored by not more than four authors.

Book Review: This consists of a critical appraisal of selected books on Anatomy. Potential authors or publishers may submit books, as well as a list of suggested reviewers, to the editorial office. The author/publisher has to pay INR 10,000 per book review.

Other:

Editorial, Guest Editorial, Commentary and Opinion are solicited by the editorial board.

References

References should be *numbered* consecutively in the order in which they are first mentioned in the text (not in alphabetic order). Identify references *in text*, tables, and legends by Arabic numerals in superscript with square bracket after the punctuation *marks. References cited only* in tables or figure legends should be numbered in accordance with the sequence established by the first identification in the text of the particular table or figure. Use the style of the examples below, which are based on the formats used by the NLM *in Index Medicus*. The titles of journals *should be abbreviated* according to the style used in Index Medicus. Use complete name of the journal for non-indexed journals. Avoid using abstracts as references. Information from manuscripts submitted but not accepted should be cited in the text as "unpublished observations" with written permission from the source. Avoid citing a "personal communication" unless it provides essential information not available from a public source, in which case the name of the person and date of communication should be cited in parentheses in the text. The commonly cited types of references are shown here, for other types of references such as newspaper items please refer to ICMJE Guidelines (http://www.icmje.org or http://www.nlm.nih.gov/bsd/uniform_requirements.html).

Articles in Journals

1. Standard journal article (for up to six authors): Parija S C, Ravinder PT, Shariff M. Detection of hydatid antigen in the fluid samples from hydatid cysts by co-agglutination. Trans. R.Soc. Trop. Med. Hyg.1996; 90:255–256.
2. Standard journal article (for more than six authors): List the first six contributors followed by *et al*.

Roddy P, Goiri J, Flevaud L, Palma PP, Morote S, Lima N. *et al*., Field Evaluation of a Rapid Immunochromatographic Assay for Detection of Trypanosoma cruzi Infection by Use of Whole Blood. J. Clin. Microbiol. 2008; 46: 2022-2027.

3. Volume with supplement: Otranto D, Capelli G, Genchi C: Changing distribution patterns of canine vector borne diseases in Italy: leishmaniosis vs. dirofilariosis. Parasites & Vectors 2009; Suppl 1:S2.

Books and Other Monographs

1. Personal author(s): Parija SC. Textbook of Medical Parasitology. 3rd ed. All India Publishers and Distributors. 2008.
2. Editor(s), compiler(s) as author: Garcia LS, Filarial Nematodes In: Garcia LS (editor) Diagnostic Medical Parasitology ASM press Washington DC 2007: pp 319-356.
3. Chapter in a book: Nesheim M C. Ascariasis and human nutrition. In Ascariasis and its prevention and control, D. W. T. Crompton, M. C. Nesbemi, and Z. S. Pawlowski (eds.). Taylor and Francis,London, U.K.1989, pp. 87–100.

Electronic Sources as reference

Journal article on the Internet: Parija SC, Khairnar K. Detection of excretory *Entamoeba histolytica* DNA in the urine, and detection of *E. histolytica* DNA and lectin antigen in the liver abscess pus for the diagnosis of amoebic liver abscess. *BMC Microbiology* 2007, **7**:41. doi:10.1186/1471-2180-7-41. http://www.biomedcentral.com/1471-2180/7/41

Tables

- Tables should be self-explanatory and should not duplicate textual material.
- Tables with more than 10 columns and 25 rows are not acceptable.
- Number tables, in Arabic numerals, consecutively in the order of their first citation in the text and supply a brief title for each.
- Place explanatory matter in footnotes, not in the heading.
- Explain in footnotes all non-standard abbreviations that are used in each table.
- Obtain permission for all fully borrowed, adapted, and modified tables and provide a credit line in the footnote.
- For footnotes use the following symbols, in this sequence: *, †, ‡, §, ‖,¶ , **, ††, ‡‡
- Tables with their legends should be provided at the end of the text after the references. The tables along with their number should be cited at the relevant place in the text

Illustrations (Figures)

- Upload the images in JPEG format. The file size should be within 1024 kb in size while uploading.
- Figures should be numbered consecutively according to the order in which they have been first cited in the text.
- Labels, numbers, and symbols should be clear and of uniform size. The lettering for figures should be large enough to be legible after reduction to fit the width of a printed column.
- Symbols, arrows, or letters used in photomicrographs

should contrast with the background and should be marked neatly with transfer type or by tissue overlay and not by pen.
- Titles and detailed explanations belong in the legends for illustrations not on the illustrations themselves.
- When graphs, scatter-grams or histograms are submitted the numerical data on which they are based should also be supplied.
- The photographs and figures should be trimmed to remove all the unwanted areas.
- If photographs of individuals are used, their pictures must be accompanied by written permission to use the photograph.
- If a figure has been published elsewhere, acknowledge the original source and submit written permission from the copyright holder to reproduce the material. A credit line should appear in the legend for such figures.
- Legends for illustrations: Type or print out legends (maximum 40 words, excluding the credit line) for illustrations using double spacing, with Arabic numerals corresponding to the illustrations. When symbols, arrows, numbers, or letters are used to identify parts of the illustrations, identify and explain each one in the legend. Explain the internal scale (magnification) and identify the method of staining in photomicrographs.
- Final figures for print production: Send sharp, glossy, un-mounted, color photographic prints, with height of 4 inches and width of 6 inches at the time of submitting the revised manuscript. Print outs of digital photographs are not acceptable. If digital images are the only source of images, ensure that the image has minimum resolution of 300 dpi or 1800 x 1600 pixels in TIFF format. Send the images on a CD. Each figure should have a label pasted (avoid use of liquid gum for pasting) on its back indicating the number of the figure, the running title, top of the figure and the legends of the figure. Do not write the contributor/s' name/s. Do not write on the back of figures, scratch, or mark them by using paper clips.
- The Journal reserves the right to crop, rotate, reduce, or enlarge the photographs to an acceptable size.

Protection of Patients' Rights to Privacy

Identifying information should not be published in written descriptions, photographs, sonograms, CT scans, etc., and pedigrees unless the information is essential for scientific purposes and the patient (or parent or guardian, wherever applicable) gives informed consent for publication. Authors should remove patients' names from figures unless they have obtained informed consent from the patients. The journal abides by ICMJE guidelines:

1. Authors, not the journals nor the publisher, need to obtain the patient consent form before the publication and have the form properly archived. The consent forms are not to be uploaded with the cover letter or sent through email to editorial or publisher offices.
2. If the manuscript contains patient images that preclude anonymity, or a description that has obvious indication to the identity of the patient, a statement about obtaining informed patient consent should be indicated in the manuscript.

Sending a revised manuscript

The revised version of the manuscript should be submitted online in a manner similar to that used for submission of the manuscript for the first time. However, there is no need to submit the "First Page" or "Covering Letter" file while submitting a revised version. When submitting a revised manuscript, contributors are requested to include, the 'referees' remarks along with point to point clarification at the beginning in the revised file itself. In addition, they are expected to mark the changes as underlined or colored text in the article.

Reprints and proofs

Journal provides no free printed reprints. Authors can purchase reprints, payment for which should be done at the time of submitting the proofs.

Publication schedule

The journal publishes articles on its website immediately on acceptance and follows a 'continuous publication' schedule. Articles are compiled in issues for 'print on demand' quarterly.

Copyrights

Checklist

Covering letter

- Signed by all contributors
- Previous publication / presentations mentioned
- Source of funding mentioned
- Conflicts of interest disclosed

Authors

- Last name and given name provided along with Middle name initials (where applicable)
- Author for correspondence, with e-mail address provided
- Number of contributors restricted as per the instructions
- Identity not revealed in paper except title page (e.g. name of the institute in Methods, citing previous study as 'our study', names on figure labels, name of institute in photographs, etc.)

Presentation and format

- Double spacing
- Margins 2.5 cm from all four sides
- Page numbers included at bottom
- Title page contains all the desired information
- Running title provided (not more than 50 characters)
- Abstract page contains the full title of the manuscript
- Abstract provided (structured abstract of 250 words for original articles, unstructured abstracts of about 150 words for all other manuscripts excluding letters to the Editor)
- Key words provided (three or more)
- Introduction of 75-100 words
- Headings in title case (not ALL CAPITALS)
- The references cited in the text should be after punctuation marks, in superscript with square bracket.
- References according to the journal's instructions, punctuation marks checked
- Send the article file without 'Track Changes'

Language and grammar

- Uniformly American English
- Write the full term for each abbreviation at its first use in the title, abstract, keywords and text separately unless it is a standard unit of measure. Numerals from 1 to 10 spelt out
- Numerals at the beginning of the sentence spelt out
- Check the manuscript for spelling, grammar and punctuation errors
- If a brand name is cited, supply the manufacturer's name and address (city and state/country).
- Species names should be in italics

Tables and figures

- No repetition of data in tables and graphs and in text
- Actual numbers from which graphs drawn, provided
- Figures necessary and of good quality (colour)
- Table and figure numbers in Arabic letters (not Roman)
- Labels pasted on back of the photographs (no names written)
- Figure legends provided (not more than 40 words)
- Patients' privacy maintained (if not permission taken)
- Credit note for borrowed figures/tables provided
- Write the full term for each abbreviation used in the table as a footnote

Journal of
The Anatomical Society of India

Salient Features:

- Publishes research articles related to all aspects of Anatomy and Allied medical/surgical sciences.
- Pre-Publication Peer Review and Post-Publication Peer Review
- Online Manuscript Submission System
- Selection of articles on the basis of MRS system
- Eminent academicians across the globe as the Editorial board members
- Electronic Table of Contents alerts
- Available in both online and print form.

The journal is registered with the following abstracting partners:
Baidu Scholar, CNKI (China National Knowledge Infrastructure), EBSCO Publishing's Electronic Databases, Ex Libris – Primo Central, Google Scholar, Hinari, Infotrieve, Netherlands ISSN center, ProQuest, TdNet, Wanfang Data

The journal is indexed with, or included in, the following:
SCOPUS, Science Citation Index Expanded, IndMed, MedInd, Scimago Journal Ranking, Emerging Sources Citation Index.

Impact Factor® as reported in the 2018 Journal Citation Reports® (Clarivate Analytics, 2019): 0.168

Editorial Office:
Dr. Vishram Singh, Editor-in-Chief, JASI
B5/3 Hahnemann Enclave, Plot No. 40, Sector 6,
Dwarka Phase – 2, New Delhi - 110 075, India.
Email: editorjasi@gmail.com
(O) | Website: www.asiindia.in

The journal is owned and run by The Anatomical Society of India